UNIVERSITY OF CALIFORNIA

Santa Barbara

Coastal Ocean pH Variability in the Context of Global Change Biology

A dissertation submitted in partial satisfaction of the

requirements for the degree Doctor of Philosophy

in Ecology, Evolution and Marine Biology

by

Lydia Kapsenberg

Committee in charge:

Professor Gretchen E. Hofmann, Chair

Dr. Carol A. Blanchette

Professor Debora Iglesias-Rodriguez

Professor Libe Washburn

September 2015

The dissertation of Lydia Kapsenberg is approved.

_____
Carol A. Blanchette

_____
Debora Iglesias-Rodriguez

_____
Libe Washburn

_____
Gretchen E. Hofmann, Committee Chair

September 2015

Coastal Ocean pH Variability in the Context of Global Change Biology

by

Lydia Kapsenberg

ACKNOWLEDGEMENTS

This dissertation is dedicated to Dr. Bruce A. Menge, who singlehandedly convinced me to pursue a PhD. He responded to my initial uncertainty by saying: "Oh, you're the type," to which I thought, "Well, he would know…!" I thank Dr. Symon A. Dworjanyn for introducing me to global change biology with such great enthusiasm for both field and lab research that my stomach often hurt from laughing.

I am grateful beyond measure for my parents, Roeland and Irma Kapsenberg. They have always encouraged me to pursue my interests and supported my decisions along the way. My brothers, Pieter and Florian, deserve a thank you for being my consultants and personal champions, despite their greatest efforts to convince me to study engineering.

My gratitude goes to my advisor and Committee Chair, Dr. Gretchen E. Hofmann, for accepting me into her lab, outstanding mentorship and offering me incredible research experiences. I thank my committee members, Drs. Libe Washburn, Debora Iglesias-Rodriguez and Carol A. Blanchette, and my fellow Hofmann Lab members from 2010 to 2015 for science support, discussions, and advice.

This dissertation was made possible through funding from the United States National Science Foundation, National Park Service, Southern California Research and Learning Center, Sea-Bird Electronics, Bureau of Ocean Energy Management, and the University of California Santa Barbara and support from the Santa Barbara Coastal Long Term Ecological Research group and Ocean Margin Ecosystems Group for Acidification Studies.

VITA OF LYDIA KAPSENBERG
September 2015

EDUCATION

2010 - 2015 **University of California Santa Barbara**

Doctor of Philosophy

Department of Ecology, Evolution and Marine Biology

Advisor: Dr. Gretchen E. Hofmann

2005 - 2009 **Oregon State University**

Bachelor of Science, *Summa Cum Laude*

Biology, Department of Biology

Minor: Chemistry, Option: Marine Biology, 13 Jun

PREVIOUS POSITIONS IN RESEARCH

2009 **Research Assistant**, full-time, 15 Jun – 15 Dec

Drs. Bruce A. Menge and Jane Lubchenco, Department of Zoology, Oregon State University, USA

2008 **Research Assistant**, full-time, 16 June – 11 Dec

Dr. Symon A. Dworjanyn, National Marine Science Centre, Southern Cross University, Australia

FELLOWSHIPS AND AWARDS

2015 - 2017 National Science Foundation Ocean Sciences Postdoctoral Research Fellowship, USA ($194,000)

2015 Nomination, 2014 Fiona Goodchild Award for Excellence as a Graduate Student Mentor of Undergraduate Research.

2015 EEMB Block Award, University of California Santa Barbara, USA

2014 - 2015 UCSB Graduate Fellowship, University of California Santa Barbara, USA

2013 Travel Award to Ocean Sciences 2014, Sea-Bird Electronics, USA ($1000)

2012 Best Poster Award, Multidisciplinary category, Scientific Committee on Antarctic Research Open Science Conference, Portland OR, USA

2012 Travel Award to XXXII Open Science Conference, Scientific Committee on Antarctic Research, Portland OR, USA ($775)

2011 - 2014 National Science Foundation Graduate Research Fellowship, USA (received in 2010)

2011 Travel Award to Friday Harbor Labs, Ocean Carbon Biogeochemistry, USA ($1000)

2010 - 2011 EEMB Block Award, University of California Santa Barbara, USA

RESEARCH GRANTS

2014 - 2015 **Research and Learning Grant** *"Characterizing Ocean pH in the Channel Islands National Park"* Southern California Research and Learning Center, USA ($3,600)

2014 - 2015 **Student Equipment Loan Program Award, *extension*** *"Quantifying drivers of pH variability in coastal Antarctica"* Sea-Bird Electronics, USA (one 37-SMP-ODO MicroCAT oceanographic sensors)

2013 - 2014 **Student Equipment Loan Program Award** *"Quantifying drivers of pH variability in the Channel Islands National Park"* Sea-Bird Electronics, USA (three 37-SMP-ODO MicroCAT oceanographic sensors, $37,000 value)

2013 - 2014 **Research and Learning Grant** *"Characterizing Ocean pH in the Channel Islands National Park"* Southern California Research and Learning Center, USA ($6,000)

2014 **Research Grant,** *"Characterizing Ocean pH in the Channel Islands National Park"* co-PIs: GE Hofmann, CA Blanchette, Bureau of Ocean Energy Management, USA ($2450 + SeaFET pH sensor, $10,000 value)

2013 **UCSB Research Fellowship**, University of California Santa Barbara, USA ($4500)

2011 - 2012 **George Melendez Wright Climate Change Fellowship "***Assessment of ocean acidification in the Channel Islands National Park and its impact on local marine species"* National Park Service, USA ($19,987)

PUBLICATIONS

7. **Kapsenberg, L**, AL Kelley, LA Francis, and SB Raskin. Exploring the complexity of ocean acidification: an ecosystem comparison of coastal pH variability. In press, *Science Scope*

6. **Kapsenberg, L**, AL Kelley, EC Shaw, TR Martz, and GE Hofmann (2015) Near-shore Antarctic pH variability has implications for the design of ocean acidification experiments. *Scientific Reports* 5, 9638. DOI:10.1038/srep09638

5. **Kapsenberg, L**, and GE Hofmann (2014) Signals of resilience to ocean change: high thermal tolerance of early stage Antarctic sea urchins (*Sterechinus neumayeri*) reared under present day and future pCO_2 and temperature. *Polar Biology* 37(7): 967-980.
4. Hofmann, GE, TG Evans, MW Kelly, JL Padilla-Gamiño, CA Blanchette, L Washburn, F Chan, MA McManus, BA Menge, B Gaylord, TM Hill, E Sanford, M LaVigne, JM Rose, **L Kapsenberg**, and JM Dutton (2014) Exploring local adaptation and the ocean acidification seascape – studies in the California Current Large Marine Ecosystem. *Biogeosciences* 11: 1053-1064.
3. Sewell, MA, R Millar, PC Yu, **L Kapsenberg**, GE Hofmann (2014) Ocean acidification and fertilization in the Antarctic sea urchin *Sterechinus neumayeri*: the importance of polyspermy. *Environmental Science & Technology* 48: 713-722.
2. Hofmann, GE, CA Blanchette, EB Rivest, and **L Kapsenberg** (2013) Taking the pulse of marine ecosystems: The importance of coupling long-term physical and biological observations in the context of global change biology. *Oceanography* 26(3): 140–148.
1. Yu, PC, MA Sewell, PG Matson, EB Rivest, **L Kapsenberg**, and GE Hofmann (2013) Growth attenuation with developmental schedule progression in embryos and early larvae of *Sterechinus neumayeri* raised under elevated CO_2. *PLoS One* 8(1): e52448.

MANUSCRIPTS

Kapsenberg, L, and GE Hofmann. Ocean pH time-series and drivers of variability along the northern Channel Islands, California, USA. In review, *Limnology & Oceanography*

PRESENTATIONS

2015	Oral *"Surprising pH from Earth's most southern sea"* 11th Annual Departmental Graduate Student Symposium, USA, 7 Feb
2014	Poster *"From kelp to ice: temporal and spatial variability in ocean pH"* Ocean Sciences Meeting, USA, 23-28 Feb
2013	Oral *"From kelp to ice: temporal and spatial variability in ocean pH"* 94th Annual Meeting of the Western Society of Naturalists, USA, 7-10 Nov
2013	Oral *"Hot but not bothered: ocean change and Antarctic sea urchin larvae"* 9th Annual Departmental Graduate Student Symposium, USA, 2 Feb
2012	Oral *"Global change biology in the Antarctic: sea urchins, SeaFETs and the anthropocene"* PC Yu, GE Hofmann, L Kapsenberg, Wednesday Night Science Lecture, McMurdo Station, Antarctica, 21 Nov
2012	Poster *"Ocean acidification: assessment of pH in the Channel Islands National Park and its effect on sea urchin fertilization"* remote presentation, 8th California Island Symposium, USA, 23-26 Oct

2012 Poster, *"Ocean acidification: assessment of pH in the Channel Islands National Park and its effect on sea urchin fertilization"* LTER All Scientist Meeting, Estes Park CO, USA, 10-13 Sep

2012 Poster "*Combatting heat in a changing ocean, sea urchins are prepared for battle"* Third Symposium on the Ocean in a High-CO_2 World, Monterey CA, USA, 24-27 Sep

2012 Poster "*Combatting heat in a changing ocean, sea urchins are prepared for battle"* XXXII Scientific Committee on Antarctic Research Open Science Conference, Portland OR, USA, 16-19 Jul

INVITED SEMINARS

2015 NOAA Channel Islands National Marine Sanctuary Advisory Council Meeting *"Ocean pH Research in the Channel Islands National Marine Sanctuary and National Park"* GE Hofmann, L Kapsenberg, Santa Barbara CA, USA, 15 May

2015 From Shore to Sea Lecture Series, Channel Islands National Park, *"Keeping up with ocean change: pH variability at the Channel Islands"* Ventura CA, USA, 12 Mar

2014 Pacific Ocean Education Team Webinar *"What biologists and resource managers need to know about ocean acidification"* CA Blanchette, L Kapsenberg, 25 Sep

2014 NOAA Channel Islands National Marine Sanctuary Advisory Council Meeting *"Drivers of natural pH variability in the Channel Islands National Park"* Santa Barbara CA, USA, 24 Jan

2014 Channel Islands National Park All Employees Meeting *"Ocean acidification… the other CO_2 problem"* Ventura CA, USA, 22 Jan

2012 Santa Barbara Museum of Natural History Science Pub *"Chills, drill, and thrills: climate change and marine life in Antarctica"* PC Yu, L Kapsenberg, Santa Barbara CA, USA 25 Jun

2012 Climate Change in America's National Parks: Climate Change Research from the Next Generation Webinar *"Ocean change in the Channel Islands National Park"* National Park Service, USA, 14 Jun

2012 NOAA Channel Islands National Marine Sanctuary Advisory Council Meeting *"Ocean acidification monitoring in the Channel Islands National Park"* Ventura CA, USA, 16 Mar

TEACHING

2015 **Teaching Assistant**, Introductory Biology Laboratory 3, Spring Quarter, UCSB, USA

2014 - 2015 **Lead Coordinator**, Ocean acidification curriculum development, in collaboration with NOAA Channel Islands National Marine Sanctuary, USA

2013 **Teaching Assistant**, Global Change Biology, Spring Quarter, UCSB, USA

2013 **Guest Lecturer**, Global Change Biology, Spring Quarter, UCSB, USA

2005 - 2008 **Assistant Swim Coach**, Crescent Valley High School, Corvallis OR, USA

CRUISE AND REMOTE FIELD RESEARCH

2014 **Research Assistant**, NOAA Channel Islands Research Cruise for Acidification Studies (CIRCAS), Santa Barbara Channel, R/V *Shearwater*, 2 days. Lead PI: JJ Lunden

2013 **Project Leader**[1], field research at McMurdo Station, Antarctica, Oct-Nov. Lead PI: GE Hofmann

2010 - 2012 **Research Assistant**, McMurdo Station, Antarctica, Oct-Dec. Lead PI: GE Hofmann

2011 **Research Assistant**, March Richard B. Gump South Pacific Research Station, University of California Berkeley, Moorea, French Polynesia, Mar. Lead PI: EB Rivest

UNIVERSITY AND PROFESSIONAL SERVICE

2015 **Graduate Student Representative,** Marine Physiology search committee, Department of Ecology, Evolution and Marine Biology, UCSB

2014 **Participant** in the National Academy of Sciences Study on Science Priorities in Antarctica, Stanford University, Stanford CA, 12 Nov

2014 **Reviewer** for *Environmental Science & Technology*, *Conservation Physiology*

2012, 2013 **Lead-, Co-Coordinator** for the Annual Graduate Student Symposium, Department of Ecology, Evolution and Marine Biology, UCSB

2012 - 2014 **Departmental Assembly Representative**, UCSB Graduate Student Association

WORKSHOPS

2014 **Keynote speaker, Co-Organizer** for Ocean Acidification Section, *"Teaching Environmental Science in a Changing Climate"* NOAA Channel Islands National Marine Sanctuary, Santa Barbara CA, USA, 20 Jun

[1] USA government shutdown in 2013 led to travel cancelation to Antarctica. L. Kapsenberg remotely coordinated and coached scientists at McMurdo Station to complete the tasks.

2013 **Co-Instructor** for SeaFET workshop for the Consortium for the Study of Ocean Change, Universidad Autónoma de Baja California, Mexico 17-20 Jun

2012 **Lead speaker, Co-Organizer** for *"LTER Ocean Acidification Data Management Workshop"* LTER All Scientists Meeting, Estes Park CO, USA, 13 Sep

STUDENT ADVISING

2014 Evan Barba (Santa Barbara Coastal LTER Research Experience), UCSB, 3 months

2013 - 2014 Mark Bitter (Santa Barbara Coastal LTER Research Experience, senior thesis), UCSB, 8 months

2012 Kylie Langlois (lab assistant), UCSB, 3 months

2011 Ella Bendrick-Chartier (lab assistant), UCSB, 3 months

OUTREACH

2014 - 2015 **Science Advisor**, Channel Coast Watershed Observatory in collaboration with SCCOOS, NOAA Channel Islands National Park, Nature Bridge, Monterey Bay Aquarium, BOEM, JASON learning, middle school STEM coordinators, USA

2013 - 2015 **Leader**, Ocean acidification education and outreach implementation, Channel Islands National Park, USA. Includes design and construction of a multi-media traveling exhibit on ocean acidification

2012 **Science Panelist**, Climate Change Student Summit, NOAA and ANDRILL, Ventura CA, USA, 28 Apr

NEWS AND MEDIA

2015 NOVA *"Lethal Seas"* documentary, 13 May

2015 Channel Islands National Park News Release *"Marine Biologist Studies Climate Change Effect on Local Sea Life"* Yvonne Menard, 6 Mar [http://www.nps.gov/chis/learn/news/pr030615.htm]

2013 Nature Comment *"Politics: The long shadow of the shutdown"* Gretchen E. Hofmann, 18 Oct [http://www.nature.com/news/politics-the-long-shadow-of-the-shutdown-1.13978]

2013 Washington Monthly *"The government shutdown is killing Antarctic science"* Rachel Cohen, 9 Oct [http://www.washingtonmonthly.com/ten-miles-square/2013/10/the_shutdown_is_killing_antarc047279.php]

2012 National Science Foundation News *"Researchers recover recorder from Antarctic waters containing critical baseline on acidification"* Peter West, 18 Oct [http://www.nsf.gov/news/news_summ.jsp?cntn_id=125761]

2012 Convergence Cover story *"Oceans of change"* Cathrine Newell, 19 Sept [http://www.convergence.ucsb.edu/article/oceans-change]

2011 Ocean Carbon Biogeochemistry News *"Impressions of the summer 2011 Ocean Acidification Course at UW Friday Harbor Labs"* 4(3) Fall

2011 Ocean Carbon Biogeochemistry News *"OCB to provide student travel support for the Friday Harbor Ocean Acidification Course"* 4(2) Spring/Summer

PROFESSIONAL AFFILIATIONS

2012 - 2015 Ocean Margins Ecosystems Group for Acidification Studies, USA

2011 - 2015 University of California Ocean Acidification Training and Research Consortium, USA

2012 - 2015 Santa Barbara Coastal Long Term Ecological Research, USA

CERTIFICATIONS

2011 - present Scientific SCUBA Certification, American Academy of Underwater Sciences, USA

2011 - present CPR, AED, First Aid, Oxygen, Scientific Diving Program, University of California Santa Barbara, USA

ABSTRACT

Coastal Ocean pH Variability in the Context of Global Change Biology

by

Lydia Kapsenberg

Anthropogenic carbon emissions are predicted to alter marine ecosystems. One such change is the decline in ocean pH, known as ocean acidification. Model predictions of ocean acidification have guided biological experiments for more than a decade. Many studies predict negative consequences of future ocean pH on marine species. To understand how species will respond to future conditions, however, knowledge of present-day pH exposures is necessary and often limited. In this dissertation, I described present-day pH variability in three coastal regions and used the data to design laboratory experiments assessing the physiological response of two organisms, sea urchins and mussels, to changing ocean conditions. As recorded by autonomous pH sensors, I found three unique patterns of coastal pH variability. Near-shore Antarctica was characterized by a steep seasonal increase in pH and pH variability during summer phytoplankton blooms. The northern Channel Islands, California, exhibited event-scale and diurnal pH variability due to primary production of phytoplankton and fixed vegetation. Only mild effects from upwelling were detected at the islands, suggesting that this region may become a spatial refuge from extreme low pH in the future. Finally, Oregon was characterized by event-scale decreases in pH due to periodic upwelling events. The results from this research show that many coastal species experience

short-term changes in pH that are within the same magnitude of change predicted for ocean acidification by the end of the century. While such present-day exposures to pH variability may promote tolerance of future pH change, these near-shore regions are also characterized by unique patterns of thermal stress. I conducted two studies to investigate the interactive effects of pH and temperature on organismal physiology. First, Antarctic sea urchin, *Sterechinus neumayeri*, early developmental stages (EDSs) currently experience < 2 °C seasonal warming and may only experience a few degrees of ocean warming over the next 100 years. Despite development under pH and temperatures outside of current exposures, *S. neumayeri* EDSs exhibited high tolerance of a one-hour heat stress test, suggesting this species may be more resilient to ocean change than previously thought. Second, unlike Antarctic species, intertidal species at mid-latitudes experience daily temperature fluctuations that can exceed four times end-century predictions of ocean warming, due to tidal cycles. In Oregon, upwelling events enhance this temperature range by periodically delivering cold, low pH water to the intertidal zone. Depending on sea water conditions simulating an upwelling event (cold, low pH) or wind relaxation (warm, high pH), the intertidal mussel *Mytilus californianus* generated different transcriptomic signatures of the cellular heat shock response, following exposure to aerial heat stress. This suggests that future changes in seawater conditions may alter the heat stress tolerance of *M. californianus* during low tides. The results from this dissertation highlight the importance of designing experiments that reflect species' present-day and future multi-stressor environment, in order to generate ecologically relevant conclusions. As anthropogenic stressors continue to take hold of coastal seas, understanding the biological consequences is critical for management and conservation efforts.

TABLE OF CONTENTS

LIST OF FIGURES

LIST OF TABLES

I. Introduction: linking oceanography with physiology

A. Introduction to ocean change

Anthropogenic carbon dioxide (CO_2) emissions are causing two major changes to the Earth's oceans: (1) warming and (2) acidification. Average global ocean temperature has increased by 0.67 ± 0.15 °C over the past century with an increased rate over the last 30 years of 0.133 ± 0.047 °C per decade (IPCC 2007b). Global sea surface temperature is predicted to increase by up to 2.6 °C by 2100 (IPCC 2007a). Ocean acidification, the addition of anthropogenic CO_2 to the ocean, alters the carbonate chemistry of seawater, which influences physiological processes of marine organisms. Thus far, global surface ocean pH has declined by 0.1 from 8.2 to 8.1 since 1750 and is predicted to further decrease up to 0.42 by 2100 and as much as 0.7 by 2300 (Caldeira and Wickett 2003; Pörtner et al. 2014). As the ocean has undergone periods of lower pH conditions previously, the critical component of ocean change in the 21st century is not necessarily the magnitude of CO_2 increase but the *rate* at which species will have to keep up with changing conditions; CO_2 in the ocean is increasing faster than any time in the last 300 million years (Hönisch et al. 2012). However, due to complexity of near-shore environments, predictions of global mean ocean pH may not capture the realized pH range experienced by many shallow, near-shore marine species. There is still a limited understanding of natural pH dynamics in the ocean, especially in near-shore systems, and how exposure to natural variability in abiotic parameters influences species physiological tolerances.

Detrimental environmental stressors, such as those associated with ocean change, can lead to four general species' responses: (1) acclimatization, (2) adaptation, (3) migration, or (4) extinction. For example, global surface warming corresponds with poleward shifts of

species ranges that are in line with known physiological tolerances (Berke et al. 2010; Parmesan and Yohe 2003; Root et al. 2003; Sunday et al. 2012; Walther et al. 2002; Wethey and Woodin 2008). In these cases, either warm adapted low latitude populations migrate to high latitudes or suffer extinction, and/or higher latitude populations are able to adapt to warmer temperatures or migrate poleward. The Earth maintains a strong thermal gradient between the poles. Sea-surface temperature ranges from ~30 to -2 °C allowing for poleward shift of species ranges to a certain extent. However, pH is relatively uniform. Due to the lack of a strong pH gradient in the marine biome and limited knowledge on current pH variability, species response to ocean acidification is less well characterized than to warming. Ocean acidification occurs across a globally homogenous abiotic parameter of pH and so migration and range shifts may not be an option for population persistence like it is for warming. The diversity in marine organisms (e.g. life histories, habitat, locomotion, feeding mode, etc.) and, in turn, their diverse sensitivities to pH and temperature, complicates our ability to predict marine ecosystem change that will be necessary to implement management strategies for ocean warming or acidification to maintain healthy marine ecosystems.

B. Overview of ocean carbonate chemistry

Since the preindustrial era, global mean atmospheric CO_2 levels have increased from 280 ppm (Caldeira and Wickett 2003) to over 400 ppm in the past 200 years (NOAA 2015, http://www.esrl.noaa.gov/gmd/ccgg/trends/global.html). From 1800 to 1994, roughly 50 % of anthropogenic CO_2 emissions remained in the atmosphere, 20 % was absorbed by the terrestrial biosphere, and the remaining 30% has been absorbed by the ocean (Sabine et al. 2004). At the air-seawater interface, CO_2 dissolves into the ocean and enters the carbon

cycle. So far, the majority of ocean-absorbed anthropogenic CO_2 remains in the first 1000 m of the ocean, with 50% residing in the first 400 m and 30% in the first 200 m (Sabine et al. 2004). Oceanic CO_2 absorption varies in water masses across the globe based on currents, winds, temperature, alkalinity, locations of landmasses, and buffer capacities (Sabine et al. 2004). Different regions will thus experience different carbonate changes, which is complicated further by local near-shore oceanographic and biological processes.

Atmospheric pCO_2 equilibrates with the sea surface such that ocean pCO_2 is increasing at a similar rate as the pCO_2 of the atmosphere (Henry's Law; Doney et al. 2009). When CO_2 dissolves into the ocean, it mixes and reacts with surface seawater to produce carbonic acid (H_2CO_3) that readily dissociates to bicarbonate (HCO_3^-), a natural buffering ion in the ocean, and a hydrogen ion (H^+) via this reversible reaction:

$$CO_2 + H_2O \rightarrow H_2CO_3 \rightarrow HCO_3^- + H^+ \qquad (1)$$

The increased H^+ concentration causes a decline in pH, ergo the phrase *'ocean acidification'*. Thus, as ocean pCO_2 increases, pH decreases. In addition, hydrogen ions (H^+) react with carbonate ions (CO_3^-) to produce more HCO_3^-.

With slow addition of CO_2 to the atmosphere, carbonate minerals (as a CO_3^{2-} source) in the ocean have time to enter the ocean carbon cycle and buffer the oceanic pH decline (Caldeira and Wickett 2003). Dissolution of calcium carbonate ($CaCO_3$) minerals balances the ocean's acidity via the following chemical reaction when calcifying organisms die and their skeletons sink, adding more CO_3^{2-} and absorbing H^+ (Feely et al. 2004):

$$CO_2 + CaCO_3 + H_2O \rightarrow 2HCO_3^- + Ca^{2+} \qquad (2)$$

The ocean's buffering capacity against ocean acidification declines as it sequesters more CO_2 (Egleston et al. 2010; Sabine et al. 2004). The rate of CO_2 change today, however, is

fast compared to events in the geological record such that ocean pH becomes more sensitive to CO_2 additions and may decline by 0.77 units by 2300 (Caldeira and Wickett 2003).

Solubility of $CaCO_3$ depends on its crystalline structure: aragonite or calcite (with varying concentrations of magnesium). The degree to which aragonite and calcite are soluble depends on the 'saturation state' (Ω) of the water with respect to those minerals. Saturation state depends on Ca^{2+} and CO_3^{2-} concentrations and the stoichiometric solubility product of the mineral form (K^*) (Feely et al. 2004):

$$\Omega_{arag} = [Ca^{2+}][CO_3^{2-}]/K^*_{arag} \qquad (3)$$

$$\Omega_{cal} = [Ca^{2+}][CO_3^{2-}]/K^*_{cal} \qquad (4)$$

Since $[Ca^{2+}]$ does not vary more than 1.5 % globally, saturation state depends primarily on $[CO_3^{2-}]$ (Feely et al. 2004). As CO_2 enters the carbon system, Ω declines with $[CO_3^{2-}]$. When seawater is saturated with respect to CO_3^{2-} and $\Omega > 1$ calcification of that mineral is favored, and when $\Omega < 1$ dissolution of biologically-unprotected $CaCO_3$ occurs (Fabry et al. 2008).

CO_2 solubility is greater at cold temperatures. As such, Ω decreases as temperature declines with depth from the surface layer. The 'carbonate saturation horizon' is the depth above which calcification is favored and below it is not. Aragonite dissolves at a higher pH threshold than calcite and therefore has a shallower saturation horizon compared to calcite (Feely et al. 2004). Calcite may additionally contain varying levels of magnesium. The higher the level of Mg^{2+} to Ca^{2+}, the more soluble the mineral is such that calcite with a Mg:Ca ratio of > 0.14 is more soluble than aragonite at the same pCO_2 level (Ries 2011). $CaCO_3$ dissolution has been documented in the Atlantic, Pacific and Indian Oceans, which corresponded with aragonite and calcite saturation horizons (Feely et al. 2004). As a direct

result of anthropogenic ocean acidification, areas of carbonate undersaturation have expanded and consequently, aragonite and calcite saturation horizons have shoaled, in some cases by up to 200 m, in large portions of these three oceans (Feely et al. 2004).

Due to different water properties, marine ecosystems differ in their sensitivity to ocean acidification. High latitude seas and deep cold seawater bought to the surface by upwelling events are known to have higher pCO_2 levels compared to the atmosphere (Feely et al. 2008; Orr et al. 2005). Ocean-carbon cycle modeling shows that the Southern Ocean will be particularly vulnerable to ocean acidification and is expected to become undersaturated with respect to aragonite as early as 2050 (Orr et al. 2005). Experimental exposure of such undersaturation resulted in shell dissolution by the subarctic-Pacific aragonite-forming pteropod *Clio pyramidata* after only 48 h of exposure (Orr et al. 2005). In contrast, tropical and subtropical waters will likely never become undersaturated with respect to calcite but biogenic calcifying rates will likely decline before saturation states are < 1 (Feely et al. 2004), and so ocean acidification still poses a risk in tropical regions. Additionally, temperate upwelling systems may be particularly sensitive to ocean acidification as they already experience drastic variations in pH on daily and seasonal time scales (Feely et al. 2008; Hauri et al. 2013). Feely et al. (2008) recorded seawater with pH < 7.75 in an upwelling zone off the northern California coast, and according to a model by Hauri et al. (2009), the California Current Large Marine Ecosystem already experiences pH levels that were not predicted to occur until several decades from now.

Carbonate undersaturation as a result of ocean acidification poses a significant challenge for marine calcifying organisms such as sea urchins, corals, mollusks, and coccolithophores (Kroeker et al. 2013), as they at least partially rely on ocean chemistry to

build calcium carbonate skeletons. For example, when reared at varying levels of Ω_{arag} (3.71 - 0.22), new coral recruits of *Favia fragum* had delayed, reduced, and altered crystal growth at lower Ω_{arag} compared to ambient conditions (Cohen et al. 2009). Cohen et al. (2009) suggested that polyp's internal Ω_{arag} must be elevated in order to continue, albeit slowly, calcification in undersaturated conditions and that reduced calcification results from a systematic decline in internal Ω_{arag} with decreasing external Ω_{arag}. Such observed negative effects of ocean acidification chemistry on calcification were the grounds to ring the alarm on ocean acidification over this past decade.

C. Current pH-seascape

1. A brief history of ocean acidification research

The past decade of ocean change research was a period of exponential growth and rapidly evolving research techniques and approaches. In 2007, development of standardized analytical carbonate chemistry methods and certified reference materials for measuring seawater pH in the field or laboratory has allowed the research community to converge on best practices (Dickson et al. 2007). As such, research methods have moved from using hydrochloric acid, to experimentally alter seawater pH in laboratory experiments to study the growth of calcifying marine invertebrates, to using CO_2-acidification of semi-enclosed aquaria in the field aimed to address ecosystem level effects of ocean change (Gattuso et al. 2014).

Traditional ocean acidification experiments exposure organisms to stable pH conditions for short periods of time. However, increased pH observations in near-shore regions reveal high temporal and spatial pH variability and indicate that IPCC (2007a) projections of ocean pH lack the resolution required to predict acidification of coastlines (Feely et al. 2008;

Hofmann et al. 2011; McElhany and Busch 2013). For example, experimental pH between 8.1 and 7.8 may not be relevant if species already experience such values on a daily basis (Figure I-1, black dots and gray line). High performance of a species under non-field-parameterized experimental conditions may lead to a false prediction of ocean acidification tolerance (Figure I-1). For example, a sensitive species (blue line) may tolerate temporary low pH exposure but appear robust in a laboratory experiment that does not include experimental treatments outside of its current pH envelope. Furthermore, lacking knowledge of a species' performance curve may lead to inaccurate predictions of 'winners and losers' (Figure I-1, red and blue lines). With ocean acidification, low pH conditions will occur more frequently and time spent in the envelope of present-day pH exposure will decline (Hauri et al. 2013; Shaw et al. 2013). Physiological performance may suffer with increased exposure time to low pH, even if the total pH range remains unchanged. Unless all components of a performance curve are known, experimental results of single point pH exposures will be difficult, if not impossible, to interpret in a way that is ecologically informative. Although some ecosystem-specific predictions of ocean acidification have been made to guide the design of biological experiments (e.g. Hauri et al. 2013; McNeil et al. 2010; Shaw et al. 2013), understanding local pH dynamics is imperative to the design and interpretation of physiological experiments. Connecting field pH exposures to laboratory performance is critical and can provide significant insight to species performance (Pansch et al. 2012; Thomsen et al. 2010; Yu et al. 2011).

2. Dawn of the pH sensors

To address the knowledge gap on local pH dynamics, one of the greatest contributions to the field of ocean acidification research has been the development of autonomous pH

Figure I-1. Schematic of physiological performance of two species (red and blue) across a range of pH. The grey boxes represent pH conditions experienced by species (light grey box is present day, dark grey line is pH observations at Santa Cruz Island, CA, in May 2012) and hypothetical future ocean acidification conditions ('OA', dark grey box). Black dots represent two experimental pH levels chosen for laboratory experiments.

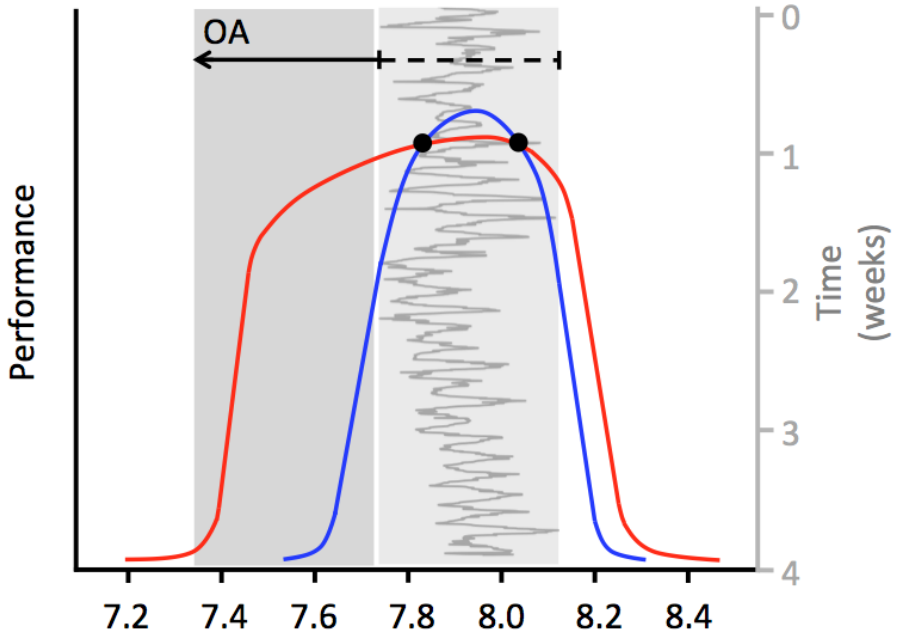

sensors (e.g. Martz et al. 2010). The goal of ocean acidification research is to ultimately understand how ecosystem function and services may change. However, not all ecosystems share the same carbon chemistry characteristics and pH can vary largely in space and time. Extensive surveys with discrete water sampling have captured ocean acidification trends and, indirectly, some degree of temporal pH variability (Bates and Peters 2007; Dore et al. 2009; González-Dávila et al. 2010). However, hourly to weekly pH variability was largely undocumented, until the development of the SeaFET pH sensor by Dr. Todd Martz and his colleagues (Martz et al. 2010). This instrument uses existing ion-sensitive field effect transistor (ISFET) technology that is adapted for autonomous sampling and deployment in the ocean environment. Early and short-term deployments of this instrument revealed previously unidentifiable spatial and temporal variability across an array of marine environments (Hofmann et al. 2011). For example, over the course of a one-month observation period, open ocean pH varied by 0.02 whereas natural CO_2 seep communities exhibited pH fluctuations on the order of 1.4 (Hofmann et al. 2011). Due to global ocean circulation, regional and seasonal weather patterns, and local geography and biological activity, different ecosystems (and even locations within them) possess unique 'pH-seascapes'. It is this pH-seascape, defined by the magnitude and temporal pH variability, which will ultimately impose selective pressures and drive the response of individual organisms.

With the development of ocean pH sensors, there has been an emerging opportunity to document pH-seascapes and use the data to link exposure to natural pH variability with physiological performance to pH. There is still a paucity of knowledge regarding the long-term natural pH dynamics of short-term pH variability in marine ecosystems. Use of

autonomous pH sensors allows us to document pH-seascapes in different ecosystems by providing high-resolution and stable pH measurements. Data of temporal and spatial pH variability can then be used to parameterize biological experiments and improve climate models. Understanding different pH-seascapes among and within ecosystems will allow us to determine to what extent organisms are able to deal with their current and local pH variability with the hopes of inferring how organisms will respond to future levels of ocean acidification.

3. Drawing pH-seascapes into experimental design

In addition to cultivating our understanding of natural pH dynamics, knowledge of an organism's pH history is necessary for the interpretation of experimental results. Laboratory studies have shown that organisms can acclimate to pH conditions and influence physiological responses to simulated ocean acidification and performance of subsequent generations (e.g. Dupont et al. 2013; Form and Riebesell 2012; Parker et al. 2012). For example, exposure to high CO_2 conditions during oyster reproductive conditioning lead to larger and faster growing larvae in high CO_2 conditions compared to larvae from adults conditioned in control CO_2 (Parker et al. 2012). Similarly, different lengths of adult sea urchin exposure time to high CO_2 led to differences in successful larval development (Dupont et al. 2013).

In reality, wild organisms will have more time to acclimatize to ocean acidification than organisms in any laboratory experiment, as the rate of ocean acidification in the field will always be slower than that simulated in laboratory experiments. Parker et al. (2012) found that oyster larvae from selected oyster lines were overall more resilient to ocean acidification than larvae from wild adults. With no knowledge of environmental conditions

of the selected lines of oysters compared to the wild oysters, it is difficult to hypothesize *why* oysters may have the ability to acclimatize and potentially adapt to ocean acidification. Perhaps selected oysters were maintained at higher densities than wild oysters, and so increased respiration lead to lower pH of the microenvironment surrounding the captive adults compared to the wild populations. If so, the selected lines may have acclimatized to reduced pH over multiple generations.

Knowledge of the pH-seascape supports the research strategy of substituting space for time (Hofmann et al. 2014). Inferred differential pH-seascapes (e.g. upwelling vs. non-upwelling dominated sites) have been linked to local adaptation of heritable ocean acidification tolerance traits in a temperate sea urchin species (Kelly et al. 2013). Such studies demonstrate a powerful research avenue for utilizing pH-seascapes as natural treatment conditions.

Given that (1) pH exposure can influence species' tolerance of low pH and (2) pH varies in the field, the environment from which the organism was collected deserves careful consideration in experimental design and interpretation, as the field exposure may impart a 'treatment' in and of itself. Therefore, quantifying the pH-history of the organisms prior to experimentation is as crucial as quantifying seawater chemistry during the experiment.

Studies that parameterize experiments with field pH observations are emerging, but even so the reported environmental data are often on the order of weeks to months, likely due to the lack of access to pH sensors in prior years. Generating multi-year datasets of pH variability will thus provide the necessary oceanographic context for biological studies.

D. Biology of ocean change

1. Ocean acidification biology

Under simulation ocean acidification (low pH), shells from dead marine organisms dissolve, yet live organisms will continue to successfully calcify at that same low pH (Findlay et al. 2011). While the dissolution of the dead shell can be attributed to reduced Ω, understanding the response of the live organisms is essential for predicting species trajectories in a changing ocean. Shell dissolution in the absence of biological control suggests an energetic cost of biogenic calcification. Changes in such energetic costs within the range of a species' natural and predicted pH exposures, may interfere with other physiological processes and lead to energetic trade-offs. One of the earlier ocean acidification studies, for example, Wood et al. (2008) found that sea stars maintained calcification under low pH but at a cost of muscle tissue loss.

Phenotypic responses to ocean acidification, such as changes in behavior and altered rates of development, growth and calcification, are all controlled by physiological processes at a cellular level. The past decade of ocean acidification research has shown that phenotypic responses vary widely across taxonomic groups and species and sometimes exhibit neutral or even positive effects (Kroeker et al. 2013; Kroeker et al. 2010). Identifying a common root driver of these phenotypic effects will improve our understanding of the limits of tolerance and adaptation potential to future ocean acidification. In temperature studies, a field much older than that of ocean acidification, the heat shock response system (HSRS) has been identified as a universal key physiological process involved in the response of organisms to environmental stressors (Lindquist 1986). Discovery of the HSRS has become the foundation for field and laboratory experiments assessing thermal adaptation (Feder and

Hofmann 1999) and provides insight to biogeographic limits and evolution (e.g. Hofmann et al. 2005). Identification of a similar unifying physiological mechanism that controls the diversity of responses to ocean acidification among marine species and lends insight the potential for pH adaptation could similarly propel ocean acidification research forward.

There are two main routes by which ocean acidification impacts marine biota. First, reduced seawater pH reduces calcium carbonate saturation states facilitating the dissolution of exposed biogenic $CaCO_3$, as described above. Second, CO_2 molecules can enter cells through passive diffusion and alter the chemical environment of the cell (i.e. reducing pH). Cell membranes are permeable to small neutral molecules including CO_2. Once diffused, CO_2 is hydrolyzed to produce charged molecules: HCO_3^- and H^+, causing acidosis in extra- and intracellular spaces. Ion concentrations, especially H^+, are tightly controlled through energetically costly transmembrane ion transport and exchange proteins in order to maintain functional physiological homeostasis (Dubyak 2004; Pörtner 2005; Reipschlager and Pörtner 1996). Changes in cellular pH influence acid-base regulation, metabolism, and overall cellular energy allocations and expenditure (Pörtner 2005; Reipschlager and Pörtner 1996). At low pH, increasing energy allocation to restore chemical homeostasis might divert energy away from growth or reproduction. For example, larval clown fish exhibit detrimental olfactory preferences under high pCO_2 exposure (Munday et al. 2009). Nilsson et al. (2012) found that high pCO_2 indirectly causes a reversal of neurotransmitter function in these larvae due to increased HCO_3^- concentrations as a product of acid-base compensation, thereby affecting olfactory responses. As such, the regulatory mechanism of acid-base balance is a proposed unifying principle by which ocean acidification affects marine organisms (Fabry et

al. 2008; Melzner et al. 2009; Pörtner 2005; Pörtner 2008; Seibel and Walsh 2003; Widdicombe and Spicer 2008).

Modes of acid-base balance and compensation can vary from tissue type to taxonomic level. Previous studies on acidosis show that organisms are largely successful at maintaining intracellular pH (pH_i) but that maintenance of extracellular pH (pH_e) is variable among organisms (Gutowska et al. 2010; Michaelidis et al. 2005; Miles et al. 2007; Spicer et al. 2011; Thomsen et al. 2010). For example, cephalopods are able to compensate pH_e (Gutowska et al. 2010) while mussels (Michaelidis et al. 2005) and sea urchins (Miles et al. 2007; Spicer et al. 2011) are less competent. Along with different modes of calcification (e.g. aragonite vs. calcite), species-specific strategies of maintaining acid-base equilibrium may in part explain the wide range of phenotypic responses to ocean acidification among marine organisms.

2. A note on multiple stressors

In addition to ocean acidification, the global ocean is warming (Rhein et al. 2013). Ocean warming and acidification affect the physiology of marine species differently and such effects can also be highly species-specific. In general, biological reactions and processes speed up with increasing temperature up to a thermal threshold (Hochachka and Somero 1984). For example, sea urchin larvae will develop at a faster rate at 18°C compared to 14°C. Multi-stressors scenarios, where both temperature and CO_2 are considered in synergy, often exacerbate the effects of a single stressor, whether positive or negative (Harvey et al. 2013). In some cases, positive effects of warming (e.g. increased growth) can actually offset some negative effects of CO_2 (e.g. decrease growth of sea urchin larvae, (Byrne 2011). Just as it is necessary to incorporate environmental pH levels into

experimental biology, temperature should also be considered. Therefore, in the biological portions of this dissertation, temperature and pH combinations are considered synergistically and outlined in the chapter introductions.

E. Dissertation initiation

The overarching theme of this dissertation is the importance of environmental realism, such as considering ocean pH variability, in the context of global change biology. Given that IPCC projections of ocean pH are based on open ocean data and models, these thresholds for ocean acidification may not be relevant for coastal species. Previous studies have shown that the magnitude of pH change predicted for the coming century influence animal physiology. These studies, however, often utilize stable pH exposures without the context of the organism's pH history. The goal of my dissertation is to characterize pH-seascapes from vulnerable ecosystems (i.e. high-latitude, upwelling ecosystems) in order to generate baseline datasets necessary to improve experimental design. My multidisciplinary endeavor requires characterization of the (1) marine environment (i.e. oceanography) and (2) response of marine species to varying ocean conditions (i.e. physiology). Past and current environmental conditions influence the present-day assemblage of tolerances and adaptive potential of functional traits. Thus, throughout this dissertation, measures of ambient conditions are emphasized in corroboration with biological experiments addressing animal physiology (e.g. thermotolerance and gene expression) under present day and future conditions (Figure I-2). This body of work has been conducted in the two most sensitive coastal marine ecosystems to ocean acidification (Gruber et al. 2012) and represents case studies for this multidisciplinary research approach.

Figure I-2. Schematic of research framework. The past environment has shaped the physiological plasticity of organisms today. It is this current plasticity that will determine whether or not species will be able to acclimate to rapid environmental change in order to tolerate future conditions. Current plasticity can be assessed it the context of current environmental conditions and future conditions with experimental manipulations.

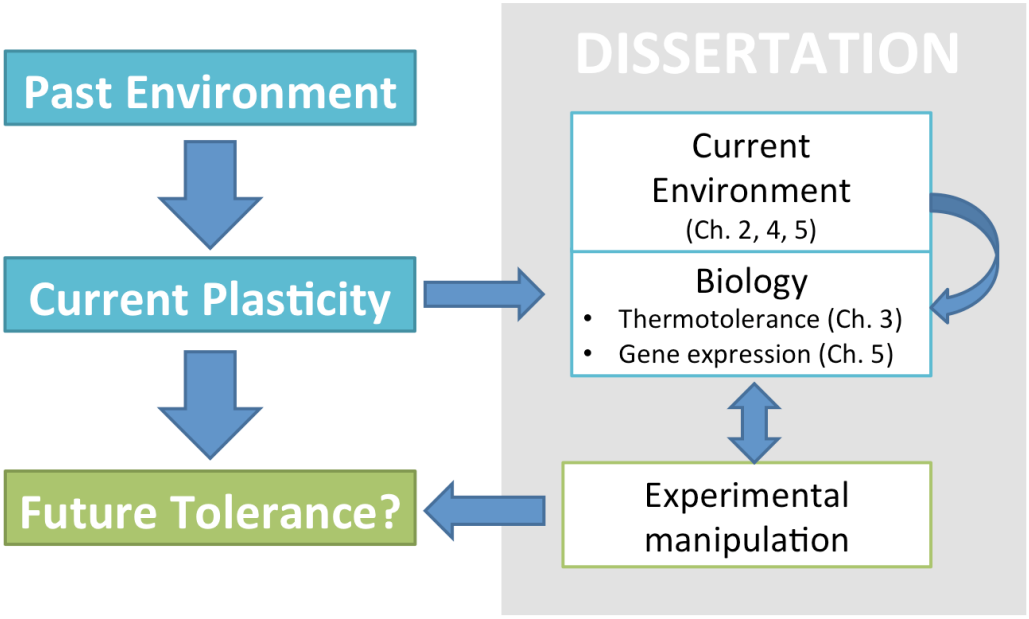

F. References

Bates, N. R., and A. J. Peters. 2007. The contribution of atmospheric acid deposition to ocean acidification in the subtropical North Atlantic Ocean. Mar. Chem. **107:** 547-558.

Berke, S. K., A. R. Mahon, F. P. Lima, K. M. Halanych, D. S. Wethey, and S. A. Woodin. 2010. Range shifts and species diversity in marine ecosystem engineers: patterns and predictions for European sedimentary habitats. Global Ecol. Biogeogr. **19:** 223-232.

Byrne, M. 2011. Impact of ocean warming and ocean acidification on marine invertebrate life history stages: vulnerabilities and potential for persistence in a changing ocean. Oceanogr. Mar. Biol. Annu. Rev. **49:** 1-42.

Caldeira, K., and M. E. Wickett. 2003. Anthropogenic carbon and ocean pH. Nature **425:** 365-365.

Cohen, A. L., D. C. Mccorkle, S. De Putron, G. A. Gaetani, and K. A. Rose. 2009. Morphological and compositional changes in the skeletons of new coral recruits reared in acidified seawater: Insights into the biomineralization response to ocean acidification. Geochemistry Geophysics Geosystems **10**.

Dickson, A. G., C. L. Sabine, and J. R. Christian. 2007. Guide to best practices for ocean CO_2 measurements. PICES Special Publication **3:** 191 pp.

Doney, S. C., V. J. Fabry, R. A. Feely, and J. A. Kleypas. 2009. Ocean acidification: the other CO_2 problem. Ann. Rev. Mar. Sci. **1:** 169-192.

Dore, J. E., R. Lukas, D. W. Sadler, M. J. Church, and D. M. Karl. 2009. Physical and biogeochemical modulation of ocean acidification in the central North Pacific. Proc. Natl. Acad. Sci. **106:** 12235-12240.

Dubyak, G. R. 2004. Ion homeostasis, channels, and transporters: an update on cellular mechanisms. Advances in Physiology Education **28:** 143-154.

Dupont, S., N. Dorey, M. Stumpp, F. Melzner, and M. Thorndyke. 2013. Long-term and trans-life-cycle effects of exposure to ocean acidification in the green sea urchin *Strongylocentrotus droebachiensis*. Mar. Biol. **160:** 1835-1843.

Egleston, E. S., C. L. Sabine, and F. M. Morel. 2010. Revelle revisited: buffer factors that quantify the response of ocean chemistry to changes in DIC and alkalinity. Global Biogeochem. Cycles **24:** GB1002.

Fabry, V. J., B. A. Seibel, R. A. Feely, and J. C. Orr. 2008. Impacts of ocean acidification on marine fauna and ecosystem processes. ICES J. Mar. Sci. **65:** 414-432.

Feder, M. E., and G. E. Hofmann. 1999. Heat-shock proteins, molecular chaperones, and the stress response: evolutionary and ecological physiology. Annu. Rev. Physiol. **61:** 243-282.

Feely, R. A., C. L. Sabine, J. M. Hernandez-Ayon, D. Ianson, and B. Hales. 2008. Evidence for upwelling of corrosive "acidified" water onto the continental shelf. Science **320:** 1490-1492.

Feely, R. A. and others 2004. Impact of anthropogenic CO_2 on the $CaCO_3$ system in the oceans. Science **305:** 362-366.

Findlay, H. S., H. L. Wood, M. A. Kendall, J. I. Spicer, R. J. Twitchett, and S. Widdicombe. 2011. Comparing the impact of high CO_2 on calcium carbonate structures in different marine organisms. Mar. Biol. Res. **7:** 565-575.

Form, A. U., and U. Riebesell. 2012. Acclimation to ocean acidification during long-term CO_2 exposure in the cold-water coral *Lophelia pertusa*. Global Change Biol. **18:** 843-853.

Gattuso, J.-P. and others 2014. Free Ocean CO_2 Enrichment (FOCE) systems: present status and future developments. Biogeosciences **11:** 4057-4075.

González-Dávila, M., J. M. Santana-Casiano, M. J. Rueda, and O. Llinás. 2010. The water column distribution of carbonate system variables at the ESTOC site from 1995 to 2004. Biogeosci. Disc. **7:** 1995-2032.

Gruber, N., C. Hauri, Z. Lachkar, D. Loher, T. L. Frölicher, and G.-K. Plattner. 2012. Rapid progression of ocean acidification in the California Current System. Science **337:** 220-223.

Gutowska, M. A., F. Melzner, M. Langenbuch, C. Bock, G. Claireaux, and H. O. Pörtner. 2010. Acid-base regulatory ability of the cephalopod (*Sepia officinalis*) in response to environmental hypercapnia. Journal of Comparative Physiology B-Biochemical Systemic and Environmental Physiology **180:** 323-335.

Harvey, B. P., D. Gwynn-Jones, and P. J. Moore. 2013. Meta-analysis reveals complex marine biological responses to the interactive effects of ocean acidification and warming. Ecology and Evolution **3:** 1016-1030.

Hauri, C. and others 2009. Ocean acidification in the California Current System. Oceanography **22:** 60-71.

Hauri, C. and others 2013. Spatiotemporal variability and long-term trends of ocean acidification in the California Current System. Biogeosciences **10:** 193–216.

Hochachka, P. W., and G. N. Somero. 1984. Biochemical adaptation. Princeton: University Press Princeton.

Hofmann, G. E. and others 2014. Exploring local adaptation and the ocean acidification seascape – studies in the California Current Large Marine Ecosystem. Biogeosciences **11:** 1053-1064.

Hofmann, G. E., S. G. Lund, S. P. Place, and A. C. Whitmer. 2005. Some like it hot, some like it cold: the heat shock response is found in New Zealand but not Antarctic notothenioid fishes. J. Exp. Mar. Biol. Ecol. **316:** 79-89.

Hofmann, G. E. and others 2011. High-frequency dynamics of ocean pH: a multi-ecosystem comparison. PLoS One **6:** e28983.

Hönisch, B. and others 2012. The geological record of ocean acidification. Science **335:** 1058-1063.

IPCC. 2007a. Contribution of Working Group II to the Fourth Assessment Report of the Intergovernmental Panel on Climate Change. (eds.) ML Parry, OF Canziani, JP Palutikof, PJ van der Linden and CE Hanson. Cambridge University Press, Cambridge, United Kingdom and New York, NY, USA.

IPCC. 2007b. Contribution of Working Groups I, II and III to the Fourth Assessment Report of the Intergovernmental Panel on Climate Change Core Writing Team. (eds) RK Pachauri and A Reisinger. Geneva, Switzerland.

Kelly, M. W., J. L. Padilla-Gamiño, and G. E. Hofmann. 2013. Natural variation and the capacity to adapt to ocean acidification in the keystone sea urchin *Strongylocentrotus purpuratus*. Global Change Biol. **19:** 2536-2546.

Kroeker, K. J. and others 2013. Impacts of ocean acidification on marine organisms: quantifying sensitivities and interaction with warming. Global Change Biol. **19:** 1884-1896.

Kroeker, K. J., R. L. Kordas, R. N. Crim, and G. G. Singh. 2010. Meta-analysis reveals negative yet variable effects of ocean acidification on marine organisms. Ecol. Lett. **13:** 1419-1434.

Lindquist, S. 1986. The heat-shock response. Annu. Rev. Biochem. **55:** 1151-1191.

Martz, T. R., J. G. Connery, and K. S. Johnson. 2010. Testing the Honeywell Durafet® for seawater pH applications. Limnol. Oceanogr. Methods **8:** 172-184.

McElhany, P., and D. S. Busch. 2013. Appropriate pCO_2 treatments in ocean acidification experiments. Mar. Biol. **160:** 1807-1812.

McNeil, B. I., A. Tagliabue, and C. Sweeney. 2010. A multi-decadal delay in the onset of corrosive 'acidified' waters in the Ross Sea of Antarctica due to strong air-sea CO_2 disequilibrium. Geophys. Res. Lett. **37:** L19607.

Melzner, F. and others 2009. Physiological basis for high CO_2 tolerance in marine ectothermic animals: pre-adaptation through lifestyle and ontogeny? Biogeosciences **6:** 2313-2331.

Michaelidis, B., C. Ouzounis, A. Paleras, and H. O. Pörtner. 2005. Effects of long-term moderate hypercapnia on acid-base balance and growth rate in marine mussels *Mytilus galloprovincialis*. Mar. Ecol. Prog. Ser. **293:** 109-118.

Miles, H., S. Widdicombe, J. I. Spicer, and J. Hall-Spencer. 2007. Effects of anthropogenic seawater acidification on acid-base balance in the sea urchin *Psammechinus miliaris*. Mar. Pollut. Bull. **54:** 89-96.

Munday, P. L. and others 2009. Ocean acidification impairs olfactory discrimination and homing ability of a marine fish. Proc. Natl. Acad. Sci. **106:** 1848-1852.

Nilsson, G. E. and others 2012. Near-future carbon dioxide levels alter fish behaviour by interfering with neurotransmitter function. Nature Climate Change **2**.

Orr, J. C. and others 2005. Anthropogenic ocean acidification over the twenty-first century and its impact on calcifying organisms. Nature **437:** 681-686.

Pansch, C., A. Nasrolahi, Y. S. Appelhans, and M. Wahl. 2012. Impacts of ocean warming and acidification on the larval development of the barnacle Amphibalanus improvisus. J. Exp. Mar. Biol. Ecol. **420:** 48-55.

Parker, L. M., P. M. Ross, W. A. O'connor, L. Borysko, D. A. Raftos, and H.-O. Pörtner. 2012. Adult exposure influences offspring response to ocean acidification in oysters. Global Change Biol. **18:** 82-92.

Parmesan, C., and G. Yohe. 2003. A globally coherent fingerprint of climate change impacts across natural systems. Nature **421:** 37-42.

Pörtner, H.-O. and others 2014. Ocean systems, p. 411-484. *In* C. B. Field et al. [eds.], Climate Change 2014: Impacts, Adaptation, and Vulnerability. Part A: Global and Sectoral Aspects. Contribution of Working Group II to the Fifth Assessment Report of the Intergovernmental Panel on Climate Change. Cambridge University Press.

Pörtner, H.-O. 2005. Synergistic effects of temperature extremes, hypoxia, and increases in CO_2 on marine animals: from Earth history to global change. Journal of Geophysical Research **110**.

Pörtner, H.-O. 2008. Ecosystem effects of ocean acidification in times of ocean warming: a physiologist's view. Mar. Ecol. Prog. Ser. **373:** 203-217.

Reipschlager, A., and H. O. Pörtner. 1996. Metabolic depression during environmental stress: the role of extracellular versus intracellular pH in *Sipunculus nudus*. J. Exp. Biol. **199:** 1801-1807.

Rhein, M. and others 2013. Observations: Ocean. *In* T. F. Stocker et al. [eds.], Climate Change 2013: Contribution of Working Group I to the Fifth Assessment Report of the Intergovernmental Panel on Climate Change.

Ries, J. B. 2011. Skeletal mineralogy in a high-CO_2 world. J. Exp. Mar. Biol. Ecol. **403:** 54-64.

Root, T. L., J. T. Price, K. R. Hall, S. H. Schneider, C. Rosenzweig, and J. A. Pounds. 2003. Fingerprints of global warming on wild animals and plants. Nature **421:** 57-60.

Sabine, C. L. and others 2004. The oceanic sink for anthropogenic CO_2. Science **305:** 367-371.

Seibel, B. A., and P. J. Walsh. 2003. Biological impacts of deep-sea carbon dioxide injection inferred from indices of physiological performance. J. Exp. Biol. **206:** 641-650.

Shaw, E. C., B. I. McNeil, B. Tilbrook, R. Matear, and M. L. Bates. 2013. Anthropogenic changes to seawater buffer capacity combined with natural reef metabolism induce extreme future coral reef CO_2 conditions. Global Change Biol. **19:** 1632-1641.

Spicer, J. I., S. Widdicombe, H. R. Needham, and J. A. Berge. 2011. Impact of CO_2-acidified seawater on the extracellular acid-base balance of the northern sea urchin *Strongylocentrotus droebachiensis*. J. Exp. Mar. Biol. Ecol. **407:** 19-25.

Sunday, J. M., A. E. Bates, and N. K. Dulvy. 2012. Thermal tolerance and the global redistribution of animals. Nature Climate Change **2:** 686-690.

Thomsen, J. and others 2010. Calcifying invertebrates succeed in a naturally CO_2-rich coastal habitat but are threatened by high levels of future acidification. Biogeosciences **7:** 3879-3891.

Walther, G. R. and others 2002. Ecological responses to recent climate change. Nature **416:** 389-395.

Wethey, D. S., and S. A. Woodin. 2008. Ecological hindcasting of biogeographic responses to climate change in the European intertidal zone. Hydrobiologia **606:** 139-151.

Widdicombe, S., and J. I. Spicer. 2008. Predicting the impact of ocean acidification on benthic biodiversity: what can animal physiology tell us? J. Exp. Mar. Biol. Ecol. **366:** 187-197.

Wood, H. L., J. I. Spicer, and S. Widdicombe. 2008. Ocean acidification may increase calcification rates, but at a cost. Proceedings of the Royal Society of London B: Biological Sciences **275:** 1767-1773.

Yu, P. C., P. G. Matson, T. R. Martz, and G. E. Hofmann. 2011. The ocean acidification seascape and its relationship to the performance of calcifying marine invertebrates: Laboratory experiments on the development of urchin larvae framed by environmentally-relevant pCO_2/pH. J. Exp. Mar. Biol. Ecol. **400:** 288-295.

II. Near-shore Antarctic pH variability has implications for the design of ocean acidification experiments[2]

A. Abstract

Understanding how declining seawater pH caused by anthropogenic carbon emissions, or ocean acidification, impacts Southern Ocean biota is limited by a paucity of pH time-series. Here, we present the first high-frequency in-situ pH time-series in near-shore Antarctica from spring to winter under annual sea ice. Observations from autonomous pH sensors revealed a seasonal increase of 0.3 pH units. The summer season was marked by an increase in temporal pH variability relative to spring and early winter, matching coastal pH variability observed at lower latitudes. Using our data, simulations of ocean acidification show a future period of deleterious wintertime pH levels potentially expanding to 7 - 11 months annually by 2100. Given the presence of (sub)seasonal pH variability, Antarctic marine species have an existing physiological tolerance of temporal pH change that may influence adaptation to future acidification. Yet, pH-induced ecosystem changes remain difficult to characterize in the absence of sufficient physiological data on present-day tolerances. It is therefore essential to incorporate natural and projected temporal pH variability in the design of experiments intended to study ocean acidification biology.

[2] Published in *Scientific Reports*: Kapsenberg, L, AL Kelley, EC Shaw, TR Martz, and GE Hofmann. Near-shore Antarctic pH variability has implications for the design of ocean acidification experiments. Sci. Rep. **5**, 9638; DOI:10.1038/srep09638 (2015). Copyright: re-use permitted under License to Publish – Open Access Agreement for SREP-14-10902A.

B. Introduction

The extensive effects of ocean acidification, the systematic reduction of ocean pH due to the absorption of anthropogenic carbon dioxide (CO_2) by surface oceans (Doney et al. 2009), are predicted to be first observed in high-latitude seas (Orr et al. 2005). Cold waters of the Southern Ocean are naturally rich with CO_2, which results in low carbonate (aragonite and calcite) saturation states (Orr et al. 2005). As ocean acidification progresses, pH and aragonite saturation state (Ω_{arag}) will decrease and facilitate the dissolution of marine calcium carbonate. From a biological perspective, evolution in the absence of shell-crushing predators in the near-shore Antarctic has left many benthic biogenic calcifiers with relatively brittle shells (Aronson et al. 2007) that may be vulnerable to ocean acidification. Shell dissolution in live Southern Ocean pteropods, *Limacina helicina antarctica*, has already been observed in CO_2-rich upwelled waters ($\Omega_{arag} \approx 1$, Bednaršek et al. 2012). Antarctic marine biota is hypothesized to be highly sensitive to ocean acidification (Fabry et al. 2009), and predicting the impact of this anthropogenic process and the potential for future organismal adaptation is a research priority (Kennicutt et al. 2014).

To predict how future ocean acidification will affect any marine ecosystem, it is first necessary to understand present-day pH variability. In the Southern Ocean, there are strong seasonal cycles in carbonate chemistry (Gibson and Trull 1999; Roden et al. 2013; Takahashi et al. 2002) due to the temporal partitioning of summertime primary production and wintertime heterotrophy (Rivkin 1991). Summertime phytoplankton blooms regularly drive the partial pressure of CO_2 in seawater (pCO_2) well below atmospheric equilibrium and are the primary source for pCO_2 variability in the Southern Ocean (Takahashi et al. 2002). This seasonal carbonate chemistry cycle corresponds to a summertime pH increase of

0.06 units on a regional scale in the Southern Ocean (McNeil and Matear 2008) and as much as 0.6 units locally in Prydz Bay (Gibson and Trull 1999) and the Ross Sea (McNeil et al. 2010). The summertime pH increase (e.g. 0.6) can thus exceed the 0.4 pH unit magnitude of ocean acidification predicted for 2100 (IPCC 2013).

Future ocean carbonate chemistry remains challenging to predict due to other environmental processes and biological feedbacks (Riebesell et al. 2009). Southern Ocean aragonite undersaturation (approx. pH $\leq$ 7.9) is predicted to occur first during the winter season in the next 20 years (McNeil and Matear 2008). However, seasonal ice cover may delay the onset of ocean acidification thresholds by a few decades due to reduced air-sea gas exchange (McNeil et al. 2010). Likewise, decreasing seasonal ice cover, due to changes in wind and air temperature, are estimated to yield at least a 14% increase in primary production in the Ross Sea by 2100 (Smith et al. 2014). This could potentially increase pH and Ω_{arag} in summer. Furthermore, increased stratification in the future may result in phytoplankton community shifts (Smith et al. 2014). As an example, diatom communities dominate periods of highly stratified waters in the Ross Sea but drawdown less CO_2 compared to the dominant bloom algae *Phaeocystis antarctica* that proliferate in deeply mixed waters (Arrigo et al. 1999). Thus, seasonal changes in carbonate chemistry (for example, from primary production) may yield alternative scenarios for ocean acidification outcomes (Shaw et al. 2013). Currently, projections of ocean acidification for near-shore Antarctica are largely based on discrete sampling (McNeil and Matear 2008), which may not have detected sub-seasonal (e.g. daily, weekly) pH variability that could be important for biological processes.

Although ocean acidification is generally predicted to be deleterious to marine life, not all taxa and species respond similarly to future conditions (Kroeker et al. 2010). There is emerging evidence that an organism's pH-exposure history can influence its tolerance of ocean acidification. For example, Lewis et al. (2013) showed that an Arctic copepod species that experienced varied depth-dependent pH exposure was more tolerant of CO_2-acidified seawater treatments compared to another Arctic copepod species that experiences a smaller range in pH. Comprehensive characterization of the 'pH-seascape' is thus necessary to link CO_2-perturbation experiments with present-day and future organismal performance in the field. Such field time-series are sparse in near-shore Antarctica and are either extremely short (Kapsenberg and Hofmann 2014; Matson et al. 2011) or low in sampling frequency (Gibson and Trull 1999; McNeil et al. 2010; Roden et al. 2013).

In this study, our main goal was to describe pH variability experienced by organisms in near-shore Antarctica across seasonal transitions in an area with annual sea ice cover. In addition, we use the data to explore how pH variability and changes in seasonal CO_2 drawdown (as a proxy for changes in primary production) may impact future trajectories of ocean acidification in our study region.

C. Methods

1. Study sites and deployment.

Autonomous SeaFET pH sensors containing Honeywell DuraFET® electrodes (Martz et al. 2010) were deployed in the austral spring at two sites in separate years on subtidal moorings in near-shore east McMurdo Sound (Figure II-1). Two SeaFETs were deployed side-by-side in December 2011 at a site near McMurdo Station (the Jetty, -77.85115, 166.66425), and one SeaFET was deployed during November 2012 at Cape Evans (-

Figure II-1. **Map of pH sensor deployments in McMurdo Sound, Antarctica.** Sensors were deployed at the Jetty (J) in 2011 and at Cape Evans (CE) in 2012. Annual sea ice contour (marble color) approximates November conditions for 2011 (RISCO Rapid*Ice* Viewer). Mapping data are courtesy of the Scientific Committee on Antarctic Research, Antarctic Digital Database. Map was constructed in QGIS (Version 2.0.1) and sea ice contour was added using GIMP (Version 2.6.11).

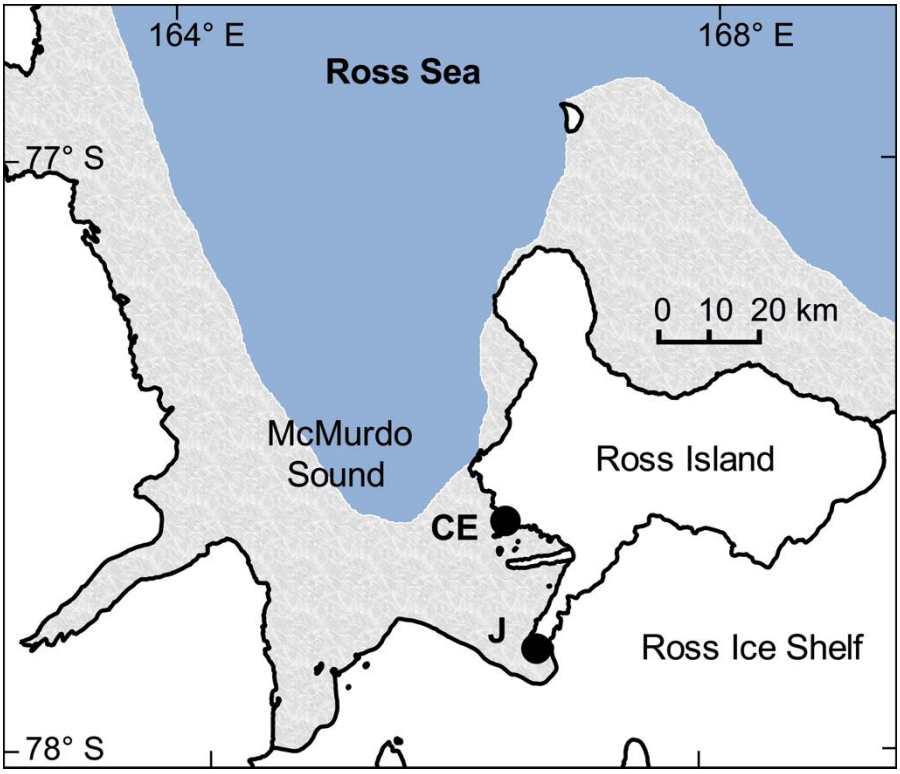

77.634617, 166.4159). Cape Evans is located 25 km north of the Jetty and is a highly productive site with an abundance of fish, macrophytes and marine invertebrates, including the sea urchin *S. neumayeri*. This site has previously been important for ocean acidification biology (Kapsenberg and Hofmann 2014; Yu et al. 2013). Subtidal moorings were anchored at approximately 27 m with sensor depth of 18 m. SeaFETs sampled on a two-hour frequency.

2. Calibration

All reported pH is on a total hydrogen ion scale and listed as 'pH'. Raw voltage recorded by the SeaFETs was converted to pH using one discrete seawater sample per sensor deployment following methods from Bresnahan et al. (2014). Calibration samples were collected via SCUBA following sensor conditioning to seawater within the first two weeks of each deployment, using a 5 L GO-FLO sampling bottle. Ideally, additional validation samples are collected throughout a sensor deployment. However, the remoteness of our sites restricted this work to one discrete sample per sensor deployment.

Calibration samples were preserved with saturated mercuric chloride according to Standard Operating Procedure (SOP) 1 (Dickson et al. 2007). Spectrophotometric pH was determined at 25 °C following SOP 6b (Dickson et al. 2007) using m-cresol purple from Sigma-Aldrich®. Total alkalinity (A_T) was measured via open-cell titration with a Mettler-Toledo T50 (SOP 3b, Dickson et al. 2007). Salinity was measured using a calibrated YSI 3100 Conductivity Instrument. Certified Reference Materials of seawater (CRMs) and acid titrant were supplied by Dr. Andrew G. Dickson (University of California San Diego, Scripps Institution of Oceanography). pH at in situ temperature was calculated from spectrophotometric measurements of $pH_{25\,°C}$ and A_T and salinity on the bottle sample using

the program CO2Calc (Robbins et al. 2010) with CO_2 constants from Mehrbach et al. (1973) refit by Dickson and Millero (1987). All reported carbonate system calculation we conducted according to these constants.

3. Data processing and analysis

Raw data from the SeaFETs were cropped based on battery exhaustion, which occurred before sensor recovery. One of the two sensors deployed at the Jetty failed quality control analyses, and data from this instrument is not reported. Inspections of raw voltages recorded by the functional SeaFETs confirmed that the calibration samples were collected after the period of sensor conditioning to seawater. In the absence of biofouling (as was the case for our sensors), sensor stability has been demonstrated over similar deployment times (Bresnahan et al. 2014) thereby generating high-quality pH datasets. A comparison of pH from each site was conducted using a Mann-Whitney Wilcoxon test, as pH values were not normally distributed (Minitab® 16, Kolmogorov-Smirnov test, $p < 0.10$, for each site). All time is reported as UTC.

Time-series carbonate parameters were calculated from pH measurements using CO2calc for a depth of 18 m. Monthly mean salinity data was used from prior measurements in McMurdo Sound (Littlepage 1965, Table II-1). A_T was calculated from the empirical relationship between sea surface salinity (SSS) and sea surface temperature (SST, as measured by SeaFETs) for the Southern Ocean as reported by Lee et al. (2006):

$$A_T = 2305 + 52.48 \times (SSS - 35) + 2.85 \times (SSS - 35)^2 - 0.49 \times (SST - 20) + 0.086 \times (SST - 20)^2 \quad (1)$$

Table II-1. Model inputs for seasonally variable parameters. See Methods for details.

Month	pH	Temp. (°C)	Salinity (Littlepage 1965)	Total Alkalinity (μmol kgSW^{-1}) ∞	Total PO4 (μmol kgSW^{-1})	Total Si (μmol kgSW^{-1})
*Nov**	8.01	-1.9	34.82	2348	1.9 (Barry 1988; Gordon et al. 2000; Noble et al. 2013; Rivkin 1991)	65.1 (Gordon et al. 2000; Rivkin 1991)
Dec	8.09	-1.6	34.76	2343	1.3 (Gordon et al. 2000; Rivkin 1991; Smith et al. 2003)	62.1 (Gordon et al. 2000; Rivkin 1991; Smith et al. 2003)
Jan	8.21	-1.0	34.65	2335	0.9 (Gordon et al. 2000; Rivkin 1991; Smith et al. 2003)	50.7 (Gordon et al. 2000; Rivkin 1991; Smith et al. 2003)
Feb	8.17	-1.1	34.37	2322	1.3 (Smith et al. 2003)	54.5 (Smith et al. 2003)
Mar	8.13	-1.6	34.44	2327	1.5 (Gordon et al. 2000)	70.5 (Gordon et al. 2000)
Apr	8.08	-1.8	34.50	2331	2.1 (McNeil et al. 2010)	78.9 (McNeil et al. 2010)
May	7.99	-1.9	34.62	2337	2.1 (McNeil et al. 2010)	78.9 (McNeil et al. 2010)
*Jun**	7.93	-1.9	34.69	2341	2.1 (McNeil et al. 2010)	78.9 (McNeil et al. 2010)
*mean**	8.05	-1.6	34.65	2335	1.6	67.5
*min**	7.90	-1.9	34.62	2337	2.1	78.9
max[§]	8.40	-0.4	34.61	2336	0.9	50.7

* pH and temperature data from Cape Evans only, based on data collected in this study and in Hofmann et al. (2011), Kapsenberg and Hofmann (2014), Matson et al. (2014)

[§] pH and temperature data from the Jetty only

∞ Calculated from salinity and temperature (Lee et al. 2006)

A_T measurements on SeaFET calibration samples matched the calculated A_T within the accuracy of titrator (A_T and salinity were 2342 μmol $kgSW^{-1}$ and 34.3 for the Jetty; 2351 μmol $kgSW^{-1}$ and 34.6 for Cape Evans, respectively). Monthly mean nutrient concentrations were estimated from the literature for McMurdo Sound and various Ross Sea stations in close proximity following the directions of ocean currents (max measurements $month^{-1}$ = 4). Due to the lack of published phosphate measurements for this region, the Redfield ratio was applied to estimate phosphate from nitrate and silicic acid concentrations, in some cases (W. O. Smith, Jr. pers. comm.).

Summertime decrease in DIC was calculated for both sites from stable fall mean DIC conditions to minimum DIC observed in summer. Temperature and pH data were analyzed for event-scale to seasonal (10-day low-pass filter) and short-term (10-day high-pass filter) trends. Standard deviation of a 10-day moving average window on high-pass filtered data was calculated to describe seasonal changes in short-term pH and temperature variability. Unfiltered and 10-day high-pass filtered pH and temperature data from the duration of the entire deployment was investigated for each site using a linear correlation analysis (Matlab R2012b, Minitab® 16).

4. Error estimates

SeaFET thermistors were not individually calibrated resulting in a maximum estimated temperature error of ~0.3 °C. The estimate of the combined standard uncertainty associated with the pH measurement of the calibration samples is ± 0.026 pH units (quadratic sum of partial uncertainties). The quantified sources in pH error are: use of unpurified m-cresol dye (0.02, Liu et al. 2011), spatio-temporal mismatch of the calibration sample (± 0.015, Bresnahan et al. 2014), user differences (± 0.006), and use of an uncalibrated SeaFET

thermistor with ± 0.03 °C error (± 0.005 pH). Measurements of spectrophotometric pH on CRMs, although not specified by the SOP, suggest that our bench top methods may underestimate $pH_{25°C}$ by 0.032 (± 0.006, n = 18, across different users and days) relative to theoretical CRM pH calculated from DIC, A_T, and salinity. It is hoped that, in the future, purified indicator dye will become widely available to the oceanography community in order to improve accuracy of pH measurements. The estimated uncertainty for the pH of calibration samples does not impact the relative changes in pH recorded by the SeaFET on hourly to monthly time scales, which in the absence of biofouling can be resolved to better than 0.001. Thermistors provide a stable temperature reading with resolution of better than 0.01 °C. Based on replicate analyses of CRMs, the precision of the titration system used for calibration samples is ± ≤10 μmol $kgSW^{-1}$ and did not impact the pH calculation of our calibration samples at in situ temperatures. Errors in salinity were not quantified. Instead, calculations of DIC, pCO_2, and Ω_{arag} from the pH time-series were conducted using monthly estimates of A_T and salinity (Table II-1). For reference, a +0.026 pH error corresponds to errors under November (January) conditions of -9 (-11) μmol $kgSW^{-1}$ DIC, -27 (-17) μatm pCO_2, and +0.07 (+0.10) Ω_{arag}.

5. Ocean acidification scenarios

Representative Concentration Pathway 8.5 (RCP8.5), which predicts atmospheric CO_2 to reach 935.87 ppm by 2100 (Riahi et al. 2007), was used to generate four ocean acidification scenarios. The equilibrium scenario assumes an increase in DIC at the same rate as would be expected if seawater pCO_2 tracks the atmospheric value (~100 μmol $kgSW^{-1}$ increase in DIC by 2100) and (2) the disequilibrium scenario assumes a DIC increase at a 65% slower rate due to seasonal ice cover (McNeil et al. 2010). Secondary simulations of a ± 20% change in

the observed seasonal amplitude of DIC are included along with the CO_2 forcing scenarios. The disequilibrium model likely overestimates pH and Ω_{arag}, as horizontal advection of northern ice-free water masses with longer surface residence times was not accounted for (McNeil et al. 2010).

First, November was used as a baseline for CO_2 forcing scenarios because it is a period of stable pH and has been measured for three consecutive years at Cape Evans (Hofmann et al. 2011; Kapsenberg and Hofmann 2014; Matson et al. 2014). Based on these prior studies and data collected in November 2012 during this study, mean November pH from 2010-2012 was pH 8.01. Calculated mean November seawater pCO_2 was then forced with pCO_2 from the RCP8.5 emission scenario assuming air-sea equilibrium, and annual changes in pCO_2 were used to calculate annual changes in November DIC up to 2100.

Second, monthly mean pH and temperature observations from the Jetty and Cape Evans from 2011-2013 were averaged to calculate a partial (8-month), present-day, regional DIC climatology. Calculations were performed in CO2calc following methods listed above, with the exception that monthly mean temperature in June at Cape Evans was corrected from -2.0 °C up to -1.9 °C to match previous long-term observations (Cziko et al. 2014). Input variables are listed in Table II-1. Starting from the November baseline, present-day changes in DIC where calculated by month (December – June) and for the maximum and minimum observed DIC and overall mean. Monthly changes in DIC were assumed constant for future projections and were applied to end-century November DIC to generate a DIC climatology for 2100. Annual DIC trajectories were modeled for observed minimum and maximum DIC, November, January, June, and overall mean. For simulations of ± 20% change in seasonal DIC amplitude, monthly changes in DIC were increased or decreased by 20%. Owing to the

lack of projections of future warming for coastal Antarctica, the effects of future temperature change were not included in our simulation.

D. Results

1. pH data

To collect high-resolution pH data, we deployed autonomous SeaFET pH sensors (Martz et al. 2010) in the austral spring at two sites in near-shore McMurdo Sound, Jetty and Cape Evans, on subtidal moorings in separate years (Figure II-1). Both the Jetty and Cape Evans showed four general sequences of pH variation during the observed period (Figure II-2a, II-2b; Table II-1). First, pH (reported on the total hydrogen ion scale for all measurements) rapidly increased from approximately 8.0 to 8.3 units in the early austral summer from December to January. Second, monthly pH variability from December through April (s.d. ± 0.03 to 0.08 units) was higher than that observed in November (s.d. ± 0.01 units). The increase in short-term pH variability remained after removing low-frequency pH variability that was inherently included in the monthly standard deviations listed in Table II-2. Standard deviation of the 10-day moving average of high-pass filtered pH data was greater during the summer months relative to November, May, and June and peaked in January at both sites (<0.05 pH units, Figure II-3a, II-3b). Third, following peak pH in January, pH and short-term pH variability generally declined to the end of April, but remained higher than November and early-December conditions. Fourth, around the onset of 24 h darkness at the end of April and during stabilized temperature pH declined and was followed by lower mean monthly pH and variability in May (s.d. ± 0.02 units) and in June (s.d. ± 0.01 units) relative to summer months. The initial pH increase from fall to peak January conditions

Figure II-2. pH and temperature cycles in McMurdo Sound, Antarctica. Time-series pH (a, b) and temperature (c, d) at the Jetty and Cape Evans as recorded by SeaFET pH sensors (grey line). A 10-day low-pass filter (10-d LPF) was applied to the pH and temperature observations (blue line). Daylight is noted by colored x-axis bars where 'sunsets' indicates decreasing day length. Arrows indicate anecdotal events of phytoplankton blooms as observed by United States Antarctic Program SCUBA divers. Calibration samples are noted (circle). Ticks on x-axes denote the first day of the month.

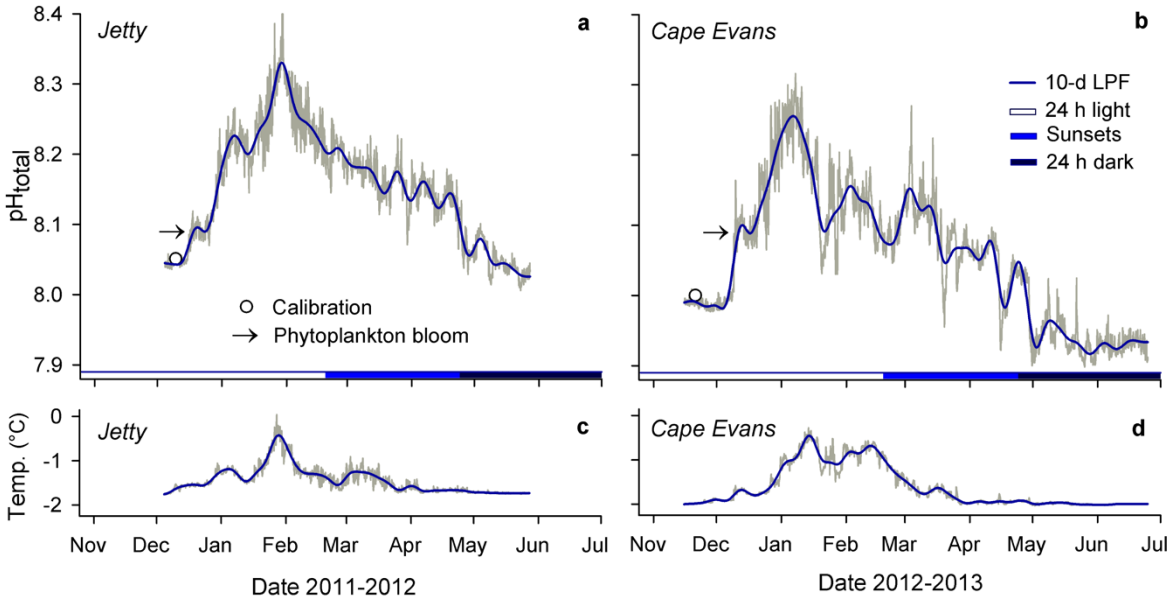

Table II-2. Carbonate parameters at two sites in McMurdo Sound, Antarctica.

Site, year		pH	T (°C)	DIC (μmol kgSW^{-1})*	pCO_2 (μatm)*	Ω_{arag}*
Jetty	*mean*	8.15 ± 0.08	-1.45 ± 0.31	2179 ± 37	302 ± 62	1.68 ± 0.29
2011-2012	*median*	8.16	-1.50	2177	292	1.66
	min	8.01	-1.80	2058	152	1.22
	max	8.40	0.00	2238	428	2.81
	range	0.40	1.80	181	276	1.60
	Dec	8.08 ± 0.04	-1.54 ± 0.14	2216 ± 17	355 ± 36	1.45 ± 0.14
	Jan	8.24 ± 0.05	-1.08 ± 0.36	2142 ± 26	236 ± 31	2.03 ± 0.23
	Feb	8.23 ± 0.04	-1.28 ± 0.25	2138 ± 17	241 ± 23	1.95 ± 0.16
	Mar	8.17 ± 0.03	-1.42 ± 0.19	2170 ± 10	286 ± 19	1.70 ± 0.09
	Apr	8.12 ± 0.04	-1.67 ± 0.05	2191 ± 14	319 ± 31	1.55 ± 0.11
	May	8.05 ± 0.02	-1.73 ± 0.01	2224 ± 7	387 ± 20	1.33 ± 0.06
Cape Evans	*mean*	8.05 ± 0.10	-1.63 ± 0.47	2218 ± 39	391 ± 92	1.37 ± 0.30
2012-2013	*median*	8.06	-1.90	2216	372	1.36
	min	7.90	-2.04	2107	192	0.96
	max	8.32	-0.27	2276	559	2.34
	range	0.42	1.77	168	367	1.39
	Nov	7.99 ± 0.01	-1.96 ± 0.0	2256 ± 2	450 ± 6	1.17 ± 0.01
	Dec	8.09 ± 0.08	-1.73 ± 0.2	2212 ± 30	349 ± 67	1.49 ± 0.25
	Jan	8.17 ± 0.07	-0.90 ± 0.3	2170 ± 29	285 ± 53	1.79 ± 0.25
	Feb	8.11 ± 0.04	-0.96 ± 0.3	2183 ± 15	327 ± 31	1.56 ± 0.12
	Mar	8.1 ± 0.05	-1.75 ± 0.1	2198 ± 18	342 ± 42	1.46 ± 0.15
	Apr	8.03 ± 0.04	-1.95 ± 0.0	2225 ± 14	403 ± 44	1.27 ± 0.10
	May	7.94 ± 0.02	-1.99 ± 0.0	2262 ± 7	508 ± 29	1.04 ± 0.05
	Jun	7.93 ± 0.01	-2.00 ± 0.0	2268 ± 3	518 ± 18	1.03 ± 0.02

Error is ± s.d.
*Calculated parameter

Figure II-3. Seasonal increase in short-term pH and temperature variability. High-pass filtered pH (a, b) and temperature (c, d) at the Jetty and Cape Evans (10-day, 10-d HPF). Blue lines are the s.d. of a 10-day moving average on the high frequency data (grey line). Daylight is noted by colored x-axis bars.

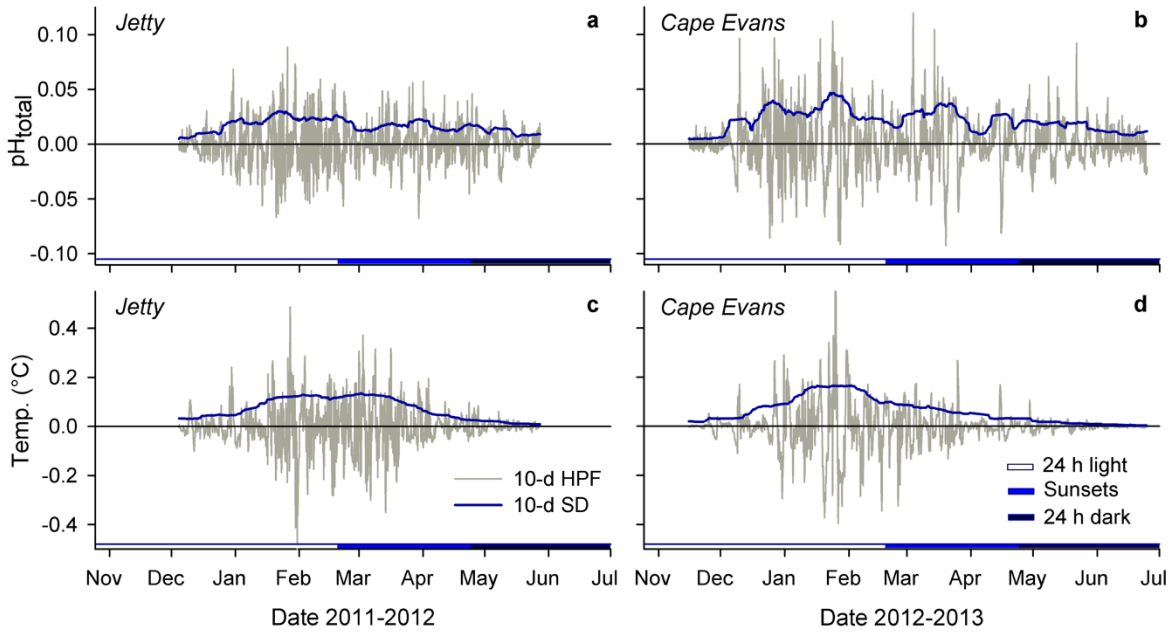

corresponded to a decline in the calculated dissolved inorganic carbon (DIC) of 167 and 137 μmol kgSW^{-1} at the Jetty (54 days) and Cape Evans (31 days), respectively.

The seasonal pH range was 0.30 and 0.33 pH units for the Jetty and Cape Evans, respectively (Figure II-1a, II-1b), based on a 10-day low-pass filter. Short-term pH variability contributed to a total range of observed pH from summer to winter conditions of 0.40 and 0.42 units, at the Jetty and Cape Evans, respectively. Maximum pH was observed in January and minimum pH was observed in May at both sites. Mean pH differed between the Jetty and Cape Evans when comparing pH observations of the same date range (8.15 ± 0.08 at the Jetty ; 8.08 ± 0.09 at Cape Evans; Mann-Whitney Wilcoxon test, $p < 0.001$, $W = 3481992$, $n = 2103$). In general, summertime sub-seasonal (Figure II-2a, II-2b) and short-term pH variability (Figure II-3a, II-3b) was greater at Cape Evans in 2013 compared to the Jetty in 2012. Changes in pH of ± 0.13 units occurred various times over the course of hours to a day at Cape Evans. The largest pH change over a relatively short period was -0.27 units over 5.5 days in March at Cape Evans.

Within the same site, temperature data showed similar patterns in variability as pH: temperature increased from the start of the recording period, peaked in January, after which it declined and stabilized in early April to similar temperatures observed in November and early December (Figure II-2c, 2d). Low-pass filtered data show a seasonal warming of 1.33 °C and 1.55 °C at the Jetty and Cape Evans, respectively. Like pH, high-pass filtered temperature data showed a seasonal increase in short-term variability from January through April (Figure II-3d, 3d). Absolute seasonal temperature change was 1.8 °C and 1.7 °C at the Jetty and Cape Evans, respectively.

At both the Jetty and Cape Evans, temperature was significantly and positively correlated with pH over the deployment period ($p < 0.001$; Table II-3), opposing the thermodynamic relationship. High-pass filtered temperature was significantly correlated with pH at both sites (Table II-3), but the direction of this relationship was different at both sites and explains little of the overall pH variation (< 5 %, Table II-3).

When used for carbonate calculations (DIC, pCO_2, Ω_{arag}), pH data indicate that McMurdo Sound is currently supersaturated with respect to aragonite (Table II-2). Monthly mean Ω_{arag} in late fall and early winter approached 1. Conditions may have actually reached undersaturation (Ω_{arag} <1) for brief periods at Cape Evans in May and June (minimum of Ω_{arag} 0.96), depending on the error in pH measurements (see Methods).

2. Ocean acidification scenarios

McMurdo Sound regional ocean acidification trajectories were made using averaged pH observations from 2011-2013 and forced with the Representative Concentration Pathway 8.5 (RCP8.5) CO_2 emission scenario (Riahi et al. 2007). Due to the potential offset in pH measurements associated with use of unpurified m-cresol dye (~0.03 pH units, see Methods), our results may slightly overestimate acidification trends. The equilibrium scenario, which represents an increase in seawater pCO_2 that tracks atmospheric levels, predicted more extreme acidification than the disequilibrium scenario, which represents a 65% reduced CO_2 uptake due to seasonal ice cover (Figure II-4, II-5).

In both scenarios, CO_2 forcing increased the seasonal pH amplitude and reflects the process of reduced ocean buffer capacity as CO_2 is absorbed (Egleston et al. 2010). For example, present-day range of observed monthly mean pH from January to June was 0.28 units and increased to 0.31 and 0.35 units under the disequilibrium and equilibrium scenario,

Table II-3. Linear regression analysis of pH and temperature.

Site	Predictor	Coef	SE Coef	*T*	*p*	R^2
Jetty	*Temperature*	0.20526	0.00358	57.27	<0.001*	0.61
	Temperature 10-d HPF	-0.04749	0.00453	-10.49	<0.001*	0.05
Cape Evans	*Temperature*	0.14985	0.00275	54.51	<0.001*	0.53
	Temperature 10-d HPF	0.02912	0.0058	5.02	<0.001*	0.01

*Statistically significant
10-d HPF, 10-day high-pass filtered data

respectively. For all scenarios, wintertime pH of ~7.9 (approximate aragonite undersaturation) occurred by the end of the century (Figure II-4, II-5). Assuming that pH < 7.9 persists for the period that we lack data for (July through October), the disequilibrium and equilibrium models suggest a 7- and 11-month annual duration of pH conditions < 7.9 units and undersaturation by 2100, respectively.

As a proxy for simulating changes in net community production, DIC amplitude was perturbed by ± 20% (Figure II-4). A 20 % increase in seasonal DIC amplitude raised pH and Ω_{arag} during the summer and fall but failed to raise pH and Ω_{arag} to present-day levels. For example, under the equilibrium model, a 20 % increase in seasonal DIC amplitude marginally extended end-century duration of summertime pH > 7.9 from January (pH 7.93, Ω_{arag} 1.07) to January (pH 7.99, Ω_{arag} 1.21) and February (pH 7.93, Ω_{arag} 1.05).

Any reduction in the amplitude of seasonal DIC will exacerbate the effects of ocean acidification. For example, during the month of peak pH, mean January pH remained above 7.9 units in all scenarios, except under the equilibrium scenario with a simulated 20% reduction in seasonal DIC amplitude (January pH 7.87, Figure II-4). This latter scenario was the only scenario that exhibited permanent aragonite undersaturation in McMurdo Sound by 2100.

Due to the increase in pH variability observed during summer months (Figure II-3), organisms at our study sites will likely still periodically experience pH > 7.9 and Ω_{arag} > 1 by 2100 (Figure II-5). For instance, under the equilibrium scenario, maximum pH was pH 8.19, and 0.47 units above mean January conditions (pH 7.72). Acidification thresholds (pH ~7.9 and Ω_{arag} < 1) were crossed earlier under the equilibrium model compared to the disequilibrium model (Figure II-5). Here, onset of June (i.e. winter) undersaturation was

Figure II-4. Present-day and end-century pH and aragonite saturation state. Present–day (circle) and end-century monthly mean pH (a) and aragonite saturation state, Ω_{arag} (b), in McMurdo Sound, Antarctica, using a disequilibrium and equilibrium scenario (solid line). Within each scenario, a simulated 20% increase (upper dashed lines) and decrease (lower dashed lines) in seasonal DIC amplitude is used to simulated changes in net community production. Dotted lines reference pH 7.9 and Ω_{arag} of 1.

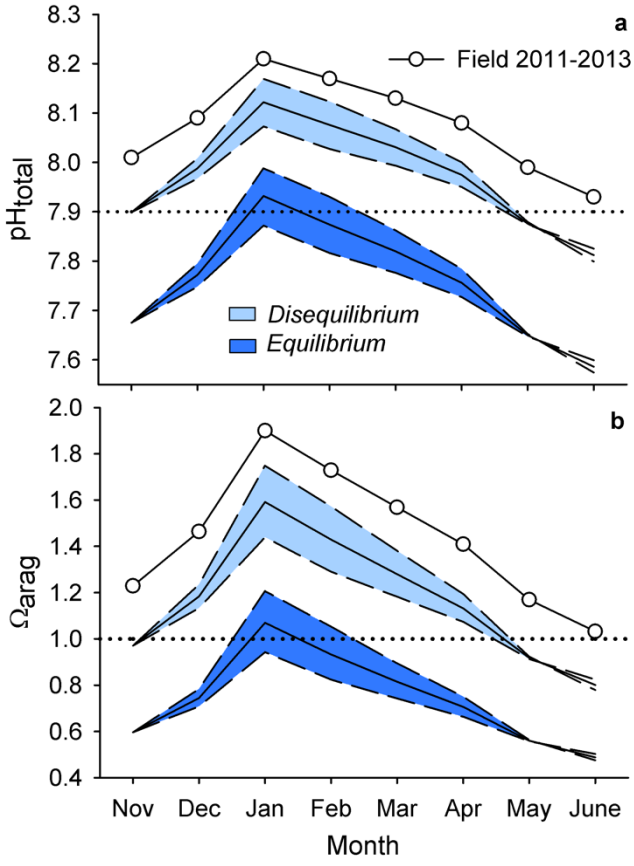

Figure II-5. Annual changes in pH and aragonite saturation state ranges. Projections of yearly changes in pH and aragonite saturation state, Ω_{arag}, in McMurdo Sound, Antarctica, using a disequilibrium (a, c) and equilibrium (b, d) scenario. Annual range in pH increases and Ω_{arag} decreases with future acidification. End-century maximum pH and Ω_{arag} remain above acidification thresholds of pH 7.9 and Ω_{arag} of 1. Projections are based on field data collected in 2011-2013 (circle). January and June monthly means represent mid-summer and winter conditions, respectively. The overall mean represent mean values from spring into winter conditions. Onset of aragonite undersaturation (triangles) is marked for each parameter and additionally for November monthly mean conditions.

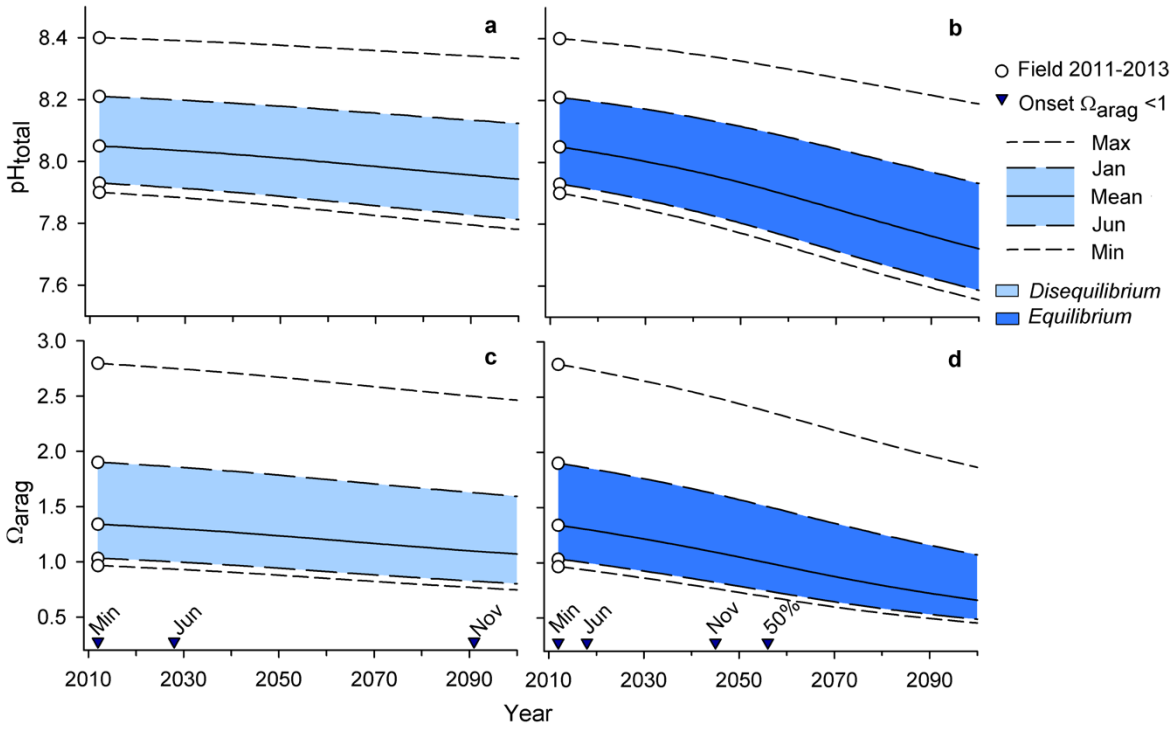

projected to occur by 2018, a decade earlier than under the disequilibrium scenario. November (i.e. spring) aragonite undersaturation was predicted to first occur by 2045 in the equilibrium model, 46 years earlier than predicted by the disequilibrium model. Timing of the threshold crossings may be delayed given the potential offset in Ω_{arag} associated with the pH measurement error.

E. Discussion

The observed pH regime in McMurdo Sound can be grouped into two seasonal patterns: (1) stable pH with low variability during the winter and spring, and (2) elevated pH with high variability during the summer and fall. While our pH sensors did not record data from July through October, previous studies of pH (in October, Matson et al. 2011) and temperature (Cziko et al. 2014) in this region support our hypothesis of low environmental variability during the winter. Note, observations from Prydz Bay (Roden et al. 2013) (68 °S) suggest that pH may decline slightly (<0.1 units) from June to September.

The amplitude of summertime pH elevation (0.3-0.4 units) observed in McMurdo Sound is among one of the greatest observed in the ocean and matches pH cycles at a northern coastal site in Prydz Bay, Antarctica (Gibson and Trull 1999; Roden et al. 2013). In McMurdo Sound, the intense summertime DIC drawdown started in December and matched the timing of the annually recurring *Phaeocystis* sp. phytoplankton blooms, which are well-described and typically centered on 10 December (R. Robbins pers. comm., Putt et al. 1994). The initial pH increase at Cape Evans (pH 8.01 to 8.12) occurred within 24 h on 9 December 2012 during which SCUBA divers noted sudden increase in phytoplankton presence in McMurdo Sound (R. Robbins pers. comm.).

Given that (1) the sudden increase in pH at our study sites followed a period of extremely stable pH conditions (Kapsenberg and Hofmann 2014; Matson et al. 2011), (2) maximum observed pH corresponded to pCO_2 ~200 μatm below atmospheric equilibrium, and (3) productive waters from the Ross Sea are advected south into east McMurdo Sound (Rivkin 1991), the initial rapid pH increase in December is likely the signature of phytoplankton blooms that originated in the Ross Sea and reached our coastal sites. Calculated DIC drawdown from fall to summer at the Jetty and Cape Evans (167 and 137 μmol $kgSW^{-1}$ DIC) matches the timing and magnitude of CO_2 cycles observed at similar depths in the Ross Sea (Sweeney 2003) and Prydz Bay (~135-200 μatm $kgSW^{-1}$ DIC, Gibson and Trull 1999; Roden et al. 2013).

Following the peak pH in January, pH steadily declined to pre-summer conditions by the end of April. A recent study of autonomous pCO_2 measurements on incoming seawater at Palmer Station from Arthur Harbor (64 °S) observed a summertime increase in primary production, starting in November (Tortell et al. 2014). Here, a phytoplankton bloom was captured with peak production corresponding to an observation of 50 μatm pCO_2. Contrary to the slow return of carbonate chemistry to pre-summer conditions observed in McMurdo Sound over 4-5 months, pCO_2 at Arthur Harbor rapidly returned to atmospheric equilibrium in December and persisted to the end of the study in March. The authors attributed the crash of the bloom to physical mixing and zooplankton grazing, which would control phytoplankton density and contribute respiratory CO_2. Depending on the year-to-year pH variability on the Antarctic Peninsula, the season of high pH in Arthur Harbor may potentially be much shorter compared to that in McMurdo Sound. For example, interannual carbonate chemistry variability in the Weddell Sea is linked to the timing of sea-ice melt and

phytoplankton productivity in the mixed layer (Weeber et al. 2015). The decline in pH observed at McMurdo is likely a combination of reduced primary production, increased heterotrophy and deepening of the mixed layer, as has been suggested to occur in Prydz Bay (Gibson and Trull 1999) and observed in other notable bloom regions such as the North Atlantic (Körtzinger et al. 2008).

Calculated pCO_2 at Cape Evans in April (403 ± 44 μatm) nears observations from the Ross Sea made in April 1997 (320-400 μatm, Takahashi et al. 2002). A stabilization of pH in May and June at Cape Evans corresponded to ~500 μatm pCO_2. We were unable to collect validation samples during this period, however, biofouling was not an issue at our sites and SeaFET pH sensors have been shown to maintain stability over >9 months (Bresnahan et al. 2014). Similar observations have been made elsewhere in near-shore Antarctica. For example, high pCO_2 (~490 μatm) was observed near the Dotson Ice Shelf in the Amundsen Sea Polynya in summer and was correlated with the deepening of the mixed layer relative to the surrounding area (Mu et al. 2014). In addition, the range of Ω_{arag} from mean summer (January) to winter (May) conditions was 0.70 and 0.75 at the Jetty and Cape Evans, respectively, matching the latest observations from Prydz Bay (0.73, Roden et al. 2013) and the Weddell Sea (0.77, Weeber et al. 2015). The low pCO_2 recorded in May and June at Cape Evans may thus be a combination of water column mixing and heterotrophy, as well as a potential 37 μatm pCO_2 overestimation associated with the offset of our pH measurement.

The observed ~0.3 unit summertime increase in pH in McMurdo Sound is much larger than of northern high-latitudes (Shadwick et al. 2013). While primary productivity in Antarctic waters is comparable to that of the high-latitude North Atlantic and Pacific (Takahashi et al. 2002), the observed < 2 °C annual temperature variation is typical of

McMurdo Sound (Cziko et al. 2014) and plays almost no role in the seasonal amplitude of pH (1.8 °C warming corresponds to a pH decrease of 0.03 units). In contrast, at locations such as the North Pacific the temperature cycle can be ~5 times greater than the observed range of temperatures in this study (Takahashi et al. 2002). At our sites, the seasonal temperature forcing on pH counteracts seasonal forcing by primary production. As a result, the absence of a significant temperature forcing in near-shore Antarctica leads to a more pronounced seasonal pH cycle with greater amplitude compared to other bloom regions in the world (Shadwick et al. 2013).

As captured in our dataset, the summer season in McMurdo Sound is marked by an increase in sub-seasonal and short-term pH variability from December through April. In terms of s.d. of unfiltered (monthly s.d.) and high-pass filtered (10-day s.d.) pH, pH variability in McMurdo Sound is of similar magnitude to that observed in temperate kelp forests (e.g. ± 0.043 - 0.111) and tropical coral reefs (e.g. ± 0.022) over 30 days (Hofmann et al. 2011). This is surprising due to absence of large temperature forcing and structural macrophytes and holobionts, which induce diurnal pH cycles at lower latitudes. On a Hawaiian reef, variability in pH was correlated with environmental parameters such as wave and height, wind speed, and solar radiation (Lantz et al. 2014), suggesting a combination of influential abiotic and biotic drivers on coastal seawater pH variability.

We did not directly measure abiotic and biotic factors that influence carbonate chemistry in our study region and more measurements would be needed to quantify the sources of variability over different frequencies. For instance, air-sea gas exchange contributes to pH on a seasonal timeframe, where summertime CO_2 uptake by the ocean during ice-free periods masks the total contribution of net community production to DIC drawdown

(Gibson and Trull 1999). Likewise, summer meltwater dilutes DIC and A_T (Gibson and Trull 1999; Roden et al. 2013) and may contribute to short-term pH variability in summer. The timing of sea ice melt onset may impact the duration and magnitude of carbonate chemistry seasonality where early melting enhances phytoplankton production under optimal mixed layer depths, as has been observed in the Weddell Sea (Weeber et al. 2015). Small pH variability (8.009 ± 0.015) observed from late October through November in McMurdo Sound may be explained by algal photosynthesis, although tides may play a small role as well (Matson et al. 2014). Tidal exchanges of shallow and deeper water masses could play a larger role in summer pH variability, compared to spring (Matson et al. 2014), when the water column is highly stratified (Barry 1988). Low pH variability observed in winter and spring could also stem from a decrease in respiratory CO_2 contributions to DIC due to metabolic depression during periods of low food availablity, as has been observed to occur in pteropods (Seibel et al. 2012). In contrast, increased pH variability during the summer and fall is potentially influenced by the dominant biological forcing on the carbonate system in the Ross Sea at that time (Takahashi et al. 2002). Such phytoplankton blooms create large spatial difference in pCO_2 (Mu et al. 2014) that could lead to sub-seasonal and short-term pH variability through bloom patchiness across water mass movement. Quantification of abiotic and biotic parameters described above would improve estimations for future ocean acidification when incorporated into sensitivity models (Shaw et al. 2013).

We explored how seasonal and pH variability may influence future ocean acidification in our study region in order to provide guidelines for biological experiments assessing future species' and ecosystem responses. The equilibrium and disequilibrium models provide boundaries for potential worst- and best-case acidification under a CO_2 emission scenario

that does not account for climate mitigation efforts (Riahi et al. 2007). Within all model parameters we employed, marine biota at our study sites are anticipated to experience changes beyond the envelope of current conditions, as has been predicted for lower latitude marine ecosystems as well (Shaw et al. 2013). As atmospheric CO_2 continues to increase, (1) pH and duration of summertime high pH (> 7.9) will decrease and (2) the magnitude of seasonal and short-term pH variability may increase.

Previous studies of ocean acidification in the Southern Ocean and the Ross Sea identify the importance of seasonality and predict onset of wintertime aragonite undersaturation ($\Omega_{arag} < 1$) between 2030 and 2050 under Intergovernmental Panel on Climate Change emissions scenario IS92a (McNeil and Matear 2008; McNeil et al. 2010; Orr et al. 2005). Our calculations of Ω_{arag} show wintertime undersaturation in McMurdo Sound occurring within this same timeframe, despite the higher CO_2 emission scenario and high-resolution data used in our study, and potential over estimation of acidification trends associated with the offset in pH measurements. Given that pH and Ω_{arag} may decrease slightly from June through September (Roden et al. 2013) and the lack of pH observations during these months, it is possible that periodic aragonite undersaturation may occur sooner than our predictions based on June observations. For context, the consequences of such periodic undersaturation could lead to calcium carbonate dissolution of live animals, as was observed for *L. helicina antarctica* at $\Omega_{arag} \approx 1$ (Bednaršek et al. 2012). Likewise, studies on Antarctic sea urchin, *Sterechinus neumayeri*, early development conducted during the period of stable spring pH and urchin spawning in McMurdo Sound, suggest that persisting conditions of pH < 7.9 (approximate aragonite undersaturation) may to impair larval growth (Yu et al. 2013) and calcification (G. E. Hofmann and P. C. Yu, unpubl.). Such conditions could occur in the

latter half of this century during the sea urchin spawning season. Future carbonate chemistry conditions will ultimately depend on the rate at which anthropogenic CO_2 is released to the atmosphere and any future changes in local physical and biological processes that our model does not account for (e.g. changes in temperature, meltwater, wind, mixing and stratification, upwelling, gas-exchange, and phytoplankton blooms).

Despite the dominant biological footprint in pH seasonality in the Southern Ocean, a 20% increase in seasonal DIC amplitude (simulating an increase in net community production) failed to raise pH to present-day levels at our study site. This suggests that relatively large changes in seasonal primary productivity may have small effect on the pH exposure of coastal organisms relative to the changes induced by ocean acidification. Phytoplankton blooms, as a food source however, may impact species responses to ocean acidification. For example, a study of *L. helicina antarctica* collected in McMurdo Sound found that (1) feeding history (e.g. weeks, months, seasons) impacted oxygen consumption rates and (2) metabolic suppression due to low pH exposure was a masked during periods of food limitation (Seibel et al. 2012). This study highlights the importance of incorporating environmental history when interpreting experimental results. As the feeding history is likely correlated with pH exposure in the bloom, parsing out the effects of pH history and food availability will present a challenge for Antarctic physiology.

In Antarctic ocean acidification biology, 'control' conditions used in experiments are often ~pH 8.0 (e.g. Cummings et al. 2011; Yu et al. 2013) and represent current spring conditions in McMurdo Sound. Based on our future projections, this 'control' treatment will only occur during summer months if at all. Regardless of the exact rate of ocean acidification, the seasonal window of pH > 7.9 and $\Omega_{arag} > 1$ will likely shorten in the future.

This shrinking and seasonally shifting window of high pH may lead to unpredictable ecological consequences through changes in physiological and seasonally dependent biological processes (e.g. sea urchin larval development). It remains largely unknown how summertime pH levels currently contribute to animal physiology and whether or not a reduction in future peak pH and duration of high pH exposure influences physiological recovery following 7-11 months unprecedented low pH conditions. As an example, oxygen consumption and gene expression of heat shock protein 70 in the Antarctic bivalve *Laternula elliptica* increased when adults were exposed to experimental conditions near the habitat maxima (pH 8.32, categorized as 'glacial levels' by the authors) and below their current pH exposure (pH 7.77), relative to performance at ~pH 8.0 (Cummings et al. 2011). These results suggest that summer exposures may induce stress similar to conditions predicted with ocean acidification. Understanding how organisms are adapted to their present-day exposures will help elucidate how they will respond to future conditions.

As the exposure period of pH > 7.9 shrinks under simulated ocean acidification, the magnitude of annual pH variability increases. These changes suggest that calcifying marine biota of Antarctic coastal regions will experience larger seasonal pH cycles in addition to exposure to lower environmental pH. Due to the reduced buffer capacity of the ocean under high CO_2, it is likely that the short-term pH variability in McMurdo Sound will be amplified in the future as well (Egleston et al. 2010). This has been predicted for coral reefs under ocean acidification scenarios (Shaw et al. 2013) and shown experimentally in pelagic field mesocosms (Schulz and Riebesell 2013) where primary production drives diurnal pH cycles.

Our results provide guidance for the design of biological experiments aimed to address the potential for Antarctic species to adapt to a seasonally shrinking window of future high

pH conditions. Although ocean acidification is likely to create an unprecedented marine environment, the existing presence of high pH variability in near-shore Antarctica may have beneficial implications for biological tolerance of ocean acidification. The distinct summertime increase in pH and pH variability in near-shore McMurdo Sound suggests that marine biota here have some capacity to deal with large fluctuations in the carbonate system, as has also been suggested by McNeil et al. (2011) in relation to the seasonal pH cycle. Unlike temperate upwelling regions where pH variability frequently drops below pH 8.0 (Hofmann et al. 2014), elevation of summer pH in McMurdo Sound opposes the direction of future ocean acidification. Future studies are necessary to describe how this pH-seascape may select for physiological tolerances of ocean acidification. For example, are natural positive (e.g. near-shore Antarctica) or negative deviations (e.g. temperate upwelling systems, Hofmann et al. 2014) from pH 8.0 important to tolerance of future acidification? Will high summertime pH prepare organisms for low pH conditions in the winter? What frequency of pH variability promotes acidification tolerance?

A few recent studies have tackled such questions in temperate regions with mixed results. For example, Frieder et al. (2014) found that larval growth of mussel *Mytilus galloprovincialis* veligers was reduced under low static pH but recovered under similar conditions of low mean pH when semi-diurnal pH variability was introduced. However, congener *M. californianus* did not exhibit this 'rescued' response with diurnal cycles (Frieder et al. 2014). Although the Southern Ocean does not experience year-round diurnal photoperiods, a similar experimental approach can be used to guide studies on the impact of pH seasonality on ocean acidification tolerance (Murray et al. 2014), and ultimately, adaptation.

We highlight a coupled oceanography and biology research strategy for studying ocean acidification biology in the Southern Ocean. Studying physiological tolerance and local adaptation to variable seawater chemistry ideally requires large differences in spatial and temporal pH variability (Hofmann et al. 2014; Hofmann et al. 2011). If patterns of pH variability differ spatially around the Antarctic continent (e.g. McMurdo Sound vs. Arthur Harbor, Tortell et al. 2014), we can begin to investigate possible levels of adaptation to local pH regimes as a proxy for evolutionary adaptions to future conditions (Sanford and Kelly 2011). In other words, evidence of adaptation in space suggests that animals may be able to adapt in time, as the capacity to do so is linked directly to standing genetic diversity in populations (Sunday et al. 2014). As illustrated in the Southern Ocean, population level differences (e.g. Ross Sea vs. Western Antarctic Peninsula biota) and local adaptation in tolerance of future anthropogenic stressors may be possible due to different rates in regional warming (Steig et al. 2009). Some studies have shown genetic structure across the biogeographic boundary of the Drake Passage (reviewed by Kaiser et al. 2013). Studies regarding population differences in pH tolerances and exposures in circum-Antarctic species can be accomplished with strategic placement of oceanographic sensors and design of biological experiments with environmentally relevant pH treatments (Hofmann et al. 2014; McElhany and Busch 2013). In addition, use of autonomous pH sensors would address the need for pH observations at high-latitudes (Fabry et al. 2009; Seibel et al. 2012).

F. Acknowledgements

We thank Dr. Paul G. Matson for sensor preparation in 2011 and United States Antarctic Program staff members, Rob Robbins and Steven Rupp, for SCUBA diving support. We thank Dr. Craig A. Carlson for insightful discussions. This research was supported by U.S.

National Science Foundation (NSF) grants ANT-0944201 and PLR-1246202 to GEH. LK was supported by a NSF Graduate Research Fellowship, and ALK was supported by the NSF Postdoctoral Fellowship in Polar Regions Research, award number ANT-1204181.

G. References

Aronson, R. B. and others 2007. Climate change and invasibility of the Antarctic benthos. Annu. Rev. Ecol. Evol. Syst. **38:** 129-154.

Arrigo, K. R. and others 1999. Phytoplankton community structure and the drawdown of nutrients and CO_2 in the Southern Ocean. Science **283:** 365-367.

Barry, J. 1988. Hydrographic patterns in McMurdo Sound, Antarctica and their relationship to local benthic communities. Polar Biol. **8:** 377-391.

Bednaršek, N. and others 2012. Extensive dissolution of live pteropods in the Southern Ocean. Nat. Geosci. **5:** 881-885.

Bresnahan, P. J. J., T. R. Martz, Y. Takeshita, K. S. Johnson, and M. Lashomb. 2014. Best practices for autonomous measurement of seawater pH with the Honeywell Durafet. Methods Oceangr. **9:** 44–60.

Cummings, V. and others 2011. Ocean acidification at high latitudes: potential effects on functioning of the Antarctic bivalve *Laternula elliptica*. PLoS One **6:** e16069.

Cziko, P. A., A. L. Devries, C. W. Evans, and C.-H. C. Cheng. 2014. Antifreeze protein-induced superheating of ice inside Antarctic notothenioid fishes inhibits melting during summer warming. Proc. Natl. Acad. Sci. **111:** 14583-14588.

Dickson, A. G., and F. J. Millero. 1987. A comparison of the equilibrium constants for the dissociation of carbonic acid in seawater media. Deep-Sea Res. I **34:** 1733-1743.

Dickson, A. G., C. L. Sabine, and J. R. Christian. 2007. Guide to best practices for ocean CO_2 measurements. PICES Special Publication **3:** 191 pp.

Doney, S. C., V. J. Fabry, R. A. Feely, and J. A. Kleypas. 2009. Ocean acidification: The other CO_2 problem. Ann. Rev. Mar. Sci. **1:** 169-192.

Egleston, E. S., C. L. Sabine, and F. M. Morel. 2010. Revelle revisited: Buffer factors that quantify the response of ocean chemistry to changes in DIC and alkalinity. Global Biogeochem. Cycles **24:** GB1002.

Fabry, V. J., J. B. McClintock, J. T. Mathis, and J. M. Grebmeier. 2009. Ocean acidification at high latitudes: The bellweather. Oceanography **22:** 160-171.

Frieder, C. A., J. P. Gonzalez, E. E. Bockmon, M. O. Navarro, and L. A. Levin. 2014. Can variable pH and low oxygen moderate ocean acidification outcomes for mussel larvae? Global Change Biol. **20:** 754–764.

Gibson, J. A., and T. W. Trull. 1999. Annual cycle of fCO_2 under sea-ice and in open water in Prydz Bay, East Antarctica. Mar. Chem. **66:** 187-200.

Gordon, L., L. Codispoti, J. Jennings Jr, F. Millero, J. Morrison, and C. Sweeney. 2000. Seasonal evolution of hydrographic properties in the Ross Sea, Antarctica, 1996-1997. Deep-Sea Res. II **47:** 3095-3117.

Hofmann, G. E. and others 2014. Exploring local adaptation and the ocean acidification seascape – studies in the California Current Large Marine Ecosystem. Biogeosciences **11:** 1053-1064.

Hofmann, G. E. and others 2011. High-frequency dynamics of ocean pH: a multi-ecosystem comparison. PLoS One **6:** e28983.

IPCC. 2013. Climate Change 2013: The Physical Science Basis. Contribution of Working Group I to the Fifth Assessment Report of the Intergovernmental Panel on Climate Change [Stocker, T.F., D. Qin, G.-K. Plattner, M. Tignor, S.K. Allen, J. Boschung, A. Nauels, Y. Xia, V. Bex and P.M. Midgley (eds.)]. Cambridge University Press, Cambridge, United Kingdom and New York, NY, USA, 1535 pp.

Kaiser, S. and others 2013. Patterns, processes and vulnerability of Southern Ocean benthos: a decadal leap in knowledge and understanding. Mar. Biol. **160:** 2295-2317.

Kapsenberg, L., and G. E. Hofmann. 2014. Signals of resilience to ocean change: high thermal tolerance of early stage Antarctic sea urchins (*Sterechinus neumayeri*) reared under present-day and future pCO_2 and temperature. Polar Biol. **37:** 967–980.

Kennicutt, M. C. and others 2014. Six priorities for Antarctic science. Nature **512:** 23-25.

Körtzinger, A. and others 2008. The seasonal pCO_2 cycle at 49°N/16.5°W in the northeastern Atlantic Ocean and what it tells us about biological productivity. J. Geophys. Res. **113:** C04020.

Kroeker, K. J., R. L. Kordas, R. N. Crim, and G. G. Singh. 2010. Meta-analysis reveals negative yet variable effects of ocean acidification on marine organisms. Ecol. Lett. **13:** 1419-1434.

Lantz, C., M. Atkinson, C. Winn, and S. Kahng. 2014. Dissolved inorganic carbon and total alkalinity of a Hawaiian fringing reef: chemical techniques for monitoring the effects of ocean acidification on coral reefs. Coral Reefs **33:** 105-115.

Lee, K. and others 2006. Global relationships of total alkalinity with salinity and temperature in surface waters of the world's oceans. Geophys. Res. Lett. **33:** L19605.

Lewis, C. N., K. A. Brown, L. A. Edwards, G. Cooper, and H. S. Findlay. 2013. Sensitivity to ocean acidification parallels natural pCO_2 gradients experienced by Arctic copepods under winter sea ice. Proc. Natl. Acad. Sci. **110:** E4960-E4967.

Littlepage, J. L. 1965. Oceanographic investigations in McMurdo sound, Antarctica. Antarct. Res. Ser. **5:** 1-37.

Liu, X., M. C. Patsavas, and R. H. Byrne. 2011. Purification and characterization of meta-cresol purple for spectrophotometric seawater pH measurements. Environ. Sci. Technol. **45:** 4862-4868.

Martz, T. R., J. G. Connery, and K. S. Johnson. 2010. Testing the Honeywell Durafet® for seawater pH applications. Limnol. Oceanogr. Methods **8:** 172-184.

Matson, P. G., T. R. Martz, and G. E. Hofmann. 2011. High-frequency observations of pH under Antarctic sea ice in the southern Ross Sea. Antarct. Sci. **23:** 607-613.

Matson, P. G., L. Washburn, T. R. Martz, and G. E. Hofmann. 2014. Abiotic versus biotic drivers of ocean pH variation under fast sea ice in McMurdo Sound, Antarctica. PLoS One **9:** e107239.

McElhany, P., and D. S. Busch. 2013. Appropriate pCO_2 treatments in ocean acidification experiments. Mar. Biol. **160:** 1807-1812.

McNeil, B. I., and R. J. Matear. 2008. Southern Ocean acidification: A tipping point at 450-ppm atmospheric CO_2. Proc. Natl. Acad. Sci. **105:** 18860-18864.

McNeil, B. I., C. Sweeney, and J. a. E. Gibson. 2011. Short Note Natural seasonal variability of aragonite saturation state within two Antarctic coastal ocean sites. Antarct. Sci. **23:** 411-412.

McNeil, B. I., A. Tagliabue, and C. Sweeney. 2010. A multi-decadal delay in the onset of corrosive 'acidified' waters in the Ross Sea of Antarctica due to strong air-sea CO_2 disequilibrium. Geophys. Res. Lett. **37:** L19607.

Mehrbach, C., C. H. Culberso, J. E. Hawley, and R. M. Pytkowic. 1973. Measurement of apparent dissociation constants of carbonic acid in seawater at atmospheric pressure. Limnol. Oceanogr. **18:** 897-907.

Mu, L., S. Stammerjohn, K. Lowry, and P. Yager. 2014. Spatial variability of surface pCO_2 and air-sea CO_2 flux in the Amundsen Sea Polynya, Antarctica. Elementa: Sci. Anthrop. **2:** 000036.

Murray, C. S., A. Malvezzi, C. J. Gobler, and H. Baumann. 2014. Offspring sensitivity to ocean acidification changes seasonally in a coastal marine fish. Mar. Ecol. Prog. Ser. **504:** 1-11.

Noble, A. E., D. M. Moran, A. Allen, and M. A. Saito. 2013. Dissolved and particulate trace metal micronutrients under the McMurdo Sound seasonal sea ice: basal sea ice communities as a capacitor for iron. Front. Chem. **1:** 25.

Orr, J. C. and others 2005. Anthropogenic ocean acidification over the twenty-first century and its impact on calcifying organisms. Nature **437:** 681-686.

Putt, M., G. Miceli, and D. K. Stoecker. 1994. Association of bacteria with *Phaeocystis* sp. in McMurdo Sound, Antarctica. Mar. Ecol. Prog. Ser. **105:** 179-189.

Riahi, K., A. Grübler, and N. Nakicenovic. 2007. Scenarios of long-term socio-economic and environmental development under climate stabilization. Technol. Forecast. Soc. Change **74:** 887-935.

Riebesell, U., A. Körtzinger, and A. Oschlies. 2009. Sensitivities of marine carbon fluxes to ocean change. Proc. Natl. Acad. Sci. **106:** 20602-20609.

Rivkin, R. B. 1991. Seasonal patterns of planktonic production in McMurdo Sound, Antarctica. Am. Zool. **31:** 5-16.

Robbins, L. L., M. E. Hansen, J. A. Kleypas, and S. C. Meylan. 2010. CO2calc—A user-friendly seawater carbon calculator for Windows, Max OS X, and iOS (iPhone). U.S. Geological Survey Open-File Report 2010–1280.

Roden, N. P., E. H. Shadwick, B. Tilbrook, and T. W. Trull. 2013. Annual cycle of carbonate chemistry and decadal change in coastal Prydz Bay, East Antarctica. Mar. Chem. **155:** 135-147.

Sanford, E., and M. W. Kelly. 2011. Local adaptation in marine invertebrates. Ann. Rev. Mar. Sci. **3:** 509-535.

Schulz, K. G., and U. Riebesell. 2013. Diurnal changes in seawater carbonate chemistry speciation at increasing atmospheric carbon dioxide. Mar. Biol. **160:** 1889-1899.

Seibel, B. A., A. E. Maas, and H. M. Dierssen. 2012. Energetic plasticity underlies a variable response to ocean acidification in the pteropod, *Limacina helicina antarctica*. PLoS One **7:** e30464.

Shadwick, E., T. Trull, H. Thomas, and J. Gibson. 2013. Vulnerability of polar oceans to anthropogenic acidification: comparison of Arctic and Antarctic seasonal cycles. Sci. Rep. **3:** 2339.

Shaw, E. C., B. I. McNeil, B. Tilbrook, R. Matear, and M. L. Bates. 2013. Anthropogenic changes to seawater buffer capacity combined with natural reef metabolism induce extreme future coral reef CO_2 conditions. Global Change Biol. **19:** 1632-1641.

Smith, W. O. J., M. S. Dinniman, E. E. Hofmann, and J. M. Klinck. 2014. The effects of changing winds and temperatures on the oceanography of the Ross Sea in the 21st century. Geophys. Res. Lett. **41:** 1624-1631.

Smith, W. O. J., M. S. Dinniman, J. M. Klinck, and E. E. Hofmann. 2003. Biogeochemical climatologies in the Ross Sea, Antarctica: seasonal patterns of nutrients and biomass. Deep-Sea Res. II **50:** 3083-3101.

Steig, E. J., D. P. Schneider, S. D. Rutherford, M. E. Mann, J. C. Comiso, and D. T. Shindell. 2009. Warming of the Antarctic ice-sheet surface since the 1957 International Geophysical Year. Nature **457:** 459-462.

Sunday, J. M., P. Calosi, S. Dupont, P. L. Munday, J. H. Stillman, and T. B. Reusch. 2014. Evolution in an acidifying ocean. Trends Ecol. Evol. **29:** 117-125.

Sweeney, C. 2003. The annual cycle of surface water CO_2 and O_2 in the Ross Sea: A model for gas exchange on the continental shelves of Antarctica. Antarct. Res. Ser. **78:** 295-312.

Takahashi, T. and others 2002. Global sea-air CO_2 flux based on climatological surface ocean pCO_2, and seasonal biological and temperature effects. Deep-Sea Res. II **49:** 1601-1622.

Tortell, P. D. and others 2014. Metabolic balance of coastal Antarctic waters revealed by autonomous pCO_2 and $\Delta O_2/Ar$ measurements. Geophys. Res. Lett. **41:** 6803-6810.

Weeber, A., S. Swart, and P. Monteiro. 2015. Seasonality of sea ice controls interannual variability of summertime ΩA at the ice shelf in the Eastern Weddell Sea – an ocean acidification sensitivity study. Biogeosci. Disc. **12:** 1653–1687.

Yu, P. C., M. A. Sewell, P. G. Matson, E. B. Rivest, L. Kapsenberg, and G. E. Hofmann. 2013. Growth attenuation with developmental schedule progression in embryos and early larvae of *Sterechinus neumayeri* raised under elevated CO_2. PLoS One **8:** e52448.

III. Signals of resilience to ocean change: thermal tolerance of early stage Antarctic sea urchins (*Sterechinus neumayeri*) reared under present day and future pCO_2 and temperature[3]

A. Abstract

We tested the hypothesis that development of the Antarctic urchin *Sterechinus neumayeri* under future ocean conditions of warming and acidification would incur physiological costs reducing the tolerance of a secondary stressor. The aim of this study is two-fold: (1) describe austral spring temperature and pH near sea urchin habitat at Cape Evans in McMurdo Sound, Antarctica in order to quantify current environmental conditions, and (2) spawn *S. neumayeri* in the laboratory and raise early developmental stages (EDSs) under ambient (-0.7°C; 400 µatm pCO_2) and future (+2.6°C; 650 and 1000 µatm pCO_2) ocean conditions and expose four EDSs (blastula, gastrula, prism, 4-arm echinopluteus) to a one hour acute heat stress and assess survivorship. Results of field data from 2011 and 2012 show extremely stable inter-annual pH conditions ranging from 7.99-8.08, suggesting that future ocean acidification will drastically alter the pH-seascape for *S. neumayeri*. In the laboratory, *S. neumayeri* EDSs appear to be tolerant of temperatures and pCO_2 levels above their current habitat conditions. EDSs survived acute heat exposures >20°C above habitat temperatures of -1.9°C. No pCO_2 effect was observed for EDSs reared at -0.7°C. When reared at +2.6°C, small but significant pCO_2 effects were observed at the blastula and prism

[3] Published in *Polar Biology*: Kapsenberg, L, and GE Hofmann. Signals of resilience to ocean change: high thermal tolerance of early stage Antarctic sea urchins (*Sterechinus neumayeri*) reared under present-day and future pCO_2 and temperature. Polar Biol. **37**, 967–980, DOI:10.1007/s00300-014-1494-x (2014).

stage suggesting that multiple stressors are more detrimental than single stressors. While surprisingly tolerant overall, blastulae were the most sensitive stage to ocean warming and acidification. We conclude that *S. neumayeri* may be unexpectedly physiologically tolerant of future ocean conditions.

B. Introduction

Due to properties of persistently cold seawater, high-latitude marine ecosystems are ranked to be among the most sensitive regions to global change (Fabry et al. 2009; McClintock et al. 2008; Orr et al. 2005; Peck 2005; Turley et al. 2010). The Southern Ocean is expected to significantly change with respect to multiple factors within decades due to anthropogenic release of carbon dioxide (CO_2) to the atmosphere (McNeil and Matear 2008; Orr et al. 2005). Specifically, unprecedented rates of ocean warming and acidification are predicted (Hönisch et al. 2012; IPCC 2007; Marcott et al. 2013; Stammerjohn et al. 2008) and the fingerprints of this change are already being documented in Antarctic marine ecosystems (Bednaršek et al. 2012; McClintock et al. 2008; Montes-Hugo et al. 2009; Naveen et al. 2012; Steinberg et al. 2012). Due to the rate of environmental change and narrow adaptive capacity of Antarctic marine organisms, future shifts in the structure and function of Antarctic ecosystems are expected to be significant (Fabry et al. 2009; Peck 2005). A critical research priority is to assess the adaptive capacity of Antarctic organisms to future complex changes, which are often not considered together (Boyd 2011). In this light, the aim of this study was to assess the physiological cost of development of a circum-Antarctic marine invertebrate, the sea urchin *Sterechinus neumayeri*, under future multi-stressor scenarios.

Assessing the adaptive capacity (sensu Dawson et al. 2011) of Antarctic organisms is a critical research priority as the rate of change of waters surrounding Antarctica is expected to be rapid. As atmospheric CO_2 dissolves into the surface layers of the ocean due to differential partial pressures in the atmosphere and seawater, ocean pCO_2 increases and pH decreases. Atmospheric pCO_2 exceeded 400 ppm in May 2013 (http://www.esrl.noaa.gov/gmd/ccgg/trends/), an increase from 280 ppm pre-industrial time (Feely 2004). The Southern Ocean is the fastest acidifying ocean on the planet with an annual pCO_2 increase of 2.13 ± 0.64 µatm y^{-1} since the 1980s (Takahashi et al. 2009). Atmospheric CO_2 is predicted to reach 1000 ppm by 2100 resulting in a decrease of 0.4 ocean pH (IPCC 2007). However, biological ramifications may become apparent earlier with seasonal aragonite undersaturation predicted to occur when atmospheric CO_2 levels reach 450 ppm, as early as 2030 (McNeil and Matear 2008). Additionally, the Southern Ocean has warmed at twice the rate of global warming: 0.17^{o}C since the 1950s (Fyfe 2006; Gille 2002). Sea surface temperature is predicted to rise by an additional 2.6°C in the next 90 years (IPCC 2007).

The ‘double whammy’ of ocean acidification and ocean warming will create unprecedented marine environments and is expected to severely impact functional traits and physiological processes of polar species (Fabry et al. 2009; Sewell and Hofmann 2011). In general, species and populations may exhibit three types of responses to environmental change: (1) migrate with the changing climate envelope (Parmesan and Yohe 2003), (2) genetically adapt (Hoffmann and Sgrò 2011), and (3) acclimatize using current physiological plasticity (Gienapp et al. 2008; Hoffmann and Sgrò 2011; Visser 2008). Migration to colder water, the poleward shifts observed at lower latitudes, is not an option

for polar organisms. Here, changes in bathymetric distribution are also not viable as there is no thermocline that might preserve colder water at depth. Genetic adaptation may also be limited. Due to cold adaptation and thermal stability of the Southern Ocean over evolutionary timescales, some Antarctic species have lost the genetic capacity to deal with environmental change (Pörtner et al. 2012; Somero 2012). For example, the Antarctic notothenioid fish *Trematomus bernacchii* has lost an inducible heat shock response as a result of evolutionary adaptation to cold temperatures whereas temperate notothenioids have retained this trait (Clark and Peck 2009; Hofmann et al. 2000; Hofmann et al. 2005; Place et al. 2004). Such evolutionary adaptations may result in reduced capacities to withstand multi-stressor environments (Enzor et al. 2013). Among Antarctic invertebrate species, slow growth and long generation times reduce the potential for rapid genetic adaptation that may be required to flourish in a future ocean (Peck 2005; Pörtner et al. 2007). Finally, studies on marine invertebrates in general suggest that they are already operating at the limits of their thermal tolerance (Sunday et al. 2012), suggesting that further acclimatization to warming will be limited especially in polar species (Peck et al. 2009). Thus, success of Antarctic marine species likely depends on their current physiological plasticity and acclimatization capacity of functional traits. The importance of present-day tolerances and functional traits has been emphasized in other ecosystems when predicting climate change responses (Buckley and Kingsolver 2012; Chown 2012).

To investigate the breadth of current plasticity in a polar marine invertebrate with respect to seawater temperature and pH, we studied the early developmental stages (EDSs) of the Antarctic sea urchin *S. neumayeri*. *S. neumayeri* is an ideal study organism for ocean change experimental biology. With an extensive biogeographic range, it is the most abundant

echinoid on the shallow Antarctic benthos and a critical member of the circum-Antarctic near-shore marine ecosystem (Bosch et al. 1987). Adults can easily be spawned in the laboratory and larvae can readily be cultured (Bosch et al. 1987). In general, EDSs are predicted to be among the most sensitive stages to environmental change (Byrne 2011; Dupont and Thorndyke 2009; Kurihara 2008) especially with respect to synergistic stressors (Harvey et al. 2013). Due to a long pelagic larval duration of up to 115 days (Bosch et al. 1987), *S. neumayeri* spend a significant amount of time under direct influence of seawater conditions during its potentially most sensitive life history stage. Additionally, the slow development of *S. neumayeri* provides a unique opportunity to assess the physiological plasticity in response to multi-stressors at different EDSs. Previous studies of *S. neumayeri* EDSs have shown reduced growth (Byrne et al. 2013; Clark et al. 2009; Yu et al. 2013) and enhanced larval asymmetry (Byrne et al. 2013) under elevated pCO_2 conditions suggesting that there is in fact a physiological cost of development under these conditions.

The goal of this study was to assess, in general, the sensitivity of *S. neumayeri* EDSs (from present-day spawning) to future abiotic conditions expected for the Southern Ocean. In order to assess its current physiological plasticity, we asked whether development of sea urchin EDSs under elevated temperature and pCO_2 came at a cost of other physiological tolerances, in this case the tolerance of an acute heat stress. As an example, temperate sea urchin and abalone larvae reared under elevated pCO_2 showed reduced heat stress response following a one hour (1 h) acute heat exposure (O'Donnell et al. 2008; Zippay and Hofmann 2010a). This suggests that there are trade-offs associated with development at high pCO_2 where energy is diverted away from the cellular stress response potentially leaving the organism ill-equipped to deal with secondary stressors. Use of acute heat stress tests and

laboratory determined thermal tolerance limits can provide valuable insight into species' physiological trade-offs and energy allocations, current physiological plasticity and acclimation capacities (Terblanche et al. 2011; Tomanek 2010) and ultimately resilience in the face of climate change (Barnes et al. 2010; Buckley and Kingsolver 2012; Chown 2012; Chown and Gaston 2008).

During austral spring when natural spawning occurs, we raised larvae in the laboratory at McMurdo Station, Antarctica under multi-stressor scenarios (two temperatures and three pCO_2 levels) and exposed four developmental stages to a 1 h heat stress test and assessed survivorship. In order to place the laboratory findings in an environmentally relevant context, we also measured field pH and temperature in the water column above a sea urchin population for the duration of the larval culturing. We hypothesized that elevated pCO_2 and high temperature incur a physiological cost to *S. neumayeri* EDSs and predicted that embryos and larvae will have reduced survivorship following a 1 h temperature challenge compared to larvae reared under ambient conditions. Here we hope to address two questions: (1) what is the natural variability in the local seawater with respect to pH, and (2) does development under future conditions of ocean acidification and warming alter the acute heat tolerance of *S. neumayeri* EDSs?

C. Materials and Methods

1. Field pH measurements

In order to parameterize the CO_2 manipulation experiments of larval cultures, we measured pH near a *S. neumayeri* population using a SeaFET sensor with a Honeywell Durafet® pH electrode (Martz et al. 2010). SeaFET pH sensors were deployed above the benthos at 18 m depth on a 27 m benthic mooring at Cape Evans, Ross Island, Antarctica at

the sea urchin collection site (S 77° 38.060', E 166° 24.918'), from late October through November both years during 24 h daylight. In 2011, a temperature sensor was also deployed (Sea Bird Electronics SBE-37 SM, Matson 2012).

Raw voltage (mV) recorded by the SeaFET was converted to pH_{total} using one discrete seawater sample per sensor deployment. Single discrete calibration samples were collected via SCUBA following Standard operating procedures (SOP) 1 and processed for spectrophotometric pH analysis (total hydrogen ion concentration pH scale) at 25°C following SOP 6b (Dickson et al. 2007). Salinity was measured using a YSI 3100 Conductivity Instrument. Total alkalinity was determined according to SOP 3b using an open-cell titrator (Mettler-Toledo T50) after measuring Certified reference materials (CRMs) seawater standards from Dr. Andrew M. Dickson at Scripps Institution of Oceanography to within 10 µmol kg^{-1} accuracy (Dickson et al. 2007). *In situ* pH_{total} of the calibration sample was calculated using the *in situ* temperature recorded by the SeaFET at the time of sample collection and calculated in CO2Calc (Robbins et al. 2010) using CO_2 constants from Mehrbach et al. (1973) refit by Dickson and Millero (1987).

Accuracy of SeaFET data depends on the quality of the calibration sample and is estimated to be ~0.01 pH as compared to SOP 6b processing of CRMs (data not shown, Matson et al. 2011). pH was recorded every hour (2011) or 30 min (2012) and reported as hourly data after applying a 1 h low-pass filter.

2. Animal collection and larval cultures

In order to raise sea urchin EDSs under multi-stressor scenarios of temperatures and pCO_2 conditions, cultures were reared at -0.7°C in 2011 and +2.6°C in 2012 (hereinafter referred to 'cold' and 'warm' cultures) at three pCO_2 levels (400, 650 and 1000 µatm) as

described in Yu et al. (2013). The warm culture temperature was chosen to be an extreme future scenario. Adult *S. neumayeri* were collected from the benthos by SCUBA at Cape Evans, Ross Island, Antarctica (S 77^{o} 38.060', E 166^{o} 24.918'), in October 2011 and 2012, during the spawning season (Brey et al. 1995; Pearse and Giese 1966; Stanwell-Smith and Peck 1998). Depth of the collection site was approximately 20 m. Adults were transported in coolers to McMurdo Station and maintained in ~ -1^{o}C flow-through seawater tables for approximately two weeks until spawning.

Adult *S. neumayeri* were induced to spawn by injection of ~1 ml of ice-cold 0.55 M KCl. Females were inverted over a beaker containing filtered seawater (FSW) on ice to collect eggs, and sperm was collected dry directly from the gonopores. Sperm and eggs were kept on wet ice until use. After successful test fertilization assays, eggs from 20 (15) females were pooled and fertilized using diluted sperm from one male to >90 percent fertilization success for the cold (warm) culture. Embryos were split between culture buckets prefilled with control and two CO_2-acidified seawater treatments as described in Yu et al. (2013). Culture vessels were stocked at ~160,000 embryos/12 L.

3. Experimental seawater acidification

For experimental sea urchin cultures, seawater was acidified with CO_2 gas. Control and CO_2-acidification of 0.32 µm FSW followed methods modified from Fangue et al. (2010) and as described in Yu et al. (2013), with the exception that seawater tubing was not insulated. Briefly, pure CO_2 gas was mixed with dry air to desired levels and was subsequently dissolved into FSW in three reservoir buckets by a venturi injector. We aimed for control pCO_2 level of 400 µatm and treatment pCO_2 levels of 650 and 1000 µatm in five replicate culture vessels for a total of 15 culture vessels. Reservoir and culture vessels were

thermally controlled in flow-through seawater tables with ambient seawater (cold culture) and temperature-control immersion heaters (Process Technology) (warm culture).

Reservoir buckets were sampled daily for temperature, salinity, total alkalinity, and pH according to methods listed under 'Field pH measurements' for discrete seawater samples, with the exception that temperature was measured using a wire probe (Fluke 52 K/J Thermometer). Culture vessels were sampled daily for temperature and pH. *In situ* pH_{total} and carbonate parameters were calculated in CO2Calc (Robbins et al. 2010) using batch processing with CO_2 constants from Mehrbach et al. (1973) refit by Dickson and Millero (1987).

4. Survivorship assays

Acute thermal tolerance of *S. neumayeri* was tested at four stages of sea urchin early development - hatched blastula, mid-gastrula, prism, and 4-arm echinopluteus (hereinafter 'pluteus') - using a survivorship assay modified from Hammond and Hofmann (2010). A thermal gradient was established by cooling and warming two ends of an aluminum block containing 60 holes fabricated to fit 20 ml scintillation vials. Here thermal tolerance was tested at nine temperatures, with two technical replicates per acute heat stress temperature and pCO_2 group for each stage (Table III-3). Unlike ecologically relevant culture temperatures of -0.7 and +2.6°C, acute heat stress temperatures (up to 25°C) were chosen to study the physiology of EDSs and do not represent temperatures likely to be encountered in the field. For optimum temperature range, two assays were required for each development stage, and as a matter of protocol for all CO_2 treatments, the cooler assay was always run before the warmer assay. All assays were conducted in walk-in environmental rooms in the Crary Laboratories maintained at -1 and +4^{o}C for the cold and warm culture, respectively.

Prior to each assay, 20 ml scintillation vials were filled with 5 ml control seawater, capped, and allowed to equilibrate to temperatures within the aluminum block for two hours. Embryos and larvae were collected from all five replicate culture vessels, concentrated through 64 µm Nitex mesh and pooled. Concentrated larvae were kept on ice in environmental rooms until used for the survivorship assay, at ~-1^{o}C and 0^{o}C for the cold and warm culture, respectively. Approximately 220-300 larvae were transferred to each temperature-equilibrated vial in no more than 250 µL, location was randomized by CO_2 treatment within the aluminum block, and time of embryos/larvae addition was noted. Temperatures in the vials were measured immediately prior to embryos/larvae addition and upon removal of vials from the aluminum block after 1 h. The mean of these two temperatures is reported (Table III-3). The brief temperature change induced by the addition of embryos/larvae was negligible. Embryos/larvae were allotted a 20 h recovery period at control temperatures (cold culture: on ice in a -1^{o}C environmental room; warm culture: +2 ^{o}C water bath). For the first blastula stage assay of the cold culture, addition of larvae to the vials was staggered by 30 min for each temperature (cold to warm) and scored in order. For all remaining assays, larvae were added consecutively by temperature and scored randomly.

After a 20 h recovery period, larvae were concentrated by reverse filtration using a transfer pipette with 64 µm Nitex mesh, and the first 100 embryos/larvae viewed under a microscope on a Sedgewick Rafter counting cell slide were scored for survival in the environmental room. Abnormal embryos/larvae (due to abnormal development or evidence of cellular egression or regression) that still exhibited ciliary activity were considered dead. Tipping-point temperatures (TTs) were determined in order to compare thermal tolerance

Table III-1. Acute temperature exposure (1 h) of early developmental stages of *S. neumayeri* raised in two thermal environments: cold (-0.7 ^{o}C) and warm (+2.6 ^{o}C).

Maximum observed change in vial temperature during the 1 h incubation was 1.1 ^{o}C and 1.5 ^{o}C in cold and warm culture assays, respectively.

Culture	Stage	Temperature (°C) of 1 h exposure									Absolute change in vial temperature (°C)[a]
Cold	*Blastula*	-0.5	2.2	4.7	7.4	10.2	13.2	15.5	17.9	20.6	0.2 ± 0.1
	Gastrula	-0.4	2.3	5.0	7.5	10.2	13.0	15.3	17.8	20.3	0.2 ± 0.2
	Prism	-0.8	4.9	10.3	13.8	16.0	17.8	20.1	22.6	25.4	0.3 ± 0.3
	Pluteus	-0.6	5.3	10.9	14.4	16.4	18.4	20.6	22.8	25.2	0.1 ± 0.1
Warm	*Blastula*	2.6	7.1	10.0	13.0	14.8	17.7	19.6	22.7	25.5	0.4 ± 0.3
	Gastrula	2.8	7.3	10.2	13.1	15.0	17.9	20.2	22.5	24.7	0.2 ± 0.2
	Prism	2.8	7.3	10.2	13.2	15.2	18.1	20.0	22.0	24.2	0.5 ± 0.4
	Pluteus	3.0	7.3	10.2	13.2	14.9	17.8	19.9	22.0	24.4	0.2 ± 0.2

[a]Values are given as mean ± SD, sample size is 54

across the cold and warm cultures and are defined as the highest temperature at which both replicates of EDSs reared under control pCO_2 levels have greater than 80 percent survivorship.

5.Statistical analysis

Survivorship data of the 1 h temperature exposure were analyzed by developmental stage and separately for cold and warm larval cultures, using a 2^{nd} order logistic model with a beta-binomial distribution (JMP 9) where pCO_2, temperature (T) and T^2 were considered main effects. There were no interactions between pCO_2 and temperature effects at any stage, and the interaction was removed from the final model.

D. Results

1. Field pH measurements

In general, pH was remarkably stable over the period of the SeaFET deployment in austral spring. Continuous pH data were recorded during two separate field seasons: 33 days in 2011 (29 October – 30 November 2011, see Matson 2012) and 14 days in 2012 (31 October – 13 November 2012, this study). pH was consistent over both field seasons (Figure III-1, Table III-2). During these recording intervals, pH varied from 7.99-8.08 (2011) and 8.01-8.08 (2012) with median values of 8.01 during both seasons. Mean pH in 2011 and 2012 was 8.01 ± 0.02 and 8.02 ± 0.01, respectively. Temperature in 2011 ranged from -1.90°C to -1.78°C with a mean of -1.88 ± 0.03°C (see Matson 2012). Due to the SeaFET location under fast sea ice and stable SeaFET temperature data (not shown) and previously documented temperatures (Hunt et al. 2003), we assumed a constant temperature of -1.9°C

to calculate pCO_2 and carbonate ion saturation states (Ω) for the 2012 deployment (Table III-2).

2. Conditions of the laboratory sea urchin cultures

During the laboratory portion of the experiment, pH (as controlled by CO_2-mixing) and temperature in the sea urchin cultures were stable. The three CO_2 treatments resulted in similar pH conditions in both the cold (2011) and warm (2012) culture (Figure III-1). Average cold and warm culture temperatures were -0.7 ± 0.3 and +2.6 ± 0.1^oC respectively with little variation between culture vessels. pH and pCO_2 levels of the cold culture remained stable throughout the experiment (Table III-3). Control pH of the cold culture was 8.038 ± 0.015 (402 ± 16 µatm pCO_2) and slightly higher than observed field pH in 2011 and 2012, whereas control pH of the warm culture matched field pH at 8.009 ± 0.027 (437 ± 16 µatm pCO_2). Failure of mass-flow control valves on day 12 of the warm culture resulted in a 1 day increase of pCO_2 to 2651 ± 353 µatm in control culture vessels and decrease to 216 ± 18 µatm in the high CO_2 treatment. Subsequently on day 14, medium CO_2 treatment levels declined to 216 ± 18 µatm pCO_2 and failed to recover for the remainder of the experiment. The warm culture pluteus stage was the only larval stage affected by the valve failures in this study and this stage was still included in the heat stress experiment.

3. Developmental progression of sea urchins in the experimental cultures

Overall, development of *S. neumayeri* larvae occurred synchronously across all CO_2 treatments with development progressing faster in the culture maintained at +2.6^oC as compared to the culture maintained at -0.7^oC (Figure III-2). As measured by prevalence of >90%, at -0.7^oC, embryos reached hatched blastula at 104 hours, gastrula by day 11, prism

Figure III-1. Comparison of field pH_{total} and laboratory pH_{total} conditions of early developmental sea urchin cultures in 2011 (a) and 2012 (b). Field pH (black line) was measured by a SeaFET sensor at 20 m depth just above the *Sterechinus neumayeri* population at Cape Evans, McMurdo Sound, Antarctica. pH of CO_2-acidified experimental cultures (control pCO_2 = light gray line with dot symbols; medium pCO_2 = dark gray circles; high pCO_2 = white triangles) was measured via spectrophotometric analysis and reported as daily averages (error bars are SD). Culture temperature in 2011 was -0.7 ^{o}C and +2.6 ^{o}C in 2012. Culture pH in (b) is reported up to the prism stage (see text for details). Time is in Coordinated Universal Time.

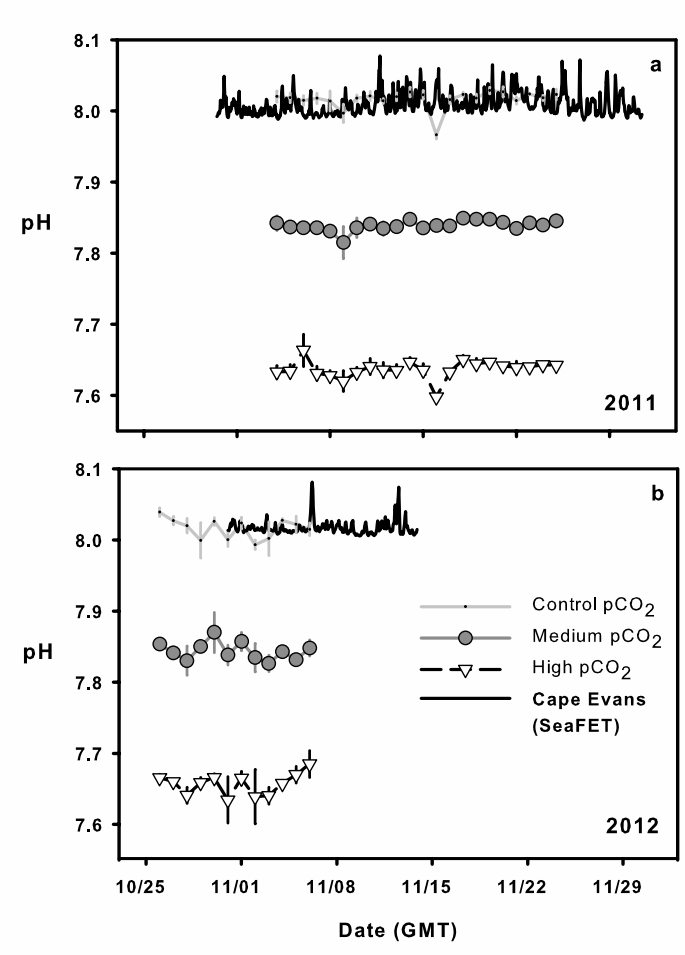

Table III-2. Field conditions at Cape Evans, McMurdo Sound, Antarctica in austral spring of 2011 (29 October – 30 November) and 2012 (31 October – 13 November) using a SeaFET pH sensor. Saturation state (Ω) and pCO_2 for 2012 were calculated in CO2calc assuming -1.9 °C and 34.7 salinity and 2346 µmol $kgSW^{-1}$ total alkalinity as measured in a discreet calibration sample. *Data are from Matson (2012).

Field parameter	2011*	2012
T (°C)	-1.88 ± 0.03	-
pH_{total}	8.01 ± 0.02	8.02 ± 0.01
pCO_2 (µatm)	426 ± 16	419 ± 10
$\Omega_{aragonite}$	1.22 ± 0.04	1.25 ± 0.03
$\Omega_{calcite}$	1.95 ± 0.06	1.99 ± 0.04
Sample size	768	335

Values are given as mean ± SD

Table III-3. *Sterechinus neumayeri* culture conditions in 2011 and 2012. TA is total alkalinity.

Parameter	*S. neumayeri* culture	
CO_2 treatment	*cold (2011)*	*warm (2012)[a]*
T (°C)		
Control	-0.7 ± 0.3 (98)	2.6 ± 0.1 (75)
Medium	-0.7 ± 0.3 (98)	2.6 ± 0.1 (70)
High	-0.7 ± 0.3 (88)	2.6 ± 0.1 (85)
pH_{total}		
Control	8.038 ± 0.015 (98)	8.009 ± 0.0268 (72)
Medium	7.858 ± 0.011 (98)	7.846 ± 0.020 (64)
High	7.652 ± 0.014 (88)	7.657 ± 0.021 (80)
pCO_2 (μatm)		
Control	402 ± 16 (98)	437 ± 31 (72)
Medium	626 ± 17 (98)	658 ± 33 (64)
High	1032 ± 37 (88)	1044 ± 55 (80)
$\Omega_{aragonite}$		
Control	1.36 ± 0.04 (98)	1.46 ± 0.07 (72)
Medium	0.92 ± 0.02 (98)	1.04 ± 0.05 (64)
High	0.59 ± 0.02 (88)	0.69 ± 0.03 (80)
TA (μmol $kgSW^{-1}$)		
Control	2348 ± 9 (22)	2348 ± 8 (17)
Medium	2341 ± 9 (22)	2349 ± 6 (17)
High	2339 ± 10 (22)	2347 ± 5 (17)
Salinity		
Control	34.2 ± 0.1 (22)	34.8 ± 0.1 (17)
Medium	34.2 ± 0.1 (22)	34.8 ± 0.1 (17)
High	34.2 ± 0.1 (22)	34.8 ± 0.1 (17)

Values are given as mean ± SD with sample size between parentheses

[a]excludes pH, pCO_2, Ω_{arag}, data on days of gas valve failures (see text for details)

Figure III-2. Sampling schedule comparison of *Sterechinus neumayeri* early developmental stages (blastula, gastrula, prism, and 4-arm pluteus) reared at -0.7 ^{o}C (white dots) and +2.6 ^{o}C (black dots) for acute heat stress survivorship assays.

Sampling was conducted once >90% of embryos or larvae reached the stage of interest. Split dot represents sampling of both cultures. Representative developmental stage photos are of *S. neumayeri* reared at +2.6 ^{o}C and assorted pCO_2 levels. Scale bar is 100 µm.

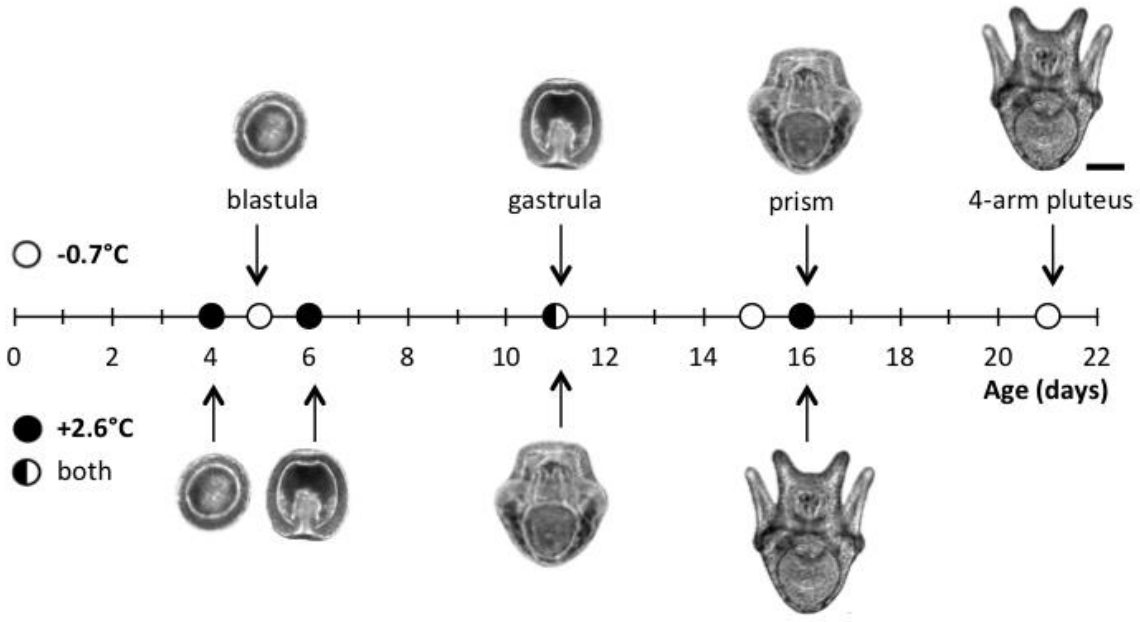

by day 15, and pluteus by day 21. In contrast at +2.6^{o}C, *S. neumayeri* reached these same stages at 84 hours, by day 6, 11, and 16, respectively. Sampling of developmental stages of the warm culture was timed as to best match developmental stages of the cold culture in the previous year as determined from daily observation. Due to the rapid development of embryos in the warm culture, there may have been a mismatch at the gastrula stage where slightly developmentally younger stage gastrulae, with smaller archenterons, were sampled in the warm culture compared to the cold culture. Some mortality was observed across all treatments at the prism and pluteus stages during the experiment but was not quantified as the requirement for experiments and sampling other than the one reported here dictated the need for large numbers of larvae.

4. Survivorship assays

Survivorship assays were used to assess whether development at elevated temperature and pCO_2 would alter the tolerance of acute heat stress in EDSs of *S. neumayeri*. All EDSs survived temperatures that greatly exceed their average habitat temperature of -1.9°C. In general survivorship curves look similar across all temperature and CO_2 treatments: survivorship following acute temperature exposure was high up to a tipping-point temperature (TT) beyond which it declined rapidly (Figure III-3).

S. neumayeri EDSs reared at -0.7°C were extremely robust to pCO_2 and no pCO_2 effect was observed in the survivorship assays (Figure III-3a-d, Table III-4). In contrast, negative pCO_2 effects were observed for two warm culture EDSs suggesting that multiple stressors are more detrimental than single stressors (Figure III-3e-h, Table III-4). First, high pCO_2 (>1000 µatm) reduced thermal tolerance of warm culture blastulae at temperatures beyond the TT of 15°C (p = 0.0005, Figure III-3e). This trend was also observed for blastulae reared

Figure III-3. Percent survivorship, following a 1 h acute heat stress and ~20 h recovery at culture temperatures, of four early developmental stages (a, e blastula; b, f gastrula; c, g prism; d, h 4-arm pluteus) of *Sterechinus neumayeri* reared at -0.7 °C (a-d) and +2.6 °C (e-h) under control (~400 µatm, black) and elevated pCO_2 (~650 µatm, gray; ~1000 µatm, perforated line). N = 100, *denotes significant pCO_2 effect.

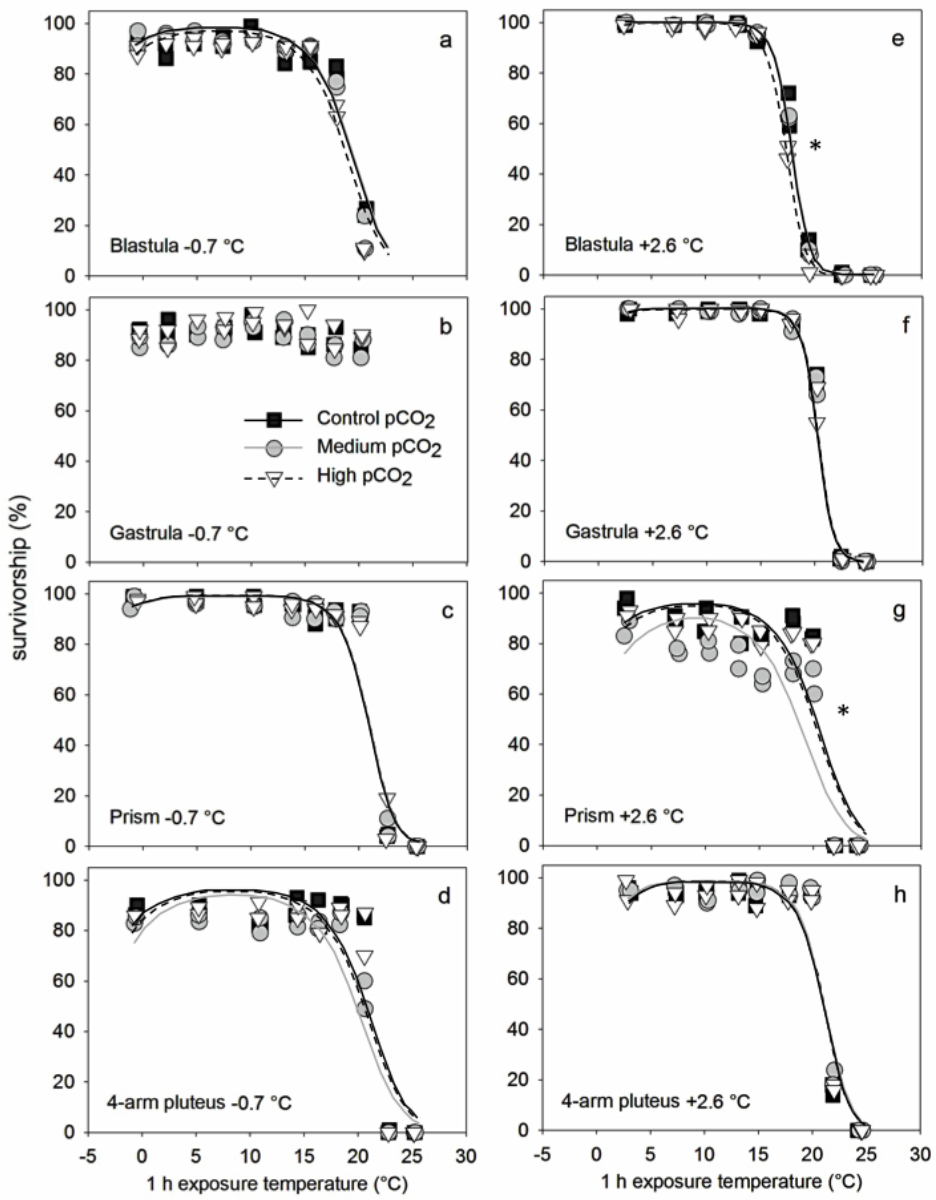

Table III-4. Logistic regression model output.

Culture	Source	*df*	L-R ChiSquare	Prob>ChiSq
Cold	*Blastula*			
	pCO_2	2	3.1213056	0.21
	T	1	198.20761	<.0001*
	T*T	1	108.22541	<.0001*
	Prism			
	pCO_2	2	0.0216827	0.9892
	T	1	331.1169	<.0001*
	T*T	1	54.107351	<.0001*
	Pluteus			
	pCO_2	2	1.7438573	0.4181
	T	1	168.85749	<.0001*
	T*T	1	65.283207	<.0001*
Warm	*Blastula*			
	pCO_2	2	15.29441	0.0005*
	T	1	3487.2801	<.0001*
	T*T	1	83.696576	<.0001*
	Gastrula			
	pCO_2	2	0.1561852	0.9249
	T	1	657.08303	<.0001*
	T*T	1	38.055269	<.0001*
	Prism			
	pCO_2	2	6.0902789	0.0476*
	T	1	155.09928	<.0001*
	T*T	1	38.090102	<.0001*
	Pluteus			
	pCO_2	2	0.2318825	0.8905
	T	1	199.23477	<.0001*
	T*T	1	61.083177	<.0001*

*significant

at -0.7°C but was not significant (p = 0.21). Second, medium pCO_2 (650 µatm) reduced thermal tolerance of prism larvae reared at +2.6°C (p = 0.0476, Figure III-3g).

Finally, due to genotypic and potential sampling differences between the cultures, direct comparisons based on culture temperature should be interpreted with caution. However, based on TTs there appears to be no strong effect of culture temperature on the thermal tolerance of *S. neumayeri* EDSs. In both the cold and warm culture, blastulae were less thermotolerant than post-blastula stages by ~5°C. Blastulae exhibit a TT of 15°C whereas post-blastula stages in both the cold and warm culture survived acute exposure up to 20°C, with the exception of warm culture gastrulae which exhibit a TT of 18°C (Figure III-4).

E. Discussion

The aim of this study was to assess the current physiological plasticity of the Antarctic sea urchin *S. neumayeri* in light of ocean warming and acidification and in the context of current ocean conditions. Here we report two salient findings. First, as measured by autonomous pH sensors, we found that *S. neumayeri* EDSs currently experience extremely stable abiotic conditions in McMurdo Sound during the austral spring. Second, we found a remarkably high acute temperature tolerance of *S. neumayeri* EDSs reared at elevated pCO_2 and temperature. Although in general, Antarctic organisms are predicted to be sensitive to environmental changes (Peck 2005; Somero 2012), here we show that *S. neumayeri* EDSs may be more physiologically tolerant of future ocean change than previously thought (Byrne et al. 2013).

Figure III-4. Summary of salient finding for the physiological toll of exposure to future ocean scenarios during *Sterechinus neumayeri* early development as assessed by a 1 h heat stress survivorship assay at four developmental stages. *S. neumayeri* embryos and larvae exhibit high tipping point temperatures independent of development at -0.7 ^{o}C and +2.6 ^{o}C. Elevated pCO_2 had an overall slight negative impact on blastulae and prisms reared at +2.6 ^{o}C. Scale bar is 100 µm.

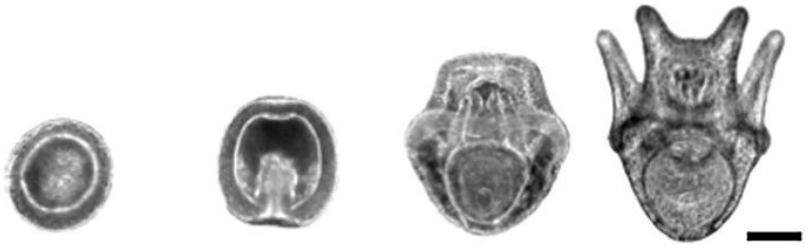

	blastula	gastrula	prism	4-arm pluteus
Tipping-point temperature	15°C	18-20°C	20°C	20°C
pCO_2 effect at -0.7°C	—	—	—	—
pCO_2 effect at +2.6°C	→	—	→	—

1. Field pH measurements

Measurements of ocean temperature and pH at Cape Evans, McMurdo Sound, Antarctica, during two seasons (austral spring 2011, 2012) were extremely stable and match previously documented environmental stability in this region (Littlepage 1965; Matson et al. 2011). For example, in 2010 pH ranged from 8.002 to 8.050 from 26 October to 15 November (Matson et al. 2011). Collectively, median pH at Cape Evans over three consecutive austral spring seasons was 8.019 (2010, Matson et al. 2011), 8.005 (2011, Matson 2012), and 8.016 (2012, this study). Relative to other ecosystems, pH data from Cape Evans show extremely stable inter-annual pH conditions. By contrast, pH in temperate and tropical reefs can vary as much as 0.544 and 0.253 pH units over only 30 days (Hofmann et al. 2011). The period of stable pH at Cape Evans coincides with the spawning season of *S. neumayeri* (Brey et al. 1995; Pearse and Giese 1966), and previous plankton tows throughout McMurdo Sound show the presence of blastulae and gastrulae from November to December (Bosch et al. 1987). Thus, depending on local retention time post-fertilization, it is likely that EDSs from the Cape Evans *S. neumayeri* spawning population consistently develop at seawater pH of 8.0-8.1 and temperature of approximately -1.9°C. Future ocean acidification and carbonate ion undersaturation such as the conditions used in the experimental portion of this study will be unprecedented for *S. neumayeri* in the coming decade

2. Survivorship assays of S. neumayeri *EDSs*

Here we report the changes in survivorship following a 1 h acute heat stress of *S. neumayeri* EDSs reared at elevated temperature and pCO_2 that mimic predicted anthropogenic changes in the Southern Ocean. We hypothesized that development of *S.*

neumayeri EDSs under seawater conditions outside their current ambient range would incur a physiological cost such that tolerance of a secondary stressor would be reduced. We measured this cost by assessing tolerance of acute heat stress (Terblanche et al. 2011). We found negative pCO_2 effects on acute thermal tolerance only when *S. neumayeri* were reared under elevated temperature of +2.6°C (Figure III-4). While these results suggest a trade-off of development under a multi-stressor scenario and ability to cope with a secondary stress, the effect is relatively small from an ecological perspective. We therefore conclude that the effect of the multi-stressor scenario (ocean acidification and ocean warming together) on acute thermal tolerance is minor. *S. neumayeri* may be one of the more tolerant Antarctic marine invertebrates, exhibiting high physiological plasticity despite living under extremely stable conditions.

Future multi-stressor scenarios, however, may impact other physiological processes and long-term tolerances. For example, in recent research, *S. neumayeri* fertilization and early cleavage was negatively impacted by temperature (+1.5 and +3°C) at a CO_2 concentration of 1370 ppm (pH 7.5, Ericson et al. 2012). However, inter-individual variation observed in *S. neumayeri* fertilization success under elevated pCO_2 may ameliorate such effects in the wild (Sewell et al. 2014). Previous studies show compromised growth of *S. neumayeri* larvae reared at elevated pCO_2 (Byrne et al. 2013; Yu et al. 2013). However, warming may increase larval growth (Byrne 2011). Byrne et al. (2013) showed that the combined effects of warming and CO_2 acidification resulted in highly altered *S. neumayeri* larval body morphology and asymmetry, suggesting that there is a significant physiological effect of multi-stressor scenarios on the development of this polar echinoderm. Byrne et al. (2013) also found that under a multi-stressor scenario of temperature (+1°C) and pCO_2 (1355 µatm,

pH 7.6) development up to the gastrula stage was not affected but was negatively affected at the prism and pluteus stages with up to 83 percent of plutei showing abnormal development. Our findings show that these negative effects do not translate to secondary physiological trade-offs such that other functional traits, namely acute thermal tolerance, are compromised. Negative effects of warming and acidification on metamorphosis, juvenile growth and reproduction may swamp the small benefit of high physiological plasticity at EDSs presented here, although these have not yet been quantified for *S. neumayeri*.

While normal development was not quantified in this study, the higher temperature of +2.6°C, a temperature 1.6 °C higher than that used by Byrne et al. (2013), may have resulted in higher mortality of abnormal larvae such that the EDSs sampled in this study were selectively more thermotolerant than those observed by Byrne et al. which were reared at +1°C. This type of outcome was observed for temperate purple sea urchin larvae, *Strongylocentrotus purpuratus*, where different genotypes were selected during culturing in various experimental future ocean acidification conditions (Pespeni et al. 2013). Ultimately we assessed the embryos and larvae that survived culture conditions long enough to be sampled. For example, the pCO_2 effect observed at the prism stage is largely due to the presence of abnormal larvae in the medium CO_2 treatment (analysis not shown) and such larvae may not have survived to the pluteus stage. It should be noted that this treatment group was exposed to low pCO_2 due to valve failures following sampling of the prism stage and higher survivorship of the pluteus stage could thus still be a factor of low pCO_2 exposure. Other studies on sea urchin species show impaired development at only a few degrees above ambient conditions (Byrne et al. 2009; Delorme and Sewell 2013; Sewell and

Young 1999; Sheppard Brennand et al. 2010) and it is likely that a culture temperature of +2.6°C is near the upper temperature limit of *S. neumayeri* early development.

Within species, developmental stages respond differently to abiotic stressors. While all *S. neumayeri* EDSs survived temperatures that greatly exceed their average habitat temperature of -1.9°C, blastulae appear to be the most sensitive stage to abiotic stressors as has been observed for other sea urchin species (Giudice et al. 1999; Roccheri et al. 1986; Sconzo et al. 1995). In this study, blastulae reared at -0.7°C exhibit a pattern of reduced acute thermal tolerance with increasing pCO_2. This pattern was statistically significant when blastulae were reared at +2.6°C suggesting that high pCO_2 affects the performance of blastulae. This has been observed previously where developmental progression of *S. neumayeri* between -0.8 and 0°C was only affected by high pCO_2 at the blastula stage (Yu et al. 2013). Additionally, in both the cold and warm culture, thermal tolerance increased as much as 5°C from 15°C to 20°C from blastula stage to gastrula, prism, and pluteus stages, respectively. In general, blastulae are one of the more sensitive developmental stages in echinoderms especially with respect to temperature (Giudice et al. 1999; Roccheri et al. 1986; Sconzo et al. 1995), and the same physiological mechanisms may affect pCO_2 tolerance. Large increases in gene expression are associated with the transition from hatched blastula to gastrula and later stages (Giudice et al. 1968; Howard-Ashby et al. 2006). Such genes include, for example, genes coding for heat shock proteins, which can increase thermal tolerance of post-blastula stages (Giudice et al. 1999; Roccheri et al. 1986; Sconzo et al. 1995). It is interesting that increased thermal tolerance coincides with increased pCO_2 tolerance. The greater tolerance of *S. neumayeri* post-blastula stages to pCO_2 and acute temperature stress may be related to alterations in the larval transcriptome. Such changes in

gene expression may allow the organism to overcome the negative effects of pCO_2 demonstrating a link between gene expression and physiological plasticity that leads to tolerance of CO_2-acidification (Evans et al. 2013). Thus, *S. neumayeri* may already harbor some genetic plasticity that allows EDSs to tolerate future ocean change, at least to some degree. Temperate sea urchin gastrulae of *S. purpuratus* exhibit large changes in gene expression relative to control conditions (pH 8.1/435 μatm pCO_2) when reared at natural levels of low pH (pH 7.77/813 μatm pCO_2) but not at pH levels lower than natural exposures (pH 7.59/1255 μatm pCO_2) suggesting that gastrulae can compensate for pCO_2 stress within the limits of natural exposure (Evans et al. 2013). Given that *S. neumayeri* EDSs experience a more stable pH environment than its temperate cousins, it is therefore unexpected that this species shows such high trait-based tolerance to elevated temperature and pCO_2. In association with this study, the transcriptomic response of *S. neumayeri* EDSs to pCO_2 and temperature stress is underway (Drs. G. Dilly and G.E. Hofmann unpublished results) and will be useful in elucidating the mechanisms that underlie the tolerance of this polar species in elevated conditions of pCO_2.

3. Comparisons to other species

EDSs among marine invertebrates are inconsistently sensitive to multi-stressor scenarios (Byrne 2011; Pörtner and Farrell 2008). For example, our results contrast with the response of invertebrate larvae of both abalone *Haliotis rufescens* (Zippay and Hofmann 2010a) and red sea urchin *Strongylocentrotus franciscanus* (O'Donnell et al. 2008) which exhibit reduced thermal tolerance following development in CO_2-acidified seawater. Many studies report much more obvious deleterious impacts of CO_2 and temperature on EDSs stages of benthic marine invertebrates (Anlauf et al. 2011; Byrne et al. 2011; Findlay et al. 2009,

2010; Parker et al. 2009, 2010; Sheppard Brennand et al. 2010). For example, Anlauf et al. (2011) found that the combined effect of elevated pCO_2 and temperature had a greater negative effect on growth of the coral *Porites panamensis* primary polyps than pCO_2 alone. Findlay et al. (2010) also found that the post-larval growth rate of the barnacle, *Semibalanus balanoides* was negatively impacted by reduced pH with a non-significant trend of further reduction in growth rate with increasing temperature of +4°C. Parker et al. (2009) found reduced successful development of D-veliger larvae of oyster *Saccostrea glomerata* at high temperature and low pH treatments compared to optimal temperature treatments. These studies highlight the importance of species-specific effects when attempting to predict biological changes to future multi-stressor scenarios using measures of current physiological plasticity.

4. S. neumayeri *temperature tolerance in context*

Successful development of *S. neumayeri* non-feeding EDSs at +2.6°C and survival of acute exposure >20°C above habitat temperatures is surprising. Firstly, Antarctic organisms are categorized as stenothermal due to evolutionary adaptation to the thermal stability of the Southern Ocean over evolutionary time scales (Peck 2005; Somero 2012). Secondly, gamete maturation in *S. neumayeri* occurs over the course of 12 to up to 24 months (Brockington et al. 2007) during which temperatures vary on an annual cycle of approximately -1.9°C to -0.5°C (Hunt et al. 2003).

Although longer temperature exposures will likely reduce upper temperature limits (Peck et al. 2009), the high acute temperature tolerance of *S. neumayeri* matches that of EDSs of eurythermal temperate species (Hammond and Hofmann 2010; Zippay and Hofmann 2010a; Zippay and Hofmann 2010b). For example, gastrulae and 4-arm

echinoplutei of temperate sea urchin *S. purpuratus* exhibit 50 percent survivorship following 1 h heat stress between 30-31°C, a value up to 20°C above average habitat temperatures (Hammond and Hofmann 2010). *S. neumayeri* are unlikely to ever experience temperatures up to 20°C, however, assessing biological response to rapid warming can provide valuable insight to a species' overall physiological tolerance and impacts on ecology (Terblanche et al. 2011). High thermal tolerance of *S. neumayeri* pelagic EDSs may be an ancestral trait stemming prior to speciation (Díaz et al. 2011) following the opening of the Drake Passage and establishment of the Antarctic Circumpolar Current (Lee et al. 2004). Such trait conservation may contribute to *S. neumayeri*'s extensive biogeographic range including colonization of warmer Antarctic archipelagos (Barnes et al. 2010). Our findings support the hypothesis that may be one of the least stenothermal Antarctic marine ectotherms (Barnes et al. 2010).

While *S. neumayeri* may be highly tolerant of acute temperature stress, this tolerance does not appear to be physiologically adaptive. Temperature of the rearing environment did not change TTs of EDSs suggesting that while EDSs can tolerate development at +2.6°C this tolerance is not physiologically adaptive. In other words, development at +3°C above -0.7°C did not shift TTs by the same magnitude. This has been shown for adult *S. neumayeri* as well. For example, a 60 day exposure of adult sea urchins to +3°C did not affect acute upper temperature limits which were approximately 15°C (Peck et al. 2010). The lethal temperatures reported here and in Peck et al. (2010) are much higher than current habitat temperatures and ecologically irrelevant for predictions of warming in the Southern Ocean. However, these data support the hypothesis that while *S. neumayeri* is less stenothermal than

previously thought (Barnes et al. 2010) its physiological adaptive capacity is limited (Peck 2005; Somero 2012).

5. Conclusion

Here we show that present day *S. neumayeri* embryos and larvae are resilient to relatively large short-term multi-stressor scenarios. Other studies show variable sensitivities of physiological measures in *S. neumayeri* EDSs (i.e. thermal tolerance, normal development, growth, and asymmetry) and it remains unclear how ocean acidification and warming will ultimately affect the life cycle of this species. These experimental results also point in the direction of a need to better understand adaptation and genetics in response to ocean acidification (Evans and Hofmann 2012; Kelly and Hofmann 2012). As the ocean changes, new selection forces will act on the existing genetic structure and individuals will be exposed to slowly changing environments which could enhance benefits of existing physiological plasticity, such as those described here, through maternal effects. It is significant that some studies show that traits of resilience are heritable (Kelly et al. 2013; Sunday et al. 2011), and other studies have shown that local adaptation likely plays a strong role as well (Pespeni et al. 2013; Schaum et al. 2013). A high degree of current physiological plasticity and genetic variability may facilitate adaptation and long-term tolerance of future conditions. Given the predictions of rapid changes in oceans (IPCC 2007), identifying resilient and vulnerable species and variably tolerant populations is crucial in order to understand future impacts of ocean change.

F. Acknowledgements

The authors would like to thank members of the U.S. Antarctic Program: R. Robbins and S. Rupp for sea urchin collections and sensor deployments and Crary Laboratory staff of 2011 and 2012 for resource support at McMurdo Station, Antarctica. We thank Professor W. Rice for advice on statistical analysis. Additionally, we especially thank Dr. P.C. Yu and other members of the Bravo-134 field team for their support during larval culture and water chemistry measurements (Professor M. Sewell, Dr. G. Dilly, E. Hunter, Dr. A. Kelley, Dr. P. Matson, E. Rivest, and O. Turnross). We are grateful for the comments from two anonymous reviewers that lead to the improvement of this manuscript. This research was supported by U.S. National Science Foundation (NSF) grant ANT-0944201 to GEH. LK was supported by a NSF Graduate Research Fellowship.

G. References

Anlauf H, D'Croz L, O'Dea A (2011) A corrosive concoction: The combined effects of ocean warming and acidification on the early growth of a stony coral are multiplicative. J Exp Mar Biol and Ecol **39**7: 13-20. doi:10.1016/j.jembe.2010.11.009

Barnes DKA, Peck LS, Morley SA (2010) Ecological relevance of laboratory determined temperature limits: colonization potential, biogeography and resilience of Antarctic invertebrates to environmental change. Glob Change Biol **16:** 3164-3169. doi:10.1111/j.1365-2486.2010.02176.x

Bednaršek N, Tarling GA, Bakker DC, Fielding S, Cohen A, Kuzirian A, McCorkle D, Lézé B, Montagna R (2012) Description and quantification of pteropod shell dissolution: a sensitive bioindicator of ocean acidification. Glob Change Biol **18:** 2378-2388

Bosch I, Beauchamp KA, Steele ME, Pearse JS (1987) Development, metamorphosis, and seasonal abundance of embryos and larvae of the Antarctic sea urchin Sterechinus neumayeri. Biol Bull **173:** 126-135. doi:10.2307/1541867

Boyd PW (2011) Beyond ocean acidification. Nat Geoscience **4** (5): 273-274. doi:10.1038/ngeo1150

Brey T, Pearse J, Basch L, McClintock J, Slattery M (1995) Growth and production of *Sterechinus neumayeri* (Echinoidea: Echinodermata) in McMurdo sound, Antarctica. Mar Biol **124:** 279-292. doi:10.1007/bf00347132

Brockington S, Peck LS, Tyler PA (2007) Gametogenesis and gonad mass cycles in the common circumpolar Antarctic echinoid *Sterechinus neumayeri*. Mar Ecol Prog Ser **330:** 139-147

Buckley LB, Kingsolver JG (2012) Functional and phylogenetic approaches to forecasting species' responses to climate change. Ann Rev Ecol Evol System **43**: 205-226

Byrne M (2011) Impact of ocean warming and ocean acidification on marine invertebrate life history stages: vulnerabilities and potential for persistence in a changing ocean. Oceanogr Mar Biol: Ann Rev **49:** 1-42

Byrne M, Ho M, Koleits L, Price C, King C, Virtue P, Tilbrook B, Lamare M (2013) Vulnerability of the calcifying larval stage of the Antarctic sea urchin *Sterechinus neumayeri* to near-future ocean acidification and warming. Glob Change Biol **19:** 2264-2275

Byrne M, Ho M, Selvakumaraswamy P, Nguyen HD, Dworjanyn SA, Davis AR (2009) Temperature, but not pH, compromises sea urchin fertilization and early

development under near-future climate change scenarios. Proc R Soc B: Biol Sci **276:** 1883-1888. doi:10.1098/rspb.2008.1935

Byrne M, Ho M, Wong E, Soars NA, Selvakumaraswamy P, Shepard-Brennand H, Dworjanyn SA, Davis AR (2011) Unshelled abalone and corrupted urchins: development of marine calcifiers in a changing ocean. Proc R Soc B: Biol Sci **278:** 2376-2383. doi:10.1098/rspb.2010.2404

Chown SL (2012) Trait-based approaches to conservation physiology: forecasting environmental change risks from the bottom up. Phil Trans R Soc B: Biol Sci **367:** 1615-1627

Chown SL, Gaston KJ (2008) Macrophysiology for a changing world. Proc R Soc B: Biol Sci **275:** 1469-1478

Clark D, Lamare M, Barker M (2009) Response of sea urchin pluteus larvae (Echinodermata: Echinoidea) to reduced seawater pH: a comparison among a tropical, temperate, and a polar species. Mar Biol **156:** 1125-1137

Clark MS, Peck LS (2009) HSP70 heat shock proteins and environmental stress in Antarctic marine organisms: a mini-review. Mar Genomics **2:** 11-18

Dawson TP, Jackson ST, House JI, Prentice IC, Mace GM (2011) Beyond predictions: biodiversity conservation in a changing climate. Sci **332:** 53-58

Delorme NJ, Sewell MA (2013) Temperature limits to early development of the New Zealand sea urchin *Evechinus chloroticus* (Valenciennes, 1846). J Thermal Biol **38:** 218-224

Díaz A, Féral J-P, David B, Saucède T, Poulin E (2011) Evolutionary pathways among shallow and deep-sea echinoids of the genus *Sterechinus* in the Southern Ocean. Deep-Sea Res Part II: Topical Studies in Oceanogr **58:** 205-211.

Dickson AG, Millero FJ (1987) A comparison of the equilibrium constants for the dissociation of carbonic acid in seawater media. Deep-Sea Res Part a-Oceanogr Res Papers **34:** 1733-1743. doi:10.1016/0198-0149(87)90021-5

Dickson AG, Sabine CL, Christian JR (Eds.) (2007) Guide to best practices for ocean CO_2 measurements. PICES Special Publication 3, 191 pp.

Dupont S, Thorndyke M (2009) Impact of CO_2-driven ocean acidification on invertebrates early life-history – What we know, what we need to know and what we can do. Biogeosc Discuss **6:** 3109–3131

Enzor LA, Zippay ML, Place SP (2013) High latitude fish in a high CO_2 world: Synergistic effects of elevated temperature and carbon dioxide on the metabolic rates of Antarctic notothenioids. Comp Biochem Physiol Part A: Molec Integrat Physiol **164:** 154-161

Ericson JA, Ho MA, Miskelly A, King CK, Virtue P, Tilbrook B, Byrne M (2012) Combined effects of two ocean change stressors, warming and acidification, on fertilization and early development of the Antarctic echinoid *Sterechinus neumayeri*. Polar Biol **35:** 1027-1034. doi:10.1007/s00300-011-1150-7

Evans TG, Chan F, Menge BA, Hofmann GE (2013) Transcriptomic responses to ocean acidification in larval sea urchins from a naturally variable pH environment. Molec Ecol **22:** 1609-1625

Evans TG, Hofmann GE (2012) Defining the limits of physiological plasticity: how gene expression can assess and predict the consequences of ocean change. Phil Trans R Soc B: Biol Sci **367:** 1733-1745

Fabry VJ, McClintock JB, Mathis JT, Grebmeier JM (2009) Ocean acidification at high latitudes: The bellweather. Oceanogr **22:** 160-171

Fangue NA, O'Donnell MJ, Sewell MA, Matson PG, MacPherson AC, Hofmann GE (2010) A laboratory-based, experimental system for the study of ocean acidification effects on marine invertebrate larvae. Limnol Oceanogr Meth **8:** 441-452. doi:10.4319/lom.2010.8.441

Feely RA (2004) Impact of anthropogenic CO_2 on the $CaCO_3$ system in the oceans. Science **305:** 362-366. doi:10.1126/science.1097329

Findlay HS, Kendall MA, Spicer JI, Widdicombe S (2009) Post-larval development of two intertidal barnacles at elevated CO_2 and temperature. Mar Biol **157:** 725-735. doi:10.1007/s00227-009-1356-1

Findlay HS, Kendall MA, Spicer JI, Widdicombe S (2010) Relative influences of ocean acidification and temperature on intertidal barnacle post-larvae at the northern edge of their geographic distribution. Estuar Coast and Shelf Sci 86:675-682. doi:10.1016/j.ecss.2009.11.036

Fyfe JC (2006) Southern Ocean warming due to human influence. Geophys Res Lett **33:** L19701

Gienapp P, Teplitsky C, Alho J, Mills J, Merilä J (2008) Climate change and evolution: disentangling environmental and genetic responses. Molec Ecol **17:** 167-178

Gille ST (2002) Warming of the Southern Ocean since the 1950s. Science **295:** 1275-1277. doi:10.1126/science.1065863

Giudice G, Mutolo V, Donatuti G (1968) Gene expression in sea urchin development. Develop Genes Evol **161:** 118-128

Giudice G, Sconzo G, Roccheri MC (1999) Studies on heat shock proteins in sea urchin development. Develop Growth Differ **41:** 375-380

Hammond LM, Hofmann GE (2010) Thermal tolerance of *Strongylocentrotus purpuratus* early life history stages: mortality, stress-induced gene expression and biogeographic patterns. Mar Biol **157:** 2677-2687. doi:10.1007/s00227-010-1528-z

Harvey BP, Gwynn-Jones D, Moore PJ (2013) Meta-analysis reveals complex marine biological responses to the interactive effects of ocean acidification and warming. Ecol Evol **3:** 1016-1030. doi:10.1002/ece3.516

Hoffmann AA, Sgrò CM (2011) Climate change and evolutionary adaptation. Nat **470:** 479-485

Hofmann GE, Buckley BA, Airaksinen S, Keen JE, Somero GN (2000) Heat-shock protein expression is absent in the Antarctic fish *Trematomus bernacchii* (family Nototheniidae). J Exp Biol **203:** 2331-2339

Hofmann GE, Lund SG, Place SP, Whitmer AC (2005) Some like it hot, some like it cold: the heat shock response is found in New Zealand but not Antarctic notothenioid fishes. J Exp Mar Biol Ecol **316:** 79-89

Hofmann GE, Smith JE, Johnson KS, Send U, Levin LA, Micheli F, Paytan A, Price NN, Peterson B, Takeshita Y, Matson PG, Crook ED, Kroeker KJ, Gambi MC, Rivest EB, Frieder CA, Yu PC, Martz TR (2011) High-frequency dynamics of ocean pH: a

multi-ecosystem comparison. PLoS One **6:** e28983. doi:10.1371/journal.pone.0028983

Hönisch B, Ridgwell A, Schmidt DN, Thomas E, Gibbs SJ, Sluijs A, Zeebe R, Kump L, Martindale RC, Greene SE, Kiessling W, Ries J, Zachos JC, Royer DL, Barker S, Marchitto TM, Jr., Moyer R, Pelejero C, Ziveri P, Foster GL, Williams B (2012) The geological record of ocean acidification.Science**335:** 1058-1063. doi:10.1126/science.1208277

Howard-Ashby M, Materna SC, Brown CT, Tu Q, Oliveri P, Cameron RA, Davidson EH (2006) High regulatory gene use in sea urchin embryogenesis: Implications for bilaterian development and evolution. Develop Biol **300:** 27-34

Hunt BM, Hoefling K, Cheng CC (2003) Annual warming episodes in seawater temperatures in McMurdo Sound in relationship to endogenous ice in notothenioid fish. Antarct Sci **15:** 333-338

IPCC (2007) Contribution of Working Group II to the Fourth Assessment Report of the Intergovernmental Panel on Climate Change. (eds.) ML Parry, OF Canziani, JP Palutikof, PJ van der Linden and CE Hanson. Cambridge University Press, Cambridge, United Kingdom and New York, NY, USA.

Kelly MW, Hofmann GE (2012) Adaptation and the physiology of ocean acidification. Func Ecol **27:** 980-990. doi:10.1111/j.1365-2435.2012.02061.x

Kelly MW, Padilla-Gamiño JL, Hofmann GE (2013) Natural variation and the capacity to adapt to ocean acidification in the keystone sea urchin *Strongylocentrotus purpuratus*. Glob Change Biol **19:** 2536-2546. doi:10.1111/gcb.12251

Kurihara H (2008) Effects of CO_2-driven ocean acidification on the early developmental stages of invertebrates. Mar Ecol Prog Ser **373:** 275-284

Lee YH, Song M, Lee S, Leon R, Godoy SO, Canete I (2004) Molecular phylogeny and divergence time of the Antarctic sea urchin (*Sterechinus neumayeri*) in relation to the South American sea urchins. Antarct Sci **16:** 29-36

Littlepage JL (1965) Oceanographic investigations in McMurdo sound, Antarctica. Antarct Res Ser **5:** 1-37

Marcott SA, Shakun JD, Clark PU, Mix AC (2013) A reconstruction of regional and global temperature for the past 11,300 years. Science **339:** 1198-1201

Martz TR, Connery JG, Johnson KS (2010) Testing the Honeywell Durafet (R) for seawater pH applications. Limnol Oceanogr Meth **8:** 172-184. doi:10.4319/lom.2010.8.172

Matson PG (2012) Ocean acidification in nearshore marine ecosystems: natural dynamics of ocean pH variation and impacts on sea urchin larvae. Dissertation, University of California Santa Barbara

Matson PG, Martz TR, Hofmann GE (2011) High-frequency observations of pH under Antarctic sea ice in the southern Ross Sea. Antarct Sci **23:** 607-613. doi:10.1017/s0954102011000551

McClintock J, Ducklow H, Fraser W (2008) Ecological responses to climate change on the Antarctic Peninsula. Am Sci **96:** 302-310

McNeil BI, Matear RJ (2008) Southern Ocean acidification: A tipping point at 450-ppm atmospheric CO_2. Proc Natl Acad Sci **105:** 18860-18864. doi:10.1073/pnas.0806318105

Mehrbach C, Culberso.Ch, Hawley JE, Pytkowic.Rm (1973) Measurement of apparent dissociation constants of carbonic acid in seawater at atmospheric pressure. Limnol Oceanogr **18:** 897-907

Montes-Hugo M, Doney SC, Ducklow HW, Fraser W, Martinson D, Stammerjohn SE, Schofield O (2009) Recent changes in phytoplankton communities associated with rapid regional climate change along the western Antarctic Peninsula. Science **323:** 1470-1473

Naveen R, Lynch HJ, Forrest S, Mueller T, Polito M (2012) First direct, site-wide penguin survey at Deception Island, Antarctica, suggests significant declines in breeding chinstrap penguins. Polar Biol **35:** 1879-1888

O'Donnell MJ, Hammond LM, Hofmann GE (2008) Predicted impact of ocean acidification on a marine invertebrate: elevated CO_2 alters response to thermal stress in sea urchin larvae. Mar Biol **156:** 439-446. doi:10.1007/s00227-008-1097-6

Orr JC, Fabry VJ, Aumont O, Bopp L, Doney SC, Feely RA, Gnanadesikan A, Gruber N, Ishida A, Joos F, Key RM, Lindsay K, Maier-Reimer E, Matear R, Monfray P, Mouchet A, Najjar RG, Plattner G-K, Rodgers KB, Sabine CL, Sarmiento JL, Schlitzer R, Slater RD, Totterdell IJ, Weirig M-F, Yamanaka Y, Yool A (2005) Anthropogenic ocean acidification over the twenty-first century and its impact on calcifying organisms. Nature **437:** 681-686. doi:10.1038/nature04095

Parker LM, Ross PM, O'Connor WA (2009) The effect of ocean acidification and temperature on the fertilization and embryonic development of the Sydney rock oyster *Saccostrea glomerata* (Gould 1850). Glob Change Biol **15:** 2123-2136. doi:10.1111/j.1365-2486.2009.01895.x

Parker LM, Ross PM, O'Connor WA (2010) Comparing the effect of elevated pCO_2 and temperature on the fertilization and early development of two species of oysters. Mar Biol **157:** 2435-2452. doi:10.1007/s00227-010-1508-3

Parmesan C, Yohe G (2003) A globally coherent fingerprint of climate change impacts across natural systems. Nature **421:** 37-42

Pearse JS, Giese AC (1966) Food, reproduction and organic constitution of common Antarctic echinoid *Sterechinus neumayeri* (Meissner). Biol Bull **130:** 387-401. doi:10.2307/1539745

Peck LS (2005) Prospects for survival in the Southern Ocean: vulnerability of benthic species to temperature change. Antarct Sci **17:** 497-507. doi:10.1017/s0954102005002920

Peck LS, Clark MS, Morley SA, Massey A, Rossetti H (2009) Animal temperature limits and ecological relevance: effects of size, activity and rates of change. Func Ecol **23:** 248-256. doi:10.1111/j.1365-2435.2008.01537.x

Peck LS, Morley SA, Clark MS (2010) Poor acclimation capacities in Antarctic marine ectotherms. Mar Biol **157:** 2051-2059. doi:10.1007/s00227-010-1473-x

Pespeni MH, Sanford E, Gaylord B, Hill TM, Hosfelt JD, Jaris HK, LaVigne Ml, Lenz EA, Russell AD, Young MK (2013) Evolutionary change during experimental ocean acidification. Proc Natl Acad Sci **110:** 6937-6942

Place SP, Zippay ML, Hofmann GE (2004) Constitutive roles for inducible genes: evidence for the alteration in expression of the inducible hsp70 gene in Antarctic notothenioid fishes. Am J Physiol – Regul Integr Comp Physiol **287:** R429-R436. doi:10.1152/ajpregu.00223.2004

Pörtner HO, Farrell AP (2008) Physiology and climate change. Sci **322:** 690-692. doi:10.1126/science.1163156

Pörtner HO, Peck L, Somero G (2007) Thermal limits and adaptation in marine Antarctic ectotherms: an integrative view. Phil Trans R Soc B: Biol Sci **362:** 2233-2258. doi:10.1098/rstb.2006.1947

Pörtner HO, Peck LS, Somero GN (2012) Mechanisms defining thermal limits and adaptation in marine ectotherms: an integrative view. Antarctic Ecosystems: An Extreme Environment in a Changing World. John Wiley & Sons, Ltd, Chichester, UK. doi:10.1002/9781444347241.ch13

Robbins LL, Hansen ME, Kleypas JA, Meylan SC (2010) CO2calc—A user-friendly seawater carbon calculator for Windows, Max OS X, and iOS (iPhone). U.S. Geological Survey Open-File Report 2010–1280

Roccheri MC, Sconzo G, Larosa M, Oliva D, Abrignani A, Giudice G (1986) Response to heat shock of different sea urchin species. Cell Differ **18:** 131-135. doi:10.1016/0045-6039(86)90007-2

Schaum E, Rost B, Millar AJ, Collins S (2013) Variation in plastic responses to ocean acidification in a globally distributed picoplankton species. Nat Clim Change **3:** 298-302

Sconzo G, Ferraro MG, Amore G, Giudice G, Cascino D, Scardina G (1995) Activation by heat shock of hsp70 gene transcription in sea urchin embryos. Biochem Biophys Res Comm **217:** 1032-1038. doi:10.1006/bbrc.1995.2873

Sewell MA, Millar RB, Yu PC, Kapsenberg L, Hofmann GE (2014) Ocean acidification and fertilization in the Antarctic sea urchin *Sterechinus neumayeri*: the importance of polyspermy. Environ Sci Technol **48:** 713-722

Sewell MA, Hofmann GE (2011) Antarctic echinoids and climate change: a major impact on the brooding forms. Glob Change Biol **17:** 734-744

Sewell MA, Young CM (1999) Temperature limits to fertilization and early development in the tropical sea urchin *Echinometra lucunter*. J Exp Mar Biol Ecol **236:** 291-305. doi:10.1016/s0022-0981(98)00210-x

Sheppard Brennand H, Soars N, Dworjanyn SA, Davis AR, Byrne M (2010) Impact of ocean warming and ocean acidification on larval development and calcification in the sea urchin *Tripneustes gratilla*. PLoS One **5:** e11372. doi:10.1371/journal.pone.0011372

Somero GN (2012) The physiology of global change: linking patterns to mechanisms. Ann Rev Mar Sci **4:** 39-61

Stammerjohn SE, Martinson DG, Smith RC, Iannuzzi RA (2008) Sea ice in the western Antarctic Peninsula region: Spatio-temporal variability from ecological and climate change perspectives. Deep-Sea Res Part II: Top Stud Oceanogr **55:** 2041-2058

Stanwell-Smith D, Peck LS (1998) Temperature and embryonic development in relation to spawning and field occurrence of larvae of three Antarctic echinoderms. Biol Bull **194:** 44-52. doi:10.2307/1542512

Steinberg DK, Martinson DG, Costa DP (2012) Two decades of pelagic ecology in the Western Antarctic Peninsula. Oceanogr **25:** 56-67

Sunday JM, Bates AE, Dulvy NK (2012) Thermal tolerance and the global redistribution of animals. Nat Clim Change **2:** 686-690

Sunday JM, Crim RN, Harley CDG, Hart MW (2011) Quantifying rates of evolutionary adaptation in response to ocean acidification. PLoS One **6:** e22881. doi:10.1371/journal.pone.0022881

Takahashi T, Sutherland SC, Wanninkhof R, Sweeney C, Feely RA, Chipman DW, Hales B, Friederich G, Chavez F, Sabine C, et al. (2009) Climatological mean and decadal change in surface ocean pCO_2, and net sea-air CO_2 flux over the global oceans. Deep-Sea Res Part II: Top Stud Oceanogr **56:** 554-577

Terblanche JS, Hoffmann AA, Mitchell KA, Rako L, le Roux PC, Chown SL (2011) Ecologically relevant measures of tolerance to potentially lethal temperatures. J Exp Biol **214:** 3713-3725

Tomanek L (2010) Variation in the heat shock response and its implication for predicting the effect of global climate change on species' biogeographical distribution ranges and metabolic costs. J Exp Biol **213:** 971-979

Turley C, Eby M, Ridgwell AJ, Schmidt DN, Findlay HS, Brownlee C, Riebesell U, Fabry VJ, Feely RA, Gattuso JP (2010) The societal challenge of ocean acidification. Mar Pollut Bull **60:** 787-792. doi:10.1016/j.marpolbul.2010.05.006

Visser ME (2008) Keeping up with a warming world; assessing the rate of adaptation to climate change. Proc R Soc B: Biol Sci **275:** 649-659

Yu PC, Sewell MA, Matson PG, Rivest EB, Kapsenberg L, Hofmann GE (2013) Growth attenuation with developmental schedule progression in embryos and early larvae of *Sterechinus neumayeri* raised under elevated CO_2. PLoS One **8:** e52448

Zippay ML, Hofmann GE (2010a) Effect of pH on gene expression and thermal tolerance of early life history stages of Red Abalone (*Haliotis rufescens*). J Shellfish Res **29:** 429-439. doi:10.2983/035.029.0220

Zippay ML, Hofmann GE (2010b) Physiological tolerances across latitudes: thermal sensitivity of larval marine snails (*Nucella* spp.). Mar Biol **157:** 707-714

IV. Ocean pH time-series and drivers of variability along the northern Channel Islands, California, USA

A. Abstract

Eastern boundary current systems (EBCSs) experience dynamic fluctuations in seawater pH due to coastal upwelling and primary production. The lack of high-resolution pH observations in EBCSs limits the ability to relate field pH exposures to performance of coastal marine species under future ocean change (acidification, warming). This three-year study describes spatio-temporal pH variability across the northern Channel Islands, along a persistent temperature gradient (1 - 4 °C) within the eastern boundary California Current System. pH and CTD-oxygen sensors were deployed on island piers in eelgrass and kelp habitat and on a subtidal mooring. Due to event-scale primary production, the temperature gradient across the islands did not manifest in a pH gradient. We resolved spatial pH variability on diel (0.05 - 0.2, photosynthesis), event-scale (< 0.1 - 0.2, upwelling, phytoplankton blooms, wind relaxation), and seasonal (0.06, warming) time frames. From 2012 to 2014 in the kelp forest, summer mean pH_T (8.01 - 8.02) and magnitude of diel pH_T cycles (0.12 – 0.10) were comparable year-to-year, despite 2.1 °C warming. Compared to nearby mainland sites, the northern Channel Islands experience limited exposures to low pH with 99% of all pH_T observations > 7.8. The lowest pH observations (< 1 SD below mean pH) occurred under either warm (respiration during warm nights) or cold (advection of upwelled water) temperatures. We emphasize the importance of incorporating site-specific environmental variability in studies of ocean change biology, particularly in the design of multi-stressor experiments.

B. Introduction

Coastal marine ecosystems are complex environments with spatio-temporal variability in productivity and bulk water mass movement. Physical and biological processes give rise to spatially unique pH-seascapes and are predicted to change with climate change (Hauri et al. 2013; Hoegh-Guldberg et al. 2014; Hofmann et al. 2011; Takeshita et al. 2015). Particularly, eastern boundary current systems (EBCSs) are predicted to be one of the first coastal ecosystems to cross thresholds of ocean acidification due to coastal upwelling (Gruber et al. 2012). While upwelling is a natural phenomenon, the associated on-shore delivery of low pH water is exacerbated by ocean acidification (Feely et al. 2008). The heightened sensitivity of EBCSs to ocean change has already been realized in economic losses of shellfish production (Barton et al. 2012). The intensity of upwelling favorable winds have increased in EBCSs (Sydeman et al. 2014) and upwelling events are predicted to increase in duration and strength with future climate change (Wang et al. 2015). As upwelling replenishes surface waters with nutrients yielding phytoplankton blooms that draw pCO_2 down to below atmospheric equilibrium (Hales et al. 2005), changes in upwelling may also alter coastal pH variability through influences on primary production in the future. Our understanding of present-day patterns in coastal carbon chemistry is often under-described making it challenging to predict which coastal zones will be resistant or vulnerable to the effects of ocean change. In an effort to increase the knowledge base on coastal pH variability in an EBCS, we examined pH heterogeneity across a small geographic scale and link patterns to local and regional processes that are relevant for marine species and coastal management.

As an EBCS with seasonally strong upwelling, the California Current System (CCS), extending from south of British Columbia to Baja California, is extremely vulnerable to the effects of ocean acidification (Feely et al. 2008; Gruber et al. 2012; Hauri et al. 2013). Summertime upwelling contributes to seasonal and spatial pH variability in the CCS (Hauri et al. 2013). Individual upwelling events have increased in duration and intensity from 1967 to 2010 (Iles et al. 2012). Both field data and model simulations of future conditions show that near-shore pH is lower than offshore surface waters (Feely et al. 2008; Gruber et al. 2012). The vulnerability to ocean acidification thus lies in coastal habitats. Near-shore (50 km) CCS waters already exhibit pH levels outside of pre-industrial conditions, and a complete departure of present-day pH variability envelope is predicted to occur as early as 2040 (Hauri et al. 2013). While incorporating seasonal pH changes helps refine predictive models, extensive documentation of event-scale to short-term pH variability are lacking, making model predictions uncertain in relation to species' future exposures.

The lack of time-series pH data to inform experiments hampers the understanding of organismal pH tolerance and adaptation. Observations from autonomous pH sensors document patterns of natural pH variability in coastal ecosystems that often meet or exceed the magnitude of predicted global ocean acidification (Hofmann et al. 2011). Use of high-resolution, autonomously-collected environmental data provides a major advantage over manual sampling through the ability to identify short-term cycles and onset of events (e.g. Frieder et al. 2012). Such data are necessary to link habitat seawater chemistry to organismal pH tolerance (e.g. Frieder et al. 2014; Kapsenberg and Hofmann 2014; Price et al. 2012; Yu et al. 2011) and extend our understanding of future coastal ocean pH variability (Takeshita et al. 2015) and ocean acidification trends (Keller et al. 2014). Specifically for biological

experiments conducted on species in the CCS, treatments designed to mimic future pH conditions often do not actually extended outside the range of the species' estimated present-day pH (pCO_2) exposure (Reum et al. 2015). Moreover, a handful of such experiments revealed negative effects of present-day conditions (Reum et al. 2015), which have also been observed in the wild and in aquaculture production (Barton et al. 2012; Bednaršek et al. 2014). Although there is evidence that some species have the potential to adapt to changing pH (e.g. Kelly et al. 2013; Malvezzi et al. 2015; Pespeni et al. 2013), these efforts are in their infancy and require detailed knowledge of environmental pH exposures. Therefore, we provide such environmental data and document pH variability in a sub-region of the CCS.

One distinctive geographic feature in the CCS is the Santa Barbara Channel (SBC), located in the Southern California Bight (Figure IV-1). The SBC is formed by a ~ 90° turn in the coastline at Pt. Conception and bound by the four northern Channel Islands (San Miguel, Santa Rosa, Santa Cruz, and Anacapa Island). The SBC is ~100 km long and 40 km wide with a central basin depth of 500 m, a sill at both the eastern (220 m) and western (430 m) entrance, and shallow connections between the islands (~40m depth) (Harms and Winant 1998). In the Bight, equatorward flow is influenced by the California Current (cold, near-surface, 200-300 km offshore) and coastal poleward flow is facilitated by the Southern California Countercurrent (warm, high salinity, flow over the continental shelf that is strongest in the fall and winter) and the California Undercurrent (deep flow along the continental slope) (Dong et al. 2009; Lynn and Simpson 1987). In the SBC, these dynamics result in flow that is generally east-west along the mainland and west-east along the islands and generate a nearly persistent cyclonic flow within the SBC (Dong et al. 2009; Harms and Winant 1998).

Figure IV-1. Three-year (2012 - 2014) temperature composite of the Santa Barbara Channel region. Study sites are noted: San Miguel Island north mooring (SMN, red circle), Prisoner's Harbor pier on Santa Cruz Island (PRZ, green circle), and Anacapa Island Landing Cove pier (ALC, blue circle). Diamond indicates National Data Buoy Center station 46054.

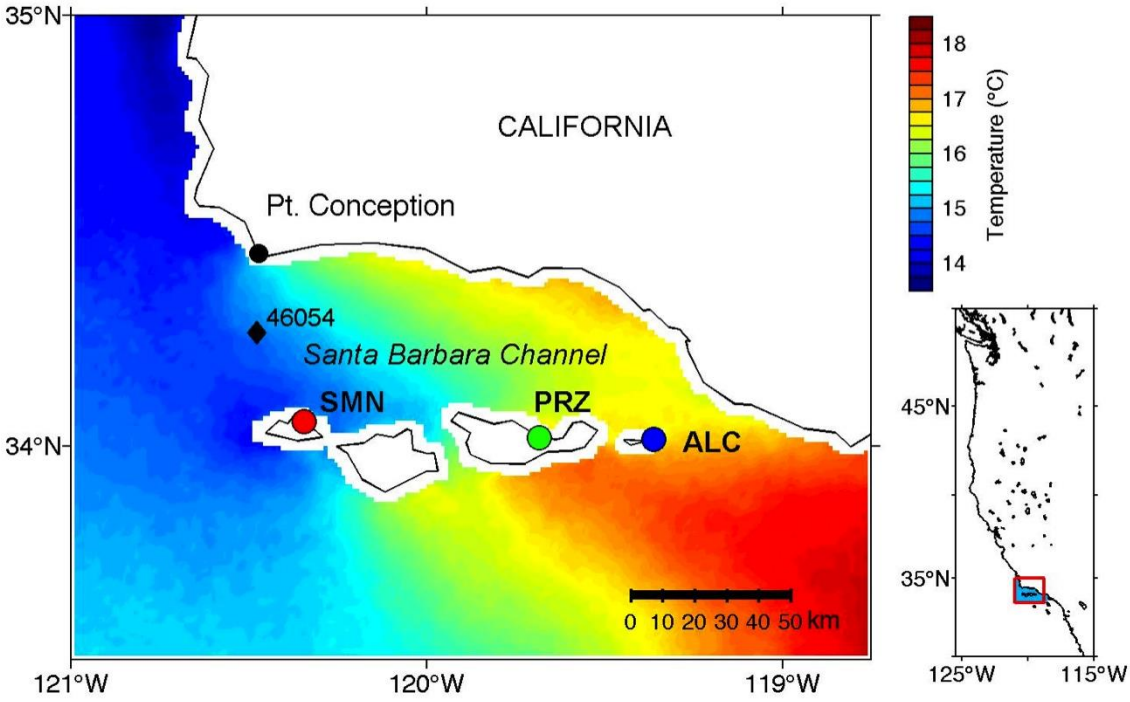

Due to the opposing flows and unique bathymetry and orientation of the SBC within the Bight, multiple abiotic gradients are established along the islands (Harms and Winant 1998), suggesting that there may be a gradient in pH as well. A persistent temperature difference of 1-4°C is maintained between San Miguel Island and Anacapa Island (Harms and Winant 1998), with a front that oscillates along the center coastline of Santa Cruz Island (Selkoe et al. 2006). Coastal upwelling north of Pt. Conception yields cool temperatures in the west and poleward flow brings in warm water in from the east (Harms and Winant 1998; Lagerloef and Bernstein 1988; Otero and Siegel 2004). In addition, Pt. Conception creates a wind shadow such that both wind and current strength decrease from west to east along the islands (Dorman and Winant 2000; Harms and Winant 1998). During upwelling-favorable wind stress, equatorward flow north of Pt. Conception extends along the islands (Harms and Winant 1998). Given the stronger winds, currents, and cooler temperatures at San Miguel Island, the pH signatures of upwelled waters may manifest as well. As part of this study, we test the hypothesis that pH decreases from west to east along the coastline of the Channel Islands. Identification of persistent pH gradients across a species' biogeographic range could aid studies of local pH adaptation and acclimatization (Hofmann et al. 2014). In this effort, we quantify pH variability along the northern Channel Islands and link observations to local and regional scale physical and biological drivers.

C. Methods

1. Sites and sensor deployments

To test the hypothesis that abiotic environmental gradients also lead to a pH gradient, we quantified pH variability on different temporal and spatial scales. SeaFET pH sensors (Martz et al. 2010) and Conductivity, Temperature, Depth, and Oxygen sensors (CTDO sensors,

Sea-Bird Electronics 37-SMP-ODO MicroCAT C-T-ODO (P) Recorder) were deployed at three sites along the northern Channel Islands: (1) Anacapa Island Landing Cove pier (ALC, 34°00.985'N, 119°21.724'W) in a marine reserve with kelp forest habitat, (2) Santa Cruz Island Prisoner's Harbor pier (PRZ, 34°01.225'N, 119°41.057'W) surrounded by a large shallow eelgrass bed (*Zostera pacifica*), and (3) San Miguel Island northern subtidal mooring (SMN, 34°03.417'N, 120°20.731'W) at 6 m in open water over a sandy bottom at 18 m depth (Figure IV-1). Sensors at ALC and PRZ were deployed at 3 - 4 m depth and < 1 m from the benthos on a pier piling. For reference, ALC and PRZ represent environmental conditions relevant to benthic marine invertebrates whereas SMN reflects environmental conditions relevant to pelagic life stages such as free-swimming invertebrate larvae. The islands are part of the Channel Islands National Park and National Marine Sanctuary.

pH sensors were first deployed in 2012 at ALC and PRZ and recorded pH and temperature every 30 min for 10 sec reading periods. pH sensors were not pumped. In May 2013, CTDO sensors were deployed in addition to pH sensors at ALC and PRZ. CTDO sensors were actively pumped through an anti-fouling passage and temperature, salinity, pressure, and dissolved oxygen were recorded every 15 min. In August 2013, the sensor array from PRZ was moved to SMN for a one-year overlapping period of data collection with ALC. During this time, a pH sensor was intermittently deployed at PRZ. At each site, sensors were swapped every 2 - 3 months. SeaFET sensor surfaces did not exhibit biofouling upon recoveries. Following the last CTDO sensor deployments in September 2014, sampling frequency on pH sensors was increased to 20 min. Following linear interpolation when necessary, all data are reported on a 30 min frequency.

2. Data processing

Calibration samples for SeaFET sensors were collected 1 – 8 times during each 2 - 3 month deployment via SCUBA, free diving, or a GO-FLOW (General Oceanics) bottle drop from the pier following Standard Operating Procedures (SOP) 1 (Dickson et al. 2007). Samples were fixed immediately with saturated mercuric chloride. Water samples were analyzed for $pH_{25\,^{\circ}C}$ (SOP 6b, using m-cresol purple from Sigma-Aldrich®), total alkalinity (SOP 3b, using open-cell titrator Mettler-Toledo T50) (Dickson et al. 2007), and salinity (YSI 3100 Conductivity Instrument) when no corresponding salinity measurements was available from a CTDO sensor. In situ pH_T (total hydrogen ion scale) was calculated using either temperature recorded by the SeaFET or CTDO sensor when available and using CO_2 constants from Mehrbach et al. (1973) refit by Dickson and Millero (1987) (CO2Calc, Robbins et al. 2010). All pH data are reported as pH_T.

SeaFET data processing followed methods from Bresnahan et al. (2014) for single and multiple calibration samples using Matlab (R2012b). When SeaFET deployments were paired with CTDO sensors (May 2013 – September 2014), temperature data from the CTDO sensors was used to correct for the offset associated with the uncalibrated SeaFET thermistor. CTDO sensors underwent factory calibration at the start and end of the project. Sensors were rinsed with DI water and dilute Triton-X, between deployments. CTDO data was interpolated onto the SeaFET sampling period and all data are reported in Coordinated Universal Time, unless specified otherwise. One 24-hour gap of CTDO data was interpolated to match the deployment length of the pH sensor at ALC when necessary for computations. Rare instances where pH declined to below pH 7.7, within two observations and independent of changes in temperature, were removed for quality control. Oxygen

saturation recorded by the CTDO sensor was converted to dissolved oxygen (DO) μmol kg^{-1} using the oxygen solubility combined fit conversion equation from (García and Gordon 1992).

3. Data analysis

Data were analyzed in raw form, as monthly means, and following a 48-h high-pass filter (to remove seasonal and event-scale signals) or low-pass filter (to remove diel cycles). The maximum daily range of pH observations within a 24 h period was calculated using 48-h high-pass filtered data and reported as 'diel pH cycles' (i.e. twice the amplitude). To investigate pH variability independent of temperature effects on pH, pH_T was normalized to 16 °C ($pH_{T\ N16°C}$). Comparisons between SMN and ALC were made using data from exactly one year: 20 August 2013 to 20 August 2014. This same date range was used to calculate anomalies where the annual site-specific mean was subtracted from the time-series (pH, oxygen, temperature, salinity). Ranges in pH_T are reported from 0.5^{th} and 99.5^{th} percentiles. In the interest of improving the design of ocean acidification research (Reum et al. 2015), low pH events were investigated in relation to temperature. Due to the lack of salinity and total alkalinity data throughout the three-year study period, we did not calculate other carbonate parameters (e.g. pCO_2, aragonite saturation state).

To investigate potential regional drivers of the observed pH variability along the northern Channel Islands, observations of regional sea surface temperature (SST, °C), Chlorophyll-a concentrations (Chl-a, mg m^{-3}), and wind stress were investigated. Satellite-derived daily SST and Chl-a images for the SBC region were downloaded from the Scripps Photobiology Group (http://spg.ucsd.edu/Satellite_Data/California_Current/, Kahru et al. 2012) and processed for composite SST and Chl-a maps during periods of positive and

negative pH anomalies. For a given time interval, all cloud-free pixels were averaged across daily images. As a guideline, Chl-a threshold indicating presence of phytoplankton blooms was considered ≥ 2 mg m^{-3} (Otero and Siegel 2004). We divided time-series pH data into phases with corresponding SST and Chl-a maps and CTDO observations to highlight drivers of pH variability. Wind data were downloaded from the National Data Buoy Center (http://www.ndbc.noaa.gov/) buoy 46054, located at the western end of the SBC, and rotated onto its principle axes. Positive wind stress denotes alongshore equatorward winds. All analyses were performed in Matlab (R2012b).

4. Error estimates

Errors in pH_T measurements of field samples are largely due to the use of unpurified m-cresol dye (0.02, Liu et al. 2011), user error (± 0.006, Kapsenberg et al. 2015), and spatio-temporal mismatch of the calibration sample as determined from multiple calibration samples in one deployment (± 0.010 for SMN, ± 0.026 for PRZ, ± 0.005 for ALC). The resultant estimated standard uncertainty of pH data differed by site and is ± 0.023 (SMN), ± 0.033 (PRZ), and ± 0.022 (ALC). The error in pH due to use of uncalibrated SeaFET thermistor (deployments February 2012 – May 2013, September 2014 - May 2015) was ± 0.005 and did not impact the estimated standard uncertainty. The accuracy of field samples is less than the resolution of SeaFET pH sensors (0.001) and pH is reported 0.01.

Post-calibration of CTDO sensors revealed negligible drifts in oxygen, salinity, and temperature. A total of six in situ water samples were collected for Winkler determination for dissolved oxygen (Wetzel and Likens 1991) and showed a mean 0.9 ± 0.9 % positive offset from sensor observations (maximum offset was 2.4 %). Post-calibration indicated oxygen sensor drift of < 1-2 % across the three instruments. The data were not corrected for

drift of the oxygen sensor and accuracy for this data is ± 2 %. A small drift in conductivity resulted in a salinity accuracy of ± 0.02. Temperature drift was < 0.001 °C for all sensors with a reported accuracy of ± 0.002 °C. Data were not corrected for sensor drift.

D. Results

1. Spatial range of pH observations

The data collected across the islands varied on temporal and spatial scales (Figure IV-2). Patterns in pH variability were detected on diel, event, seasonal time scales, with limited inter-annual variability. For all data collected, mean pH_T (± SD) at each site was: SMN 8.05 ± 0.05, PRZ 8.00 ± 0.06, and ALC 8.01 ± 0.04. At each site, 99% of pH_T observations fell between 7.92 - 8.16, 7.81 - 8.16, and 7.88 - 8.12, at SMN, PRZ and ALC, respectively. PRZ exhibited the widest range in pH_T observations 0.36 and SMN and ALC had a pH_T range of 0.24. For periods < 48 h, the range in pH_T observations was reduced to 0.27 at PRZ and 0.21 to SMN and ALC, respectively (Figure IV-3).

During the overlapping deployment period at ALC and SMN (20 August 2013 to 20 August 2014), SMN exhibited a greater range in pH_T (0.24) and higher mean pH_T (8.05 ± 0.05) compared to ALC (8.02 ± 0.03), which exhibited a pH_T range of 0.18. These differences were due to distinct positive and negative event-scale (days to weeks) pH anomalies observed at SMN and do not support the hypothesis of a persistent pH gradient across the northern Channel Islands.

Figure IV-2. Complete pH and temperature time-series (a, b) and paired CTDO sensor data and wind stress time-series for a subset of the three-year study (c-g). Positive wind stress values are equatorward. Deployment period of CTDO sensors is marked by solid vertical lines in (a) and (b).

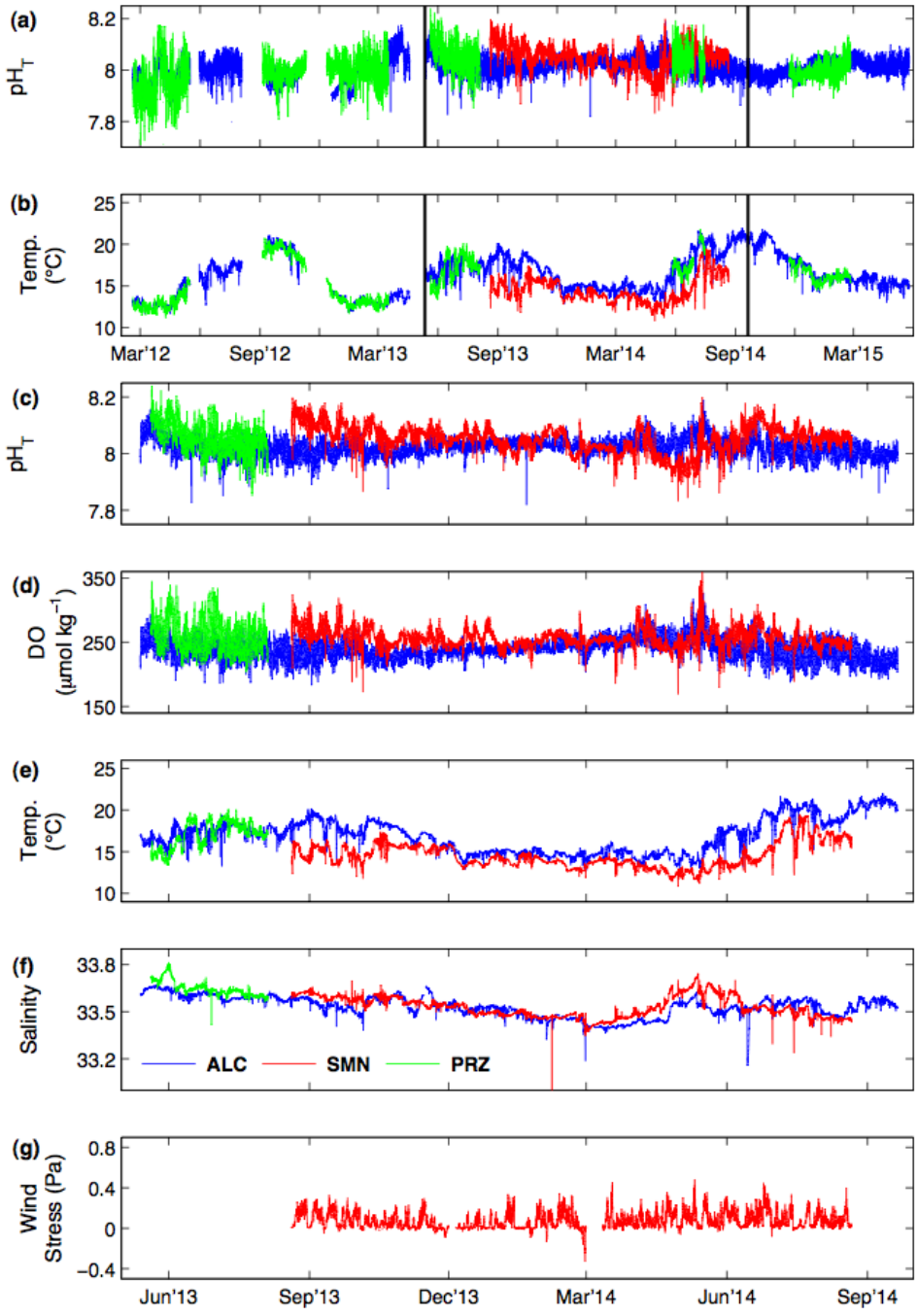

Figure IV-3. Time-series of 48 h low-pass filtered pH (a-c) and temperature (d-f) by site. Colors represent different years. Site codes are same as in Figure IV-1.

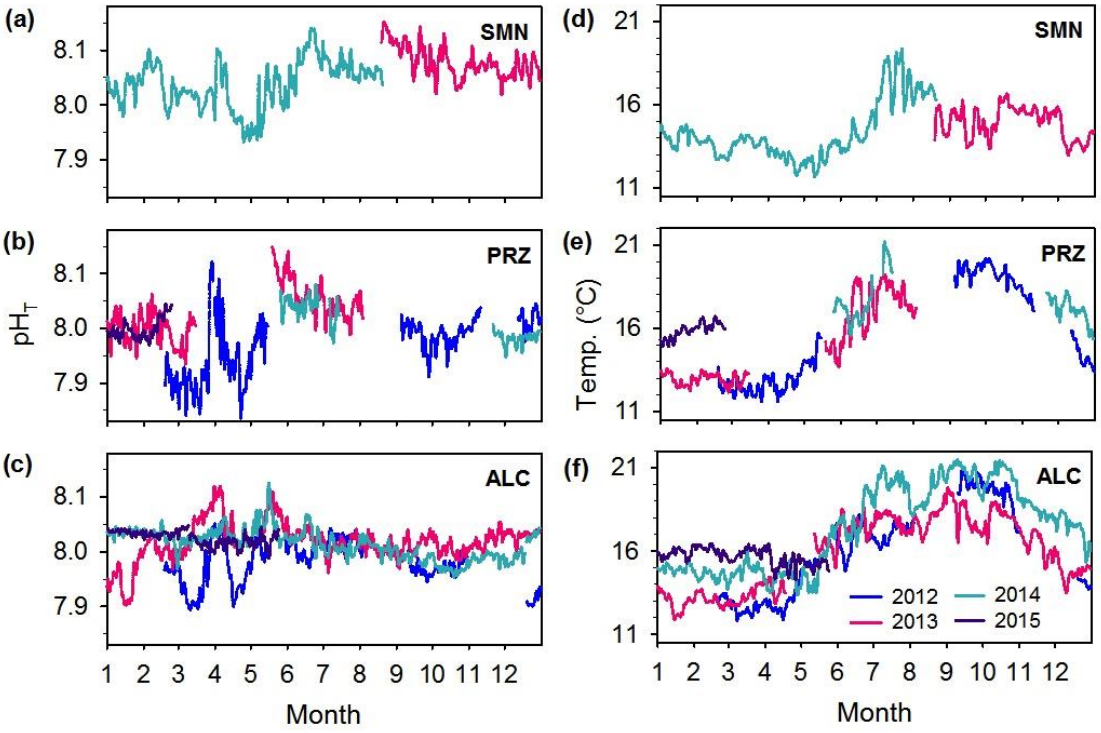

2. Diel pH cycles

Significant 24-h periodicities in pH were observed at all sites (Figure IV-4). The magnitude of diel pH cycles (twice the amplitude) was investigated following 48-h high-pass filtering to remove event-scale and seasonal signatures (Figure IV-5). In general, diel pH cycles at PRZ were larger and more variable than the other two sites, despite the fact that ALC and PRZ experienced similar thermal regimes (Figure IV-2). Peaks in the daily magnitude of pH change occurred at different times in the year at each site suggesting biotic, and not abiotic, processes govern this time-scale variability. Magnitude of diel pH cycles peaked in in spring, summer, or spring and fall, for PRZ (eelgrass), ALC (kelp forest), and SMN (open water), respectively. High-pass filtered oxygen and pH observations were positively correlated at all sites, with a stronger correlation at vegetated sites, ALC (R^2 = 0.91, F = 234156, $p < 0.001$, n = 23660) and PRZ (R^2 = 0.86, F = 2.3378, $p < 0.001$, n = 3637), compared to SMN (R^2 = 0.79, F = 64182, $p < 0.001$, n = 17437).

PRZ exhibited the largest seasonal change in diel pH_T cycles where cycles in April (0.20) were approximately tripled from November and December observations (0.07, 0.06). The largest diel pH cycles at PRZ occurred during months of lowest temperature and lowest mean pH (March, April). When comparing the vegetated sites, monthly mean diel pH cycles were always larger at PRZ compared to ALC. ALC exhibited a seasonal increase magnitude of diel pH_T cycles from, on average, 0.05 in winter to 0.10 in summer. At SMN, the magnitude of diel pH_T cycles peaked once in October (0.09) and again in May (0.11), which reflected an approximate doubling of diel pH cycles observed in winter and early spring despite being outside of vegetated habitat.

Figure IV-4. Power spectra for pH, temperature, oxygen, salinity, and pressure for all paired pH and CTDO sensor deployments. Site codes are same as in Figure IV-1.

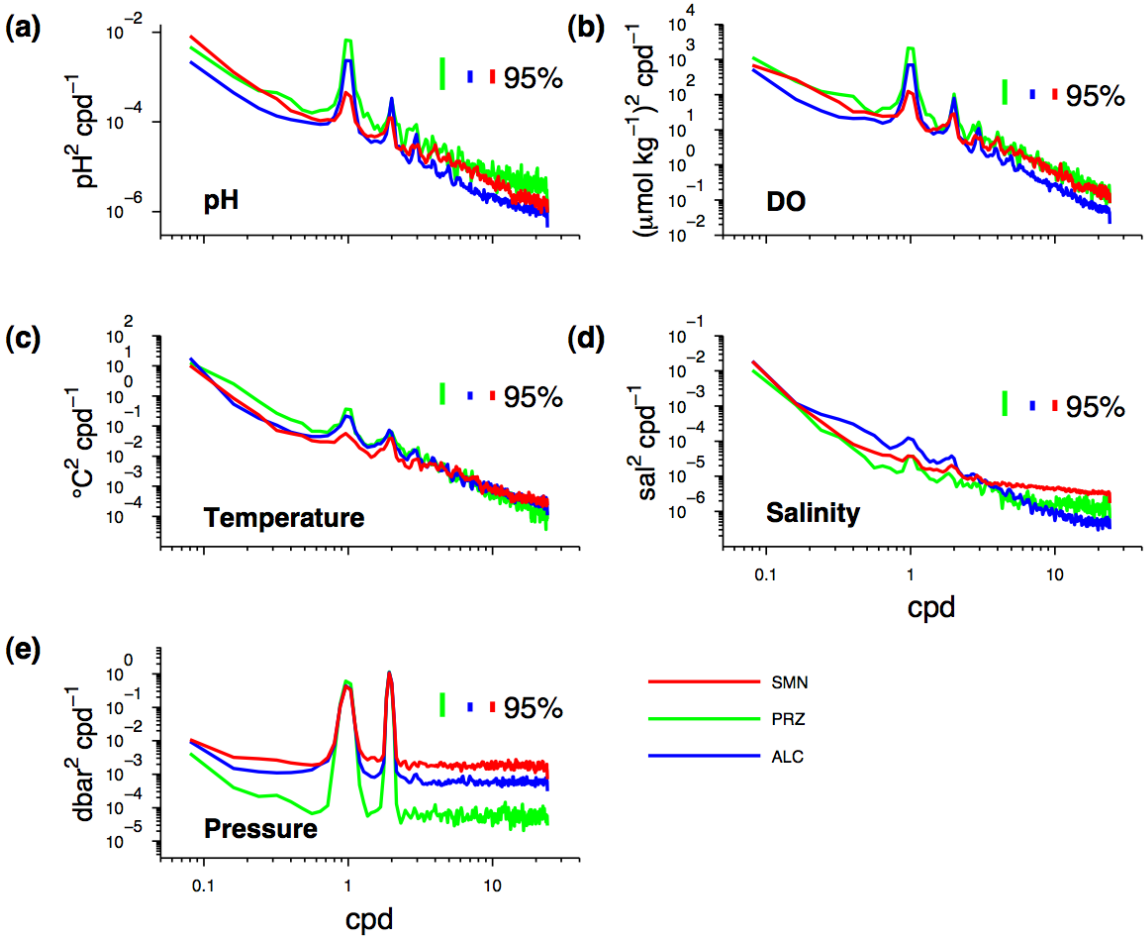

Figure IV-5. Seasonal evolution of diel pH cycles in open water (a, SMN), and in eelgrass (b, PRZ) and kelp forest (c, ALC) habitat. Tripling and doubling of diel pH cycles are shown on the right y-axis. Diel cycles were calculated following 48 h high-pass filtering. Dots represent daily observations colored by year. Squares denote combined-year monthly means ± SD. Site codes are same as in Figure IV-1.

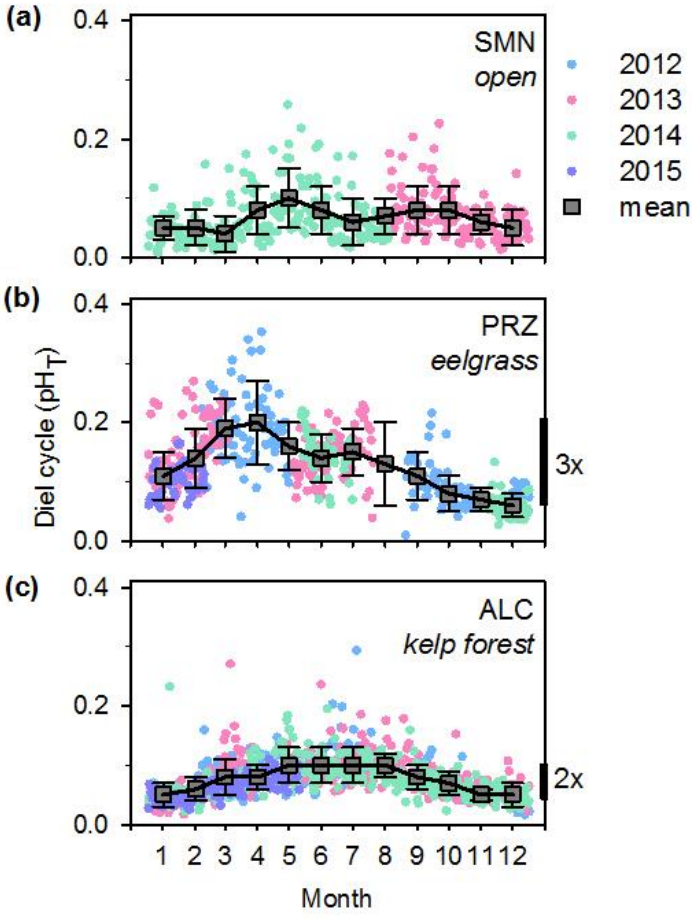

3. Event-scale variability

Event-scale pH anomalies were investigated and compared for SMN and ALC for the overlapping period of paired pH and CTDO sensor deployments. Three event-scale effects were discovered and were most apparent at SMN: (1) phytoplankton blooms (0.1 - 0.2 pH_T increase), (2) advection of upwelled water (0.1 pH_T decrease), and (3) wind relaxation (increased high-frequency, < 1 day, pH_T variability). To describe event-scale variability, we divided pH time-series data into district phases and investigated corresponding SST and Chl-a maps.

The first example describes a regionally restricted *phytoplankton bloom* that occurred during disparate pH anomalies at SMN and ALC. Here, a near-persistent positive pH and oxygen anomaly at SMN occurred from August to mid-October in 2013, but not at ALC (Figure IV-6, Phase I). During this anomaly, pH and oxygen oscillated above their annual mean and exhibited similar patters in variability. This event coincided with persistent observations of Chl-a concentrations indicative of phytoplankton blooms (Figure IV-6c). The bloom was restricted to the western end of the SBC and surrounded San Miguel Island but not Anacapa Island. The bloom subsided in the latter half of October into December at the same time that pH and oxygen turned non-anomalous at SMN (Figure IV-6, Phase II). Throughout phase I and II, pH remained slightly negatively anomalous at ALC. As (1) diel pH cycles at SMN were larger in September and October compared to November and December and (2) SMN is outside of vegetated habitat, the different patterns in pH anomalies at SMN compared to ALC are likely due to the phytoplankton blooms localized around San Miguel Island.

Figure IV-6. pH and oxygen anomalies (a, b) at SMN and ALC from August to December and corresponding surface Chl-a composites during two time periods: Phase I and II. Positive pH and oxygen anomalies (Phase I) were observed at SMN (red) but not at ALC (blue) during a phytoplankton bloom in the western end of the channel (c). Following disappearance of Chl-a in the channel (Phase II), pH and oxygen returned to non-anomalous conditions at SMN, matching observations at ALC. Bold time-series lines are 48 h low-pass filtered data. Time-series tick marks denote the 1st of the month. Dashed line indicates start of Phase II. Map coordinates are the same as in Figure IV-1. Chl-a composites represent means for cloud-free pixels using daily images. Site codes are same as in Figure IV-1.

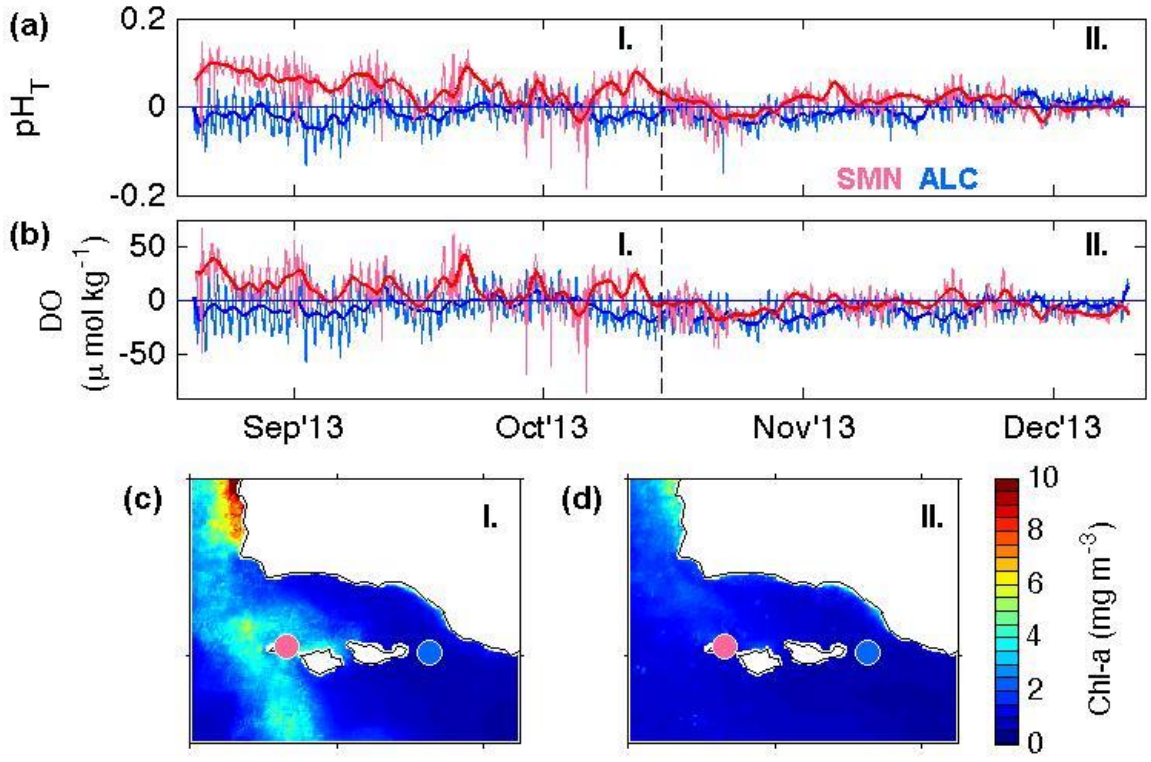

A second example of event-scale variability is described during the upwelling season. The largest variability in event-scale pH was observed during April and May at SMN. During these months, pH exhibited a mostly-negative anomaly, due to *advection of upwelled water* with high salinity and low oxygen and temperature, that was interrupted by pH increases due to phytoplankton blooms (Figure IV-7). For Figure IV-7, we focused on describing pH variability at SMN and compared with patterns observed at ALC.

At the start of the upwelling season in April, an initial pH_T increase of ~0.15 at SMN occurred on 2 April 2014 at the same time as an increase in regional Chl-a (Figure IV-7, Phase I). These conditions persisted for ten days and corresponded to a positive oxygen anomaly during which temperature declined and salinity increased (i.e. presence of an upwelled water mass). Next, pH_T declined (~0.12) over the following 26 days (Figure IV-7, Phase II). This phase marked the lowest pH and temperature and highest salinity observations at SMN. SST composites during Phase II suggest that these water masses were advected to SMN from upwelling events north of Pt. Conception. During the presence of these upwelled waters, a one-day pH_T increase (0.15) occurred with the over-night appearance of high levels of regional Chl-a (Figure IV-7, Phase III). With strengthening equatorward winds, pH_T decreased by 0.15 and remained low for two days, despite a continued increase in regional Chl-a. This marked the end of the low pH conditions in spring at SMN. Next, pH recovered to a small positive anomaly during wind relaxation (details discussed below) and intrusion of warm low salinity water from the south (Figure IV-7, Phase IV). Warm water intrusion was observable at both SMN and ALC in the time-series data and SST plots.

Figure IV-7. Shifts to negative pH anomalies and recoveries at SMN (red), compared to positive pH anomalies at ALC (blue). Transitional events, or phases, are numbered with Latin numerals. Corresponding SST and Chl-a composites were computed over the time intervals in gray and represent means for cloud-free pixels using daily images. Dark lines in time-series represent 48 h low-pass filtered data. Site codes are same as in **Figure IV-1**.

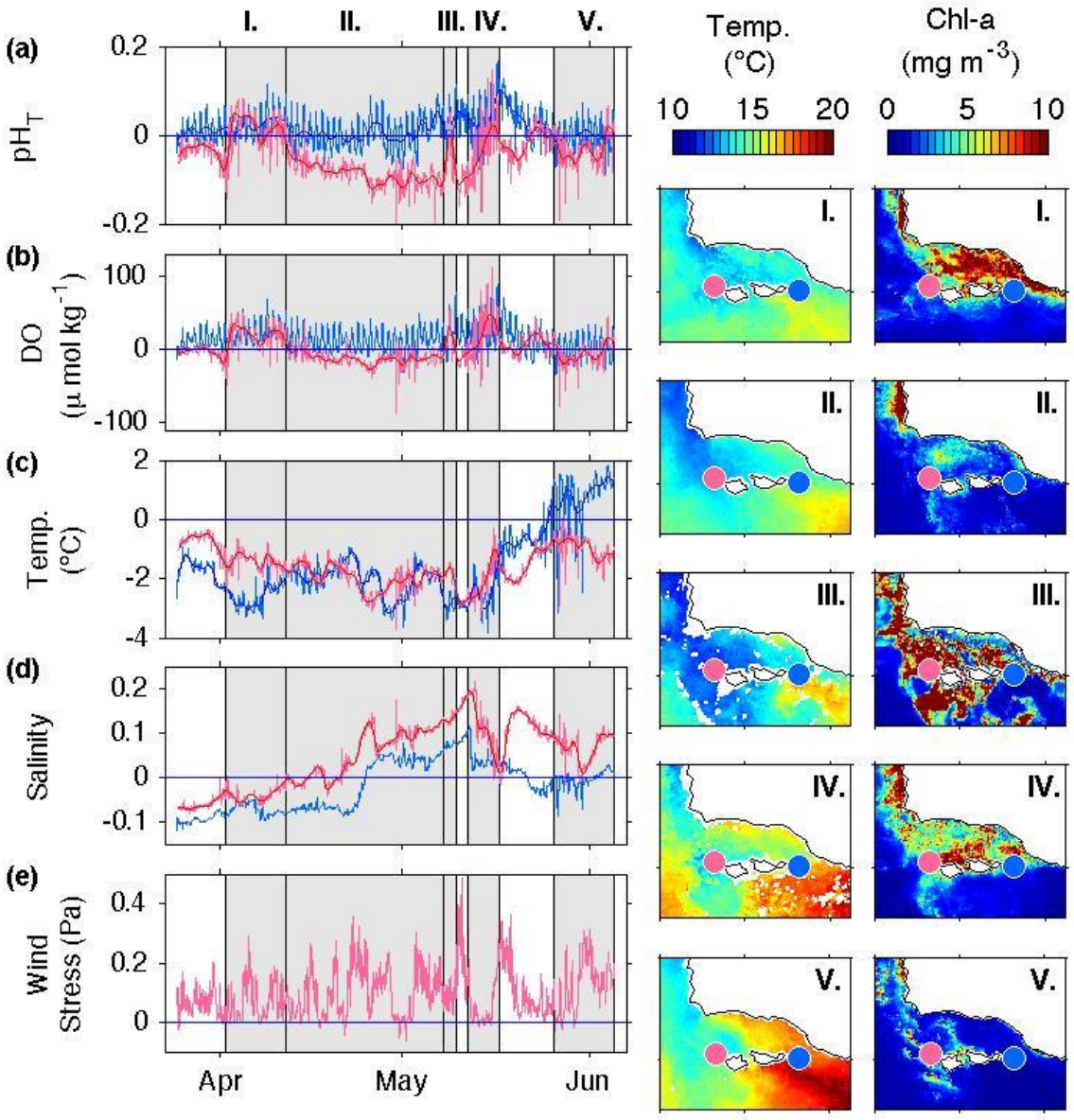

Overall, during the period of the largest pH variability at SMN, April and May, ALC generally exhibited a positive pH and oxygen anomaly following the first channel-wide Chl-a increase on 2 April 2014 (Figure IV-7, Phase I). pH and oxygen anomalies roughly returned to a non-anomalous state at ALC at the same time as (1) seasonal warming (which could partially account for a decrease in pH) and (2) the near-disappearance of Chl-a in the SBC (Figure IV-7, Phase V). Along with the disparate pH and oxygen anomalies observed between SMN and ALC in the fall (Figure IV-6), these results highlight Anacapa Island's isolation from regional processes that operate at the western end of the SBC leading to reduced pH variability at ALC compared to SMN.

The third event-scale variability we discovered related to wind stress. Due to the gradient of wind stress at the SBC (Harms and Winant 1998), wind effects were most apparent at SMN. Throughout the study period, wind relaxation events corresponded with periods of *increased high-frequency pH variability*, or alternatively, high wind stress diminished high-frequency pH variability. This effect was observable in January, a period of relatively low pH variability (Figure IV-8a-e). Here, high wind stress corresponded with decreasing pH, oxygen, and temperature and increasing salinity, signifying intrusion of upwelled water. During spring and a period of relatively high pH variability (Figure IV-8f-j), wind relaxation in May occurred with increasing pH, oxygen, temperature and decreasing salinity. In both examples, wind relaxation corresponded with an increase in high-frequency pH, oxygen, temperature, and salinity variability. As wind stress increased, these high frequencies diminished with a 1-day delayed effect. This suggests that periods of high wind stress mask the effect of processes that induce high-frequency pH variability.

Figure IV-8. Event-scale changes in variability at San Miguel Island north mooring (SMN) during wind stress in winter (a-e, shaded) and relaxation in spring during a phytoplankton bloom (f-j, shaded), in 2014. Dashed lines mark the 1-day delay in wind stress effects on variability. Note, y-axis scales are approximately double during the phytoplankton bloom (f-j), except for wind stress. Site codes are same as in Figure IV-1.

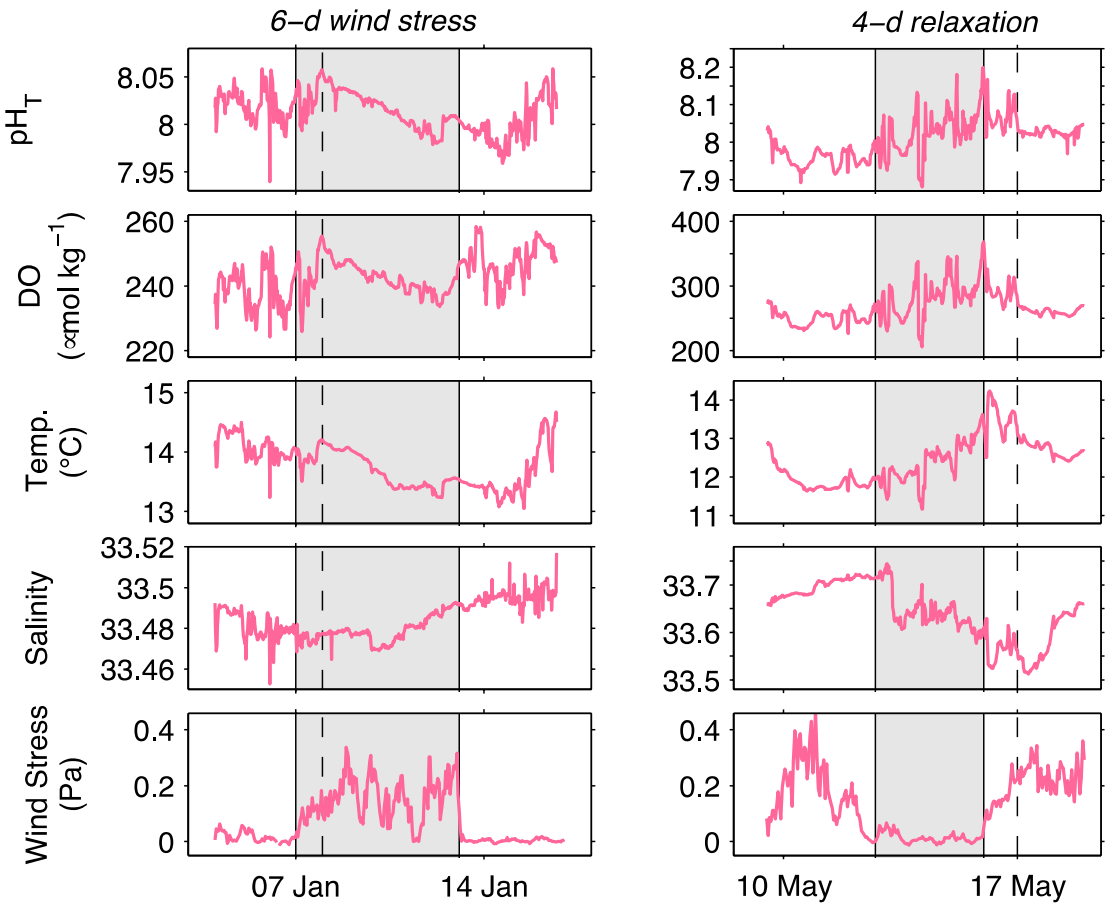

It is noteworthy that event-scale pH variability was observed at all island sites, for example at PRZ and ALC in March and April 2012 (Figure IV-3). While we lack CTDO data for that deployment period, the 0.15 - 0.20 pH_T increase over 10 days occurred with the appearance of Chl-a near the island coastlines (Chl-a composite not shown). Following a decline in pH at the same time as a reduction in Chl-a, pH_T increased again by 0.1 at both sites with a second and larger increase in regional Chl-a that was accompanied by ~ 4 °C temperature increase.

4. Seasonal trends

Evidence for a seasonal pH cycle was found across the islands (Table IV-1). ALC and PRZ appeared to share a similar trend in seasonal pH_T change of 0.06 - 0.08. At ALC, peak pH_T occurred in May (8.04 ± 0.03) and declined to October (7.98 ± 0.02). At PRZ, peak pH_T occurred in June (8.06 ± 0.02) and declined to October (7.98 ± 0.02). As a caveat, data collection was not continuous at PRZ and low monthly mean pH in March and April was biased by two low pH events in 2012, which were also observed at ALC (Figure IV-3a-c). The seasonal cycle at SMN was described over one year only and exhibited a different trend from ALC and PRZ. At SMN, pH_T generally declined from August (8.08 ± 0.04) through April and peaked in summer immediately following months of low pH_T (8.00 in April, May).

5. Interannual comparisons

Interannual comparisons of pH are only made using data from ALC as this is the most complete data record over the three-year study period. At ALC, mean pH_T (± SD) for data collected from 2012 – 2014 was 7.98 ± 0.05, 8.02 ± 0.04, and 8.01 ± 0.04, respectively.

Table IV-1. Monthly mean (± SD) temperature and pH observed during this study at San Miguel Island (SMN), Santa Cruz Island (PRZ), and Anacapa Island (ALC).

Month	Temperature (°C)			pH		
	SMN	*PRZ*	*ALC*	*SMN*	*PRZ*	*ALC*
1	14.1 ± 0.1	14.2 ± 0.2	14.6 ± 1.3	8.03 ± 0.02	8.00 ± 0.02	8.01 ± 0.04
2	13.3 ± 0.1	14.1 ± 0.2	14.4 ± 1.3	8.05 ± 0.04	7.99 ± 0.04	8.02 ± 0.02
3	13.8 ± 0.0	12.6 ± 0.1	14.1 ± 1.4	8.02 ± 0.01	7.94 ± 0.07	8.01 ± 0.05
4	12.8 ± 0.1	12.7 ± 0.1	14.1 ± 1.1	8.00 ± 0.05	7.94 ± 0.05	8.02 ± 0.04
5	12.9 ± 0.1	14.9 ± 0.2	15.4 ± 0.9	8.00 ± 0.04	8.04 ± 0.06	8.04 ± 0.03
6	14.1 ± 0.1	16.9 ± 0.1	17.4 ± 1.0	8.08 ± 0.04	8.06 ± 0.02	8.02 ± 0.02
7	17.4 ± 0.2	18.6 ± 0.2	18.3 ± 1.4	8.07 ± 0.02	8.03 ± 0.02	8.01 ± 0.02
8	16.1 ± 0.2	16.9 ± 0.1	18.6 ± 1.1	8.08 ± 0.04	8.04 ± 0.03	8.01 ± 0.01
9	14.9 ± 0.1	19.5 ± 0.1	19.7 ± 1.3	8.1 ± 0.02	7.99 ± 0.03	7.99 ± 0.02
10	15.4 ± 0.2	19.2 ± 0.1	19.3 ± 1.2	8.07 ± 0.03	7.98 ± 0.02	7.98 ± 0.02
11	15.5 ± 0.1	17.7 ± 0.1	17.5 ± 1.2	8.07 ± 0.02	8.01 ± 0.02	8.00 ± 0.02
12	14.0 ± 0.1	15.9 ± 0.2	15.8 ± 1.6	8.06 ± 0.02	7.99 ± 0.02	8.00 ± 0.04

Event-scale variability observed in winter and spring (e.g. 2012, 2013), contrasts the stability of summer pH year to year (Figure IV-3c). In the summer, for the period from 1 June to 31 July, mean pH_T was 8.01 ± 0.04, 8.02 ± 0.03, and 8.02 ± 0.03, in 2012, 2013, and 2014 respectively. Likewise, mean diel pH_T cycles changed little year to year: 0.12 ± 0.08, 0.10 ± 0.03, and 0.10 ± 0.03, for 2012, 2013, and 2014, respectively. These similar summer conditions are notable as mean temperature increased each year in summer: 16.9 ± 0.4 °C, 17.6 ± 1.0 °C, and 19.0 ± 1.5 °C, in 2012, 2013, and 2014, respectively. Summer diel pH cycles were consistently larger than the previous or following winter, from 2012 to 2014, suggesting that the seasonal change in diel pH cycles is consistent inter-annually and not driven by the changing mean temperature conditions.

6. Temperature and pH

Throughout the study period, waters warmed seasonally (Figure IV-3d-f). SMN was always colder than ALC by ~ 1 (winter) – 4 (summer) °C. PRZ and ALC exhibited similar thermal regimes where temperature peaked in September and troughed in March and April (Table IV-1). As annual warming was evident (e.g. ALC, Figure IV-3f), pH and temperature relationships were investigated by month and year.

None of the sites exhibited a significant linear relationship between mean monthly pH and temperature (SMN: R^2 = 0.28, F = 4.1963, p = 0.065, n = 13; PRZ: R^2 = 0.16, F = 3.7085, p = 0.069, n = 22; ALC: R^2 = 0.002, F = 0.0689, p = 0.794, n = 39). Monthly mean pH reached a midpoint maximum over temperature at each site (Figure IV-9a). When controlling for variability in pH due to thermal effects, $pH_{T\ N16°C}$ did not exhibit a midpoint maximum over temperature (Figure IV-9b). Instead, $pH_{T\ N16°C}$ remained low during cool months and increased during warm months relative to pH_T. This suggests that low monthly

Figure IV-9. Scatter plot of monthly mean temperature and pH at in situ temperatures (a) and temperature normalized pH ($pH_{T\ (N\ 16\ °C)}$) (b). pH 8.05 is marked with a dotted line for reference. Site codes are same as in Figure IV-1.

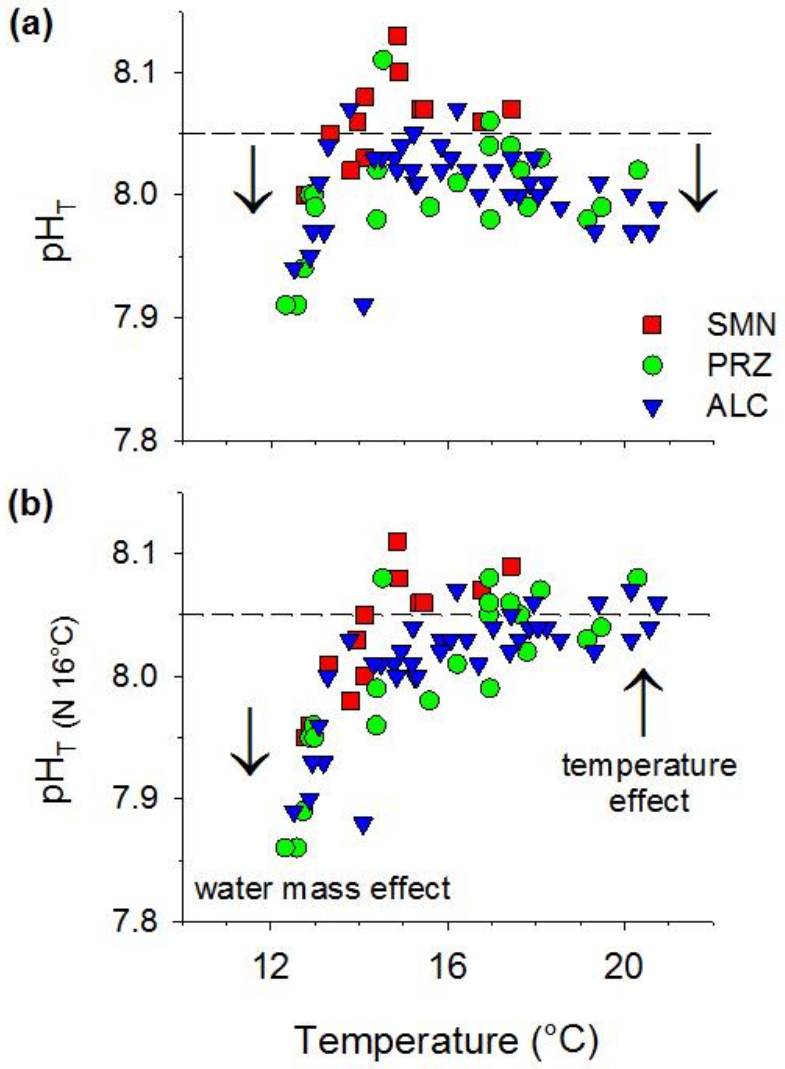

mean pH during warm months may be driven by thermal effects (i.e. 0.015 pH_T decrease per 1 °C increase) and not increased ecosystem respiration at higher temperatures. At cooler temperatures, low $pH_{T\ N16°C}$ suggests that pH was not driven by thermal effects and, instead, may be due to a higher dissolved inorganic carbon content of the water mass, for example, from upwelled water.

When comparing SMN and ALC, low pH events (pH < 1 SD below mean) spanned different temperatures and time frames (Figure IV-10). At SMN, low pH_T events ranged from 7.83 to 8.01 and were largely concentrated between 11.5 and 14 °C and occurred at all hours of the day (Figure IV-10a, b). At ALC, low pH_T events ranged from 7.82 to 7.99 under a bimodal distribution of temperatures with a division at 16.5 °C (Figure IV-10c). At temperatures ≥ 16.5 °C, lowest pH observations occurred during night hours (Figure IV-10d). These patterns suggest two different drivers of low pH events: (1) low pH events at cold temperatures (< 16.5 °C, SMN and ALC) were a function of abiotic processes (e.g. pH of upwelled water) and (2) low pH observations under warm temperatures (≥ 16.5 °C, ALC) were a function of biotic processes operating on a diel cycle (e.g. nighttime ecosystem respiration in warm summer months).

E. Discussion

1. Spatial temporal pH variability

In this study, we observed spatial and temporal pH heterogeneity across three sites in a temperate coastal region with persistent abiotic gradients, within an EBCS. Each study site was different in terms of habitat and biota with ALC and PRZ representing fixed vegetation (kelp and eelgrass, respectively) and the warmer portion of the SBC, and SMN a more open water site and cooler portion of the SBC. We hypothesized that the persistent temperature,

Figure IV-10. Low pH events (1 SD below mean pH) at SMN (red) and ALC (blue) as a function of temperature (a, c) and time of day (b, d). At ALC, boxplots of low pH events by time of day were divided between < or ≥ 16.5 °C, due to the bimodal distribution of low pH events across temperature. Data were collected on a 30 min sampling frequency from 20 Aug 2013 to 20 Aug 2014. Site codes are same as in Figure IV-1.

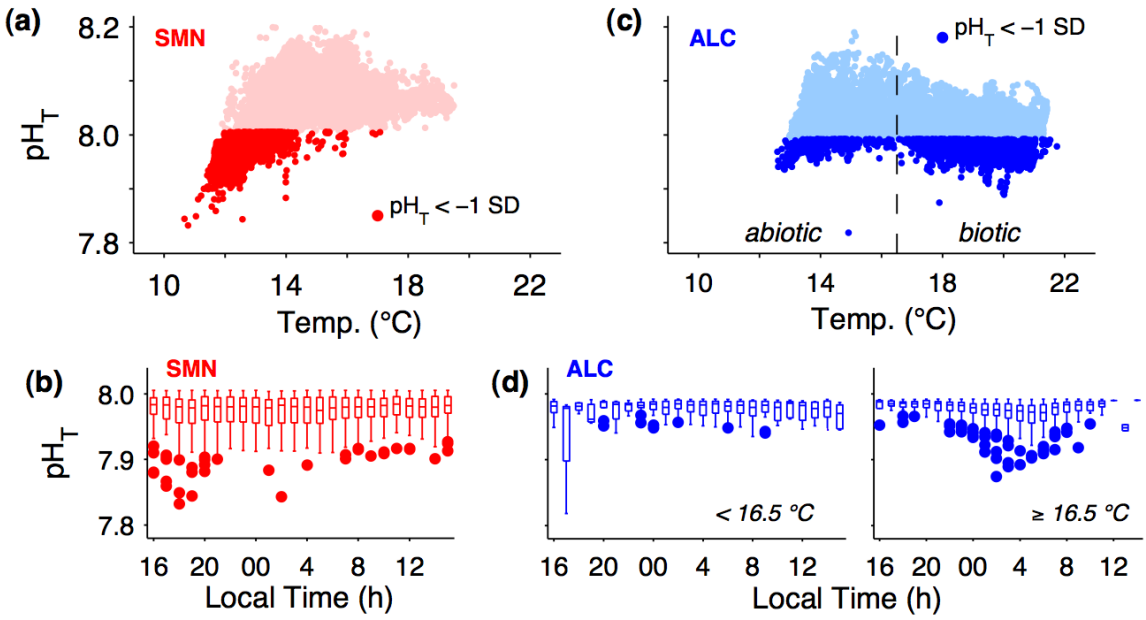

wind, and current gradients across these sites would yield a pH gradient where SMN experiences lower pH than ALC. This hypothesis was not supported due to event-scale pH variability observed across all island sites. For example, while springtime upwelling in 2014 led to a negative pH anomaly at SMN and not at ALC as hypothesized, low pH_T (7.9) events were observed at PRZ and ALC in other years. These events occurred during the coldest temperatures suggesting that seasonal upwelling may, on occasion, influence pH conditions throughout the SBC. All sites experienced event-scale pH increases that correlated with timing of local phytoplankton blooms. Variability in timing and spatial extent of advected upwelled water and phytoplankton blooms thus prevented a persistent pH gradient in this region, despite the presence of wind, current, and temperature gradients. The pH heterogeneity described here reflects a fusion of local and regional drivers and addresses a knowledge gap of how pH dynamics vary over multiple spatial and time scales in a coastal region of an EBCS.

We detected various drivers and temporal scales of pH variability (Table IV-2). One source was **diel** pH cycles, which differed by (1) site and (2) season. First, the diel pH cycles at PRZ, the eelgrass dominated site, were nearly double in magnitude compared to ALC, the kelp forest site. Previous studies show diel pH cycles of 0.06 to 0.35 in seagrass beds (Challener et al. 2015; Hendriks et al. 2014) and ~0.1 in kelp forests (Frieder et al. 2012; Krause-Jensen et al. 2015). Second, seasonal doubling or tripling of diel pH cycles was observed in the kelp forest and eelgrass bed, respectively, and was consistent between years (Figure IV-5). Such seasonality in diel pH cycles was also documented in a temperate salt marsh, where diel pH ranges increased more than threefold from winter to summer (Flax

Table IV-2. Summary of pH change associated with different time-scale processes.

Ocean acidification is referenced for comparison. Bold indicates a biotic effect. + *hf* stands for increased high-frequency variability.

Time-scale	Variable	Effect on pH	ΔpH
Centennial	Ocean acidification	-	0.42*
Seasonal	Warming (4 °C)	-	0.06
	Advection of upwelled water	-	0.1
Event	**Phytoplankton blooms**	+	0.1 - 0.2
	Wind relaxation	+ *hf*	< 0.1
Daily	**Photosynthesis/respiration**	±	0.05 - 0.2

*End century prediction, RCP8.5 climate scenario (Pörtner et al. 2014)

Pond, North Atlantic coast, USA, Baumann et al. 2015). In the Southern California Bight, Frieder et al. (2012) found that equatorward currents enhanced diel pH cycles in the La Jolla Kelp Forest, suggesting that some variability in diel pH cycles may be controlled by water mass movement. Peak diel pH cycles at SMN matched those of ALC. As SMN is located outside vegetated habitat, changes in diel pH cycles there likely reflect photosynthesis of phytoplankton blooms. If so, diel pH cycles of 0.1 from blooms could contribute to the observed diel pH cycles at ALC and PRZ.

Moving up in scale from diel cycles, we observed **event-scale** (days to weeks) changes in pH. During the overlapping period of sensor deployments at SMN and ALC, such events were more prominent at SMN as this site is influenced by equatorward wind stress and currents more so than the other sites (Harms and Winant 1998). SMN exhibited a wider range in pH observations than ALC. We discuss the three observed event-scale pH effects due to (1) upwelling, (2) phytoplankton blooms, and (3) periods of wind relaxation.

First, *upwelling* in the CCS brings low pH (< 7.75) seawater onshore (Feely et al. 2008). Outside the SBC and north of Pt. Conception on the mainland, these upwelling events decrease pH_T by 0.3 - 0.4 (Santa Barbara Coastal LTER unpublished data, Hofmann et al. 2011). As upwelling favorable winds in the CCS would result in downwelling at SMN (a north-facing coastline), the upwelling effects observed at SMN (0.1 pH_T decrease) are likely a signature of low pH, upwelled, water masses advected from north of Pt. Conception. The smaller change in pH_T associated with upwelled water at SMN (0.1) compared to north of Pt. Conception (0.3-0.4) suggest a decline in dissolved inorganic carbon as the water is advected to SMN. This could be due to CO_2 off-gassing or uptake of dissolved inorganic carbon through primary production during transport. The lack of strong upwelling at the

islands compared to north of Pt. Conception suggest that the northern Channel Islands may serve as a spatial refuge from extreme low pH and upwelling events in the future.

Second, *phytoplankton blooms* appeared to increase pH_T by 0.1 - 0.2 at all island sites. Blooms occur more frequently in the eastern portion of the SBC compared to the western end (Otero and Siegel 2004), which led to a positive pH anomaly observed at SMN in the fall but not at ALC (Figure IV-6). Channel-wide blooms typically occur in April and May during cold temperatures (Otero and Siegel 2004) and corresponded with positive pH and oxygen anomalies across all sites. Smaller near-shore phytoplankton blooms can occur throughout the year due to storm runoff (Otero and Siegel 2004) and likely contribute to the spatial variability of event-scale pH anomalies. These event-scale increases in pH may be a feature of pH variability found throughout the Southern California Bight. For example, a 0.1 increase in pH_T was observed in the La Jolla Kelp Forest during transitions from equatorward to poleward alongshore currents and were attributed to increase ecosystem production following high-density water intrusion (Frieder et al. 2012).

Third, *periods of wind relaxation* corresponded with an increase in high-frequency (< 1 day) pH, oxygen, temperature and salinity variability. This could stem from physical processes that are masked during periods of high wind stress. Wind relaxation results in restratification such that larger vertical property gradients form. Propagated internal waves and tides could deliver different water masses across the sensor surface on frequencies < 1 day (Booth et al. 2012). Tidal effects on pH have been shown for coastal ecosystems (Baumann et al. 2015; Frieder et al. 2012). Although the pH power spectra in our study showed peaks at 1 and 2 cycles per day (cpd, Figure IV-4), the peak for 1 cpd was larger than the peak for 2 cpd suggesting that tidal effects were smaller than the effect of biological

forcing on pH at our sites. During high wind stress, mixing of the water column homogenizes vertical gradients, which could thus also homogenize vertical gradients in pH.

Small **seasonal** trends in pH were observed: pH_T declined from May to October by 0.06 at both ALC and PRZ. During this time, waters warmed 4.3 and 3.9 °C, respectively. Assuming a pH_T decreases 0.015 for every degree warming, expected pH decline due to warming alone would be 0.06 and matches the observed seasonal change in pH. The ocean is not a closed system and CO_2 off gassing, primary production, and increased ecosystem respiration under warming may also contribute to seasonal changes in pH. As poleward advection of southern waters increases in fall and contributes to seasonal warming in the SBC (Lynn and Simpson 1987; Otero and Siegel 2004), the observed seasonal pH cycle at PRZ and ALC may represent a pattern present throughout the Southern California Bight. For example, a similar seasonal decrease in pH_T (< 0.1) was also observed in Santa Monica Bay, ~60 km east of the Channel Islands (Leinweber and Gruber 2013), and predicted in model simulations (0.04) of nearshore seasonal pH variability in the southern portion of the CCS (Hauri et al. 2013). In the southern region of the CCS, the timing of seasonal primary production (pH increase) counteracts seasonal warming (pH decrease), resulting in an overall small seasonal pH cycle compared to northern regions of the CCS (Hauri et al. 2013). Larger seasonal pH change has been documented in other coastal regions. For example, pH_{NBS} declined by 0.6 from early spring to late summer in Flax Pond, a temperate salt marsh (Baumann et al. 2015). In Flax Pond, lowest pH was observed in August and correlated with maximum diel pH cycles. As such, the 0.6 seasonal change in pH was attributed to seasonal changes in community production and respiration, which were influenced by seasonal warming and increases in day length (Baumann et al. 2015). This

was not the case at our sites because diel pH cycles at ALC and PRZ peaked during different seasons (Figure IV-5), supporting the conclusion that the small summertime decline in pH in our study region is likely due to seasonal warming (Hauri et al. 2013).

While our dataset has gaps, we were able to gain some inferences on pH over an **interannual** time frame. Stable pH conditions were observed each year in summer at ALC despite increasing temperatures. Late winter and spring appear to be the most variable, in terms of pH events, making predictions of future pH challenging for this portion of the year. Using the approach from (Keller et al. 2014), we can estimate how long the pH time-series needs to be in the Channel Islands before detecting an ocean acidification trend. This time of emergence (ToE) is defined as "the point in time when the trend signal (S ×ToE) exceeds two times the background variability (N)" (Keller et al. 2014):

$$\text{ToE} = (2 \times N)/S \quad (1)$$

For our estimate of ToE, we used data from ALC, which exhibited an overall pH SD of 0.04 (=N), despite occasional low pH events. Assuming a constant -0.002 yr^{-1} change in pH_T (=S) for the North Pacific (Dore et al. 2009; Ishii et al. 2011), ToE for detecting the anthropogenic signal at Anacapa Island would be 40 years and more than triple the length of time estimated to detect ocean acidification trends in the open ocean (Keller et al. 2014). Coastal acidification rates, however, may be much faster (e.g. -0.058 yr^{-1} at Tatoosh Island, Washington, USA, Wootton and Pfister 2012) and so trends may be detectable sooner.

2. Application to future research strategies

Incorporating environmental realism into laboratory experiments remains a vital research goal and challenge within ocean change biology (McElhany and Busch 2013; Reum et al. 2015; Takeshita et al. 2015). Here, the scarcity of time-series data from coastal marine

ecosystems can be a major resource gap for the research community. Such data provide present-day exposures of resident biota necessary to study pH tolerance and adaptive capacity. Here we show that the northern Channel Islands is a location within an EBCS that experiences relatively mild effects of coastal upwelling and strong biological influences within vegetated habitats. These findings have two implications for the sensitivity of local biota to ocean acidification in this region: (1) the northern Channel Islands may provide a *spatial refuge* from extreme low pH (< 7.7, sensu Feely et al. 2008) associated with upwelling and (2) pH increase due to primary production may provide a *temporal refuge* from ocean acidification, in the future. Identifying the effects of spatio-temporal pH variability on organisms and ecosystems remains an underexplored area of research. Evidence is emerging that such patterns can result in selection for tolerant genotypes (e.g. Kelly et al. 2013) and may also drive transgenerational effects (Murray et al. 2014; Parker et al. 2015; Thor and Dupont 2015). We also emphasize the importance of addressing multi-stressor scenarios in such endeavors. It is known that pH, temperature and oxygen stress co-occurs or changes seasonally in coastal habitats (Baumann et al. 2015; Reum et al. 2015). In this study, comparison of low pH events (driven by abiotic and biotic process) across sites revealed unique combinations of pH and temperature stress that may be relevant on an organismal scale (Figure IV-10). A similar perspective was gleaned from a coral reef ecosystem in Australia where anomalous pH and thermal stress were found to be asynchronous in time (Kline et al. 2015). Understanding the biological and physiological importance of environmental exposures over different timescales and various combinations is therefore critical. Simple warming and acidification treatments in laboratory experiments may not be relevant if those conditions are not reflective of realistic future exposures across

a species range (Reum et al. 2015). We recommend designing experiments that are (1) fine-tuned to local habitat conditions to which the experimental organisms are inherently acclimatized and (2) carefully designed to address biological responses on specific temporal scales (e.g. diel, seasonal, etc.). Reum et al. (2015) provide suggestions for experimental design based on habitat conditions of CO_2 and temperature for upwelling systems, and Bockmon et al. (2013) have developed a laboratory infrastructure to conduct multi-stressor experiments. pH exposures for coastal organisms cannot be assumed and studies of biology should ideally be coupled with environmental data such as those presented here.

F. Acknowledgements

Research for this project was funded by the George Melendez Wright Climate Change Fellowship (2011), Sea-Bird Electronics Student Equipment Loan Program Award (2013), and Southern California Research and Learning Grants (2013, 2014) awarded to LK. Data were collected under National Park Service (NPS) research permits CHIS-2013-SCI-0012 and CHIS-2014-SCI-0019 and Channel Islands National Marine Sanctuary Research Permit CINMS-2015-003. During the course of this project, LK was supported by a U.S. National Science Foundation (NSF) Graduate Research Fellowship. Boat travel and on-island support was facilitated by the Channel Islands NPS. Portions of this research were supported by funds from the Bureau of Ocean Energy Management to LK, GEH, and Dr. Carol A. Blanchette, the University of California in support of a multi-campus research program, Ocean Acidification: A Training and Research Consortium to GEH, and an NSF award (NSF OCE-1040960) to GEH as part of the Ocean Margins Ecosystem Group for Acidification Studies (OMEGAS - a consortium of scientists from different institutions along the U.S. West Coast). We thank Dr. Carol Janzen at Sea-Bird Electronics for advising

on use of CTDO sensors, Dr. Yui Takeshita and Chris Gotschalk for assistance with Matlab, and Dr. Libe Washburn for insightful comments on the manuscript.

G. References

Barton, A., B. Hales, G. G. Waldbusser, C. Langdon, and R. A. Feelyd. 2012. The Pacific oyster, *Crassostrea gigas*, shows negative correlation to naturally elevated carbon dioxide levels: Implications for near-term ocean acidification effects. Limnol. Oceanogr. **57:** 698-710.

Baumann, H., R. B. Wallace, T. Tagliaferri, and C. J. Gobler. 2015. Large natural pH, CO_2 and O_2 fluctuations in a temperate tidal salt marsh on diel, seasonal, and interannual time scales. Estuaries and Coasts **38:** 220-231.

Bednaršek, N. and others 2014. *Limacina helicina* shell dissolution as an indicator of declining habitat suitability owing to ocean acidification in the California Current Ecosystem. Proceedings of the Royal Society of London B: Biological Sciences **281:** 20140123.

Bockmon, E., C. Frieder, M. Navarro, L. White-Kershek, and A. Dickson. 2013. Technical note: controlled experimental aquarium system for multi-stressor investigation of carbonate chemistry, oxygen saturation, and temperature. Biogeosciences **10:** 5967-5975.

Booth, J. a. T. and others 2012. Natural intrusions of hypoxic, low pH water into nearshore marine environments on the California coast. Cont. Shelf Res. **45:** 108-115.

Bresnahan, P. J., T. R. Martz, Y. Takeshita, K. S. Johnson, and M. Lashomb. 2014. Best practices for autonomous measurement of seawater pH with the Honeywell Durafet. Methods Oceangr. **9:** 44-60.

Challener, R. C., L. L. Robbins, and J. B. McClintock. 2015. Variability of the carbonate chemistry in a shallow, seagrass-dominated ecosystem: implications for ocean acidification experiments. Marine and Freshwater Research.

Dickson, A. G., and F. J. Millero. 1987. A comparison of the equilibrium constants for the dissociation of carbonic acid in seawater media. Deep-Sea Res. I **34:** 1733-1743.

Dickson, A. G., C. L. Sabine, and J. R. Christian. 2007. Guide to best practices for ocean CO_2 measurements. PICES Special Publication **3:** 191 pp.

Dong, C., E. Y. Idica, and J. C. Mcwilliams. 2009. Circulation and multiple-scale variability in the Southern California Bight. Prog. Oceanogr. **82:** 168-190.

Dore, J. E., R. Lukas, D. W. Sadler, M. J. Church, and D. M. Karl. 2009. Physical and biogeochemical modulation of ocean acidification in the central North Pacific. Proc. Natl. Acad. Sci. **106:** 12235-12240.

Dorman, C., and C. Winant. 2000. The structure and variability of the marine atmosphere around the Santa Barbara Channel. Monthly Weather Review **128:** 261-282.

Feely, R. A., C. L. Sabine, J. M. Hernandez-Ayon, D. Ianson, and B. Hales. 2008. Evidence for upwelling of corrosive "acidified" water onto the continental shelf. Science **320:** 1490-1492.

Frieder, C., S. Nam, T. Martz, and L. Levin. 2012. High temporal and spatial variability of dissolved oxygen and pH in a nearshore California kelp forest. Biogeosciences **9:** 3917-3930.

Frieder, C. A., J. P. Gonzalez, E. E. Bockmon, M. O. Navarro, and L. A. Levin. 2014. Can variable pH and low oxygen moderate ocean acidification outcomes for mussel larvae? Global Change Biol. **20:** 754–764.

García, H. E., and L. I. Gordon. 1992. Oxygen solubility in seawater: better fitting equations. Limnol. Oceanogr. **37:** 1307-1312.

Gruber, N., C. Hauri, Z. Lachkar, D. Loher, T. L. Frölicher, and G.-K. Plattner. 2012. Rapid progression of ocean acidification in the California Current System. Science **337:** 220-223.

Hales, B., T. Takahashi, and L. Bandstra. 2005. Atmospheric CO_2 uptake by a coastal upwelling system. Global Biogeochem. Cycles **19**.

Harms, S., and C. D. Winant. 1998. Characteristic patterns of the circulation in the Santa Barbara Channel. Journal of Geophysical Research: Oceans (1978-2012) **103:** 3041-3065.

Hauri, C. and others 2013. Spatiotemporal variability and long-term trends of ocean acidification in the California Current System. Biogeosciences **10:** 193–216.

Hendriks, I. E. and others 2014. Photosynthetic activity buffers ocean acidification in seagrass meadows. Biogeosciences **11:** 333-346.

Hoegh-Guldberg, O. and others 2014. The Ocean, p. 1655-1731. *In* V.R. Barros et al. [eds.], Climate Change 2014: Impacts, Adaptation, and Vulnerability. Part B: Regional Aspects. Contribution of Working Group II to the Fifth Assessment Report of the Intergovernmental Panel on Climate Change.

Hofmann, G. E. and others 2014. Exploring local adaptation and the ocean acidification seascape – studies in the California Current Large Marine Ecosystem. Biogeosciences **11:** 1053-1064.

Hofmann, G. E. and others 2011. High-frequency dynamics of ocean pH: a multi-ecosystem comparison. PLoS One **6:** e28983.

Iles, A. C., T. C. Gouhier, B. A. Menge, J. S. Stewart, A. J. Haupt, and M. C. Lynch. 2012. Climate-driven trends and ecological implications of event-scale upwelling in the California Current System. Global Change Biol. **18:** 783-796.

Ishii, M., N. Kosugi, D. Sasano, S. Saito, T. Midorikawa, and H. Y. Inoue. 2011. Ocean acidification off the south coast of Japan: a result from time series observations of CO_2 parameters from 1994 to 2008. Journal of Geophysical Research: Oceans (1978-2012) **116:** C06022.

Kahru, M., R. M. Kudela, M. Manzano-Sarabia, and B. G. Mitchell. 2012. Trends in the surface chlorophyll of the California Current: merging data from multiple ocean color satellites. Deep Sea Research Part II: Topical Studies in Oceanography **77:** 89-98.

Kapsenberg, L., and G. E. Hofmann. 2014. Signals of resilience to ocean change: high thermal tolerance of early stage Antarctic sea urchins (*Sterechinus neumayeri*) reared under present-day and future pCO_2 and temperature. Polar Biol. **37:** 967–980.

Kapsenberg, L., A. L. Kelley, E. C. Shaw, T. R. Martz, and G. E. Hofmann. 2015. Near-shore Antarctic pH variability has implications for biological adaptation to ocean acidification. Sci. Rep. **5**: 9638.

Keller, K., F. Joos, and C. Raible. 2014. Time of emergence of trends in ocean biogeochemistry. Biogeosciences **11:** 3647-3659.

Kelly, M. W., J. L. Padilla-Gamiño, and G. E. Hofmann. 2013. Natural variation and the capacity to adapt to ocean acidification in the keystone sea urchin *Strongylocentrotus purpuratus*. Global Change Biol. **19:** 2536-2546.

Kline, D. I. and others 2015. Six month *in situ* high-resolution carbonate chemistry and temperature study on a coral reef flat reveals asynchronous pH and temperature anomalies. PLoS One **10:** e0127648.

Krause-Jensen, D. and others 2015. Macroalgae contribute to nested mosaics of pH variability in a sub-Arctic fjord. Biogeosci. Disc. **12:** 4907–4945.

Lagerloef, G. S., and R. L. Bernstein. 1988. Empirical orthogonal function analysis of advanced very high resolution radiometer surface temperature patterns in Santa Barbara Channel. Journal of Geophysical Research: Oceans (1978-2012) **93:** 6863-6873.

Leinweber, A., and N. Gruber. 2013. Variability and trends of ocean acidification in the Southern California Current System: A time series from Santa Monica Bay. J. Geophys. Res. **118:** 3622-3633.

Liu, X., M. C. Patsavas, and R. H. Byrne. 2011. Purification and characterization of meta-cresol purple for spectrophotometric seawater pH measurements. Environ. Sci. Technol. **45:** 4862-4868.

Lynn, R. J., and J. J. Simpson. 1987. The California Current System: the seasonal variability of its physical characteristics. Journal of Geophysical Research **92:** 947-912.

Malvezzi, A. J. and others 2015. A quantitative genetic approach to assess the evolutionary potential of a coastal marine fish to ocean acidification. Evolutionary Applications **8:** 352-362.

Martz, T. R., J. G. Connery, and K. S. Johnson. 2010. Testing the Honeywell Durafet® for seawater pH applications. Limnol. Oceanogr. Methods **8:** 172-184.

McElhany, P., and D. S. Busch. 2013. Appropriate pCO_2 treatments in ocean acidification experiments. Mar. Biol. **160:** 1807-1812.

Mehrbach, C., C. H. Culberso, J. E. Hawley, and R. M. Pytkowic. 1973. Measurement of apparent dissociation constants of carbonic acid in seawater at atmospheric pressure. Limnol. Oceanogr. **18:** 897-907.

Murray, C. S., A. Malvezzi, C. J. Gobler, and H. Baumann. 2014. Offspring sensitivity to ocean acidification changes seasonally in a coastal marine fish. Mar. Ecol. Prog. Ser. **504:** 1-11.

Otero, M. P., and D. Siegel. 2004. Spatial and temporal characteristics of sediment plumes and phytoplankton blooms in the Santa Barbara Channel. Deep Sea Research Part II: Topical Studies in Oceanography **51:** 1129-1149.

Parker, L. M., W. A. O'connor, D. A. Raftos, H.-O. Pörtner, and P. M. Ross. 2015. Persistence of positive carryover effects in the oyster, *Saccostrea glomerata*, following transgenerational exposure to ocean acidification. PLoS One **10:** e0132276.

Pespeni, M. H. and others 2013. Evolutionary change during experimental ocean acidification. Proc. Natl. Acad. Sci. **110:** 6937-6942.

Pörtner, H.-O. and others 2014. Ocean systems, p. 411-484. *In* C. B. Field et al. [eds.], Climate Change 2014: Impacts, Adaptation, and Vulnerability. Part A: Global and Sectoral Aspects. Contribution of Working Group II to the Fifth Assessment Report of the Intergovernmental Panel on Climate Change. Cambridge University Press.

Price, N. N., T. R. Martz, R. E. Brainard, and J. E. Smith. 2012. Diel variability in seawater pH relates to calcification and benthic community structure on coral reefs. PLoS One **7:** e43843.

Reum, J. C. and others 2015. Interpretation and design of ocean acidification experiments in upwelling systems in the context of carbonate chemistry co-variation with temperature and oxygen. ICES J. Mar. Sci.

Robbins, L. L., M. E. Hansen, J. A. Kleypas, and S. C. Meylan. 2010. CO2calc—A user-friendly seawater carbon calculator for Windows, Max OS X, and iOS (iPhone). U.S. Geological Survey Open-File Report 2010–1280.

Selkoe, K. A., S. D. Gaines, J. E. Caselle, and R. R. Warner. 2006. Current shifts and kin aggregation explain genetic patchiness in fish recruits. Ecology **87:** 3082-3094.

Sydeman, W. and others 2014. Climate change and wind intensification in coastal upwelling ecosystems. Science **345:** 77-80.

Takeshita, Y. and others 2015. Including high frequency variability in coastal ocean acidification projections. Biogeosci. Disc. **12:** 7125–7176.

Thor, P., and S. Dupont. 2015. Transgenerational effects alleviate severe fecundity loss during ocean acidification in a ubiquitous planktonic copepod. Global Change Biol. **21:** 2261-2271.

Wang, D., T. C. Gouhier, B. A. Menge, and A. R. Ganguly. 2015. Intensification and spatial homogenization of coastal upwelling under climate change. Nature **518:** 390-394.

Wetzel, R. G., and G. E. Likens. 1991. Limnological Analyses: Second Edition. Springer-Verlag New York, Inc.

Wootton, J. T., and C. A. Pfister. 2012. Carbon system measurements and potential climatic drivers at a site of rapidly declining ocean pH. PLoS One **7:** e53396.

Yu, P. C., P. G. Matson, T. R. Martz, and G. E. Hofmann. 2011. The ocean acidification seascape and its relationship to the performance of calcifying marine invertebrates: Laboratory experiments on the development of urchin larvae framed by environmentally-relevant pCO_2/pH. J. Exp. Mar. Biol. Ecol. **400:** 288-295.

V. The interaction of low tide heat stress experienced by mussels and wind-driven upwelling and relaxation events

A. Introduction

As described in Chapter 4, the California Current System (CCS) undergoes large temporal and spatial pH fluctuations that are driven by episodic upwelling and primary productivity. Due to natural low pH events associated with coastal upwelling, the CCS is considered one of the most sensitive ecosystems to ocean acidification (Feely et al. 2008; Gruber et al. 2012; Hauri et al. 2013; Hofmann et al. 2014). In the northern regions off the coast of Oregon, upwelling is seasonal and strong and contributes to high productivity in summer (Huyer 1983). In the southern portion of the CCS in south-central California, upwelling occurs year round but is generally weaker than in the north (Bograd et al. 2009). Due to this latitudinal mosaic in upwelling strength, Oregon experiences more frequent low pH events than its southern counterpart (Hofmann et al. 2014). Upwelling events can last for three weeks (Menge et al. 1997; Sanford 1999), but over the last 40 years in Oregon, duration of upwelling events has increased by 26 - 86 % (Iles et al. 2012). This increase in the frequency of upwelling events is also matched with increases in magnitude (Iles et al. 2012). These strong upwelling events bring water masses of pH 7.7 on-shore near the Oregon-California border (Feely et al. 2008). Increased upwelling intensity is related to increasing wind stress (Bakun 1990), and at the same time, ocean acidification has resulted in the shoaling of low (aragonite) saturated water in the CCS (Feely et al. 2008).

Together, these observations indicate that benthic marine organisms in the near-shore CCS are spending up to multiple weeks in seawater of low pH, sometimes lower than what is predicted for the open ocean by 2100 (Hofmann et al. 2014; Pörtner et al. 2014). For

example, during an upwelling event in Oregon, pH decreased from 8.2 to 7.6 and temperature decreased from 13 to 8 °C (Figure V-1). Predictions are that this exposure to episodic low pH events will increase in the future and that this change in abiotic conditions will interact with other physical features, such as aerial exposure during low tides. The larger goal of this chapter was to examine the interaction of these increasing bouts of low pH seawater and the stress induced by aerial exposure in the intertidal zone, a period of thermal stress for many of the resident organisms.

Specifically, the intertidal zone is one of the harshest habitats on earth. Tidal emersion rapidly changes habitat conditions from wet to dry with large changes in temperature over a period of hours while exerting considerable physical force through wave action (Menge and Branch 2001). The rocky shores of central Oregon may perhaps be one of the harshest intertidal regions in the CCS. Intertidal organisms in Oregon are exposed to multiple stressors that are separated in time: heat stress during emersion and low pH stress at cool temperatures during submersion. For example, summertime seasonal upwelling coincides with hot mid-day low tides (Helmuth et al. 2006; Helmuth et al. 2002). Within one tidal cycle, mussel body temperature can increase from 7 °C to 33 °C during a 6 h tidal emersion (Hofmann, 2005). Then, upon emersion during an upwelling event, organisms are exposed to cold, low pH conditions (Hofmann et al. 2014). Currently, bouts of heat stress during low tides are known to induce a cellular stress response (CSR) in the mussel *Mytilus californianus* (Gracey et al. 2008; Hofmann 2005), which indicates that organisms in the intertidal habitat live near the limits of their physiological tolerances. With future changes to this already harsh marine environment, it remains unclear whether or not intertidal species are at their physiological limit of tolerance or possess sufficient physiological plasticity to

Figure V-1. pH and temperature time-series at Lincoln Beach (44.86°N), Oregon, inner-shelf mooring (sensor depth = 4 m, mooring depth = 15 m) before and during an upwelling event in 2013. Temperature is in °C. Preliminary data courtesy of OMEGAS, PIs Bruce A. Menge and Gretchen E. Hofmann.

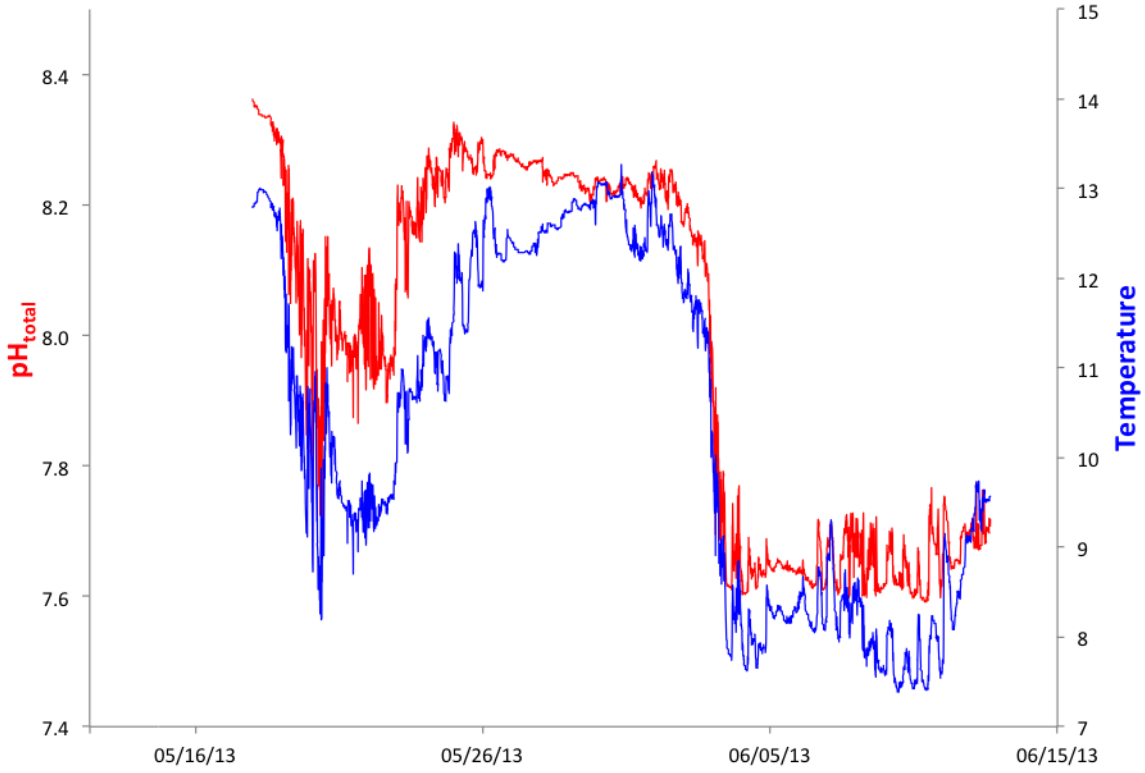

withstand future stress. In order to describe the sensitivities of species to future changes in this habitat, we must understand their present-day range of tolerance.

One evolutionarily conserved physiological mechanism to deal with environmental stress is the CSR. The CSR is composed in part of conserved genes that respond to cellular damage induced by harsh environmental conditions and temporarily extends the tolerance of individuals to harmful conditions (Kültz 2005). One particular and highly conserved suite of genes within the CSR are heat shock proteins (Hsps). Hsps are molecular chaperones that facilitate protein folding and protect the cell from stress-induced protein damage (Feder and Hofmann 1999; Somero 1995). Synthesis of Hsps following environmental stress, and particularly for temperature stress, occurs within minutes of exposure and is referred to as the Heat Shock Response (HSR, Lindquist 1986). Rapid response of the HSR to thermal stress makes this suite of genes an ideal target in studies of stress tolerance, especially at the gene expression level. Out of the Hsps, Hsp70 is the most highly conserved Hsp (Kültz 2005; Lindquist 1986) and one of the most widely used biomarkers for investigations of environmental stress (Feder and Hofmann 1999). Studies of *M. californianus* reveal that patterns of Hsp70 expression can vary in induction temperature, with seasonal acclimatization, and across populations (Buckley et al. 2001; Halpin et al. 2004; Roberts et al. 1997). As *M. californianus* already experiences temperatures high enough to induce the HSR in the field (Gracey et al. 2008; Roberts et al. 1997), it is critical to understand whether ocean acidification will compromise the HSR and alter the thermal tolerance of a species already living at the brink of its physiological limit. For instance, one study found that larvae of the red sea urchin *Mesocentrotus franciscanus* induced a suppressed expression of Hsp70 following a 1 h heat stress at pH 7.87 relative to pH 8.04 (O'Donnell et al. 2008).

Assessment of the HSR has rarely been applied ocean acidification scenarios, and design and execution of multi-stressor scenarios is currently an active area of research (Breitburg et al. 2015; Reum et al. 2015).

An ideal study organism to investigate tolerance of intertidal heat and pH stress is *M. californianus* due to its (1) ecological importance and dominance as a foundation species in the rocky intertidal zone and (2) sensitivity to low pH compared to other marine invertebrates (Gaylord et al. 2011; Kroeker et al. 2013). *M. californianus* create expansive mussel beds in the mid-intertidal zone that function as both food and habitat for other marine invertebrates. These ecosystem engineers are an integral component of intertidal community structure, food webs, and species interactions. While this foundation species thrives in the harsh intertidal environment, exposure to low pH due to ocean acidification is predicted to weaken their shell strength (Gaylord et al. 2011; Kurihara 2008) and strength of byssal thread attachments (O'Donnell et al. 2013) making *M. californianus* a target for ocean acidification research.

In general, mollusks have been found to be much more sensitive to pH than other marine organisms (Harvey et al. 2013; Kroeker et al. 2013). For early life history stages of *Mytilus* species, larvae exhibit abnormal development and juveniles exhibit reduced growth under future ocean acidification scenarios (*M. galloprovincialis*, Kurihara 2008; Michaelidis et al. 2005). Similarly, *M. californianus* larvae grow smaller, but also weaker with respect to crushing resistance when reared at low pH (Gaylord et al. 2011). While shell size is compromised under pH levels predicted for the future, response of other physiological processes vary. An eight-day incubation of adult and juvenile *M. galloprovincialis* in CO_2-acidified seawater (pH 7.3) resulted in reduced extracellular pH (Michaelidis et al. 2005).

Intracellular pH, which is biologically more tightly controlled than extracellular pH, was restored by day 2 after an initial decline. These changes were also accompanied by metabolic depression suggesting potential trade-offs in energy allocation, growth and cellular homeostasis. In contrast, *M. edulis* was found to elevate rates of oxygen consumption under low pH exposure (Thomsen and Melzner 2010). These studies suggest that cellular processes are affected by pH exposure alone and in the absence of secondary stressors, such as temperature. Given that the intertidal zone experiences a multitude of abiotic stressors from wave action and emersion desiccation and heat stress (Menge and Branch 2001), it is important to consider environmentally relevant conditions for laboratory studies of stress tolerance, such as dry heat stress during low tide emersion.

While pH can have a significant impact on growth and physiology, combined effects of warming and acidification in general result in a stronger negative biological response than either pH or temperature alone (Harvey et al. 2013). This may be particularly important for *M. californianus* as this species experiences multiple stressors in the field. As described above, in Oregon during upwelling events, *M. californianus* is exposed to low pH when underwater followed by aerial heat during day-time low tides. Recovery from heat stress following low pH exposure may thus be informative, as well as ecologically relevant, when addressing the impact of ocean acidification on the intertidal community. For example, when exposed to low pH seawater following emersion heat stress, the velvet swimming crab *Necora puber* exhibited slower recovery (e.g. removal of extracellular pCO_2 due to acidosis during emersion) compared to those exposed to high pH seawater (Rastrick et al. 2014). Similar results were found for the porcelain crab *Petrolisthes cinctipes*. Here, *P. cinctipes* exhibited metabolic suppression and enhanced thermotolerance under extreme low pH

(7.15) and temperature (30 °C), suggesting that the CSR was initiated at emersion temperatures of 30 °C during extreme low pH exposures, but not under more moderate, but low pH (7.6) exposures (Paganini et al. 2014). Changes in future seawater pH and emersion temperature may thus have negative consequences on intertidal species with the potential to influence intertidal community structure.

In addition to measurements of physiological processes, such as metabolic rate, another technique to assess organismal response to acute environmental stress is gene expression. Use of gene expression analysis gained popularity as a research technique over the past few years (Stillman and Armstrong 2015). In particular, next-generation sequencing (NGS) has revealed organismal responses to temperature and pH that support local adaptation and phenotypic plasticity of marine species to such stressors and advanced our understanding of species responses to future climate change (Stillman and Armstrong 2015). Since physiological responses can be diverse across pH and temperature stress, investigating multiple physiological pathways simultaneously can elucidate which pathways are critical for responding to environmental stress. As such, NGS provides an excellent method to investigate acute responses through high-through-put sequencing of the entire transcriptome. In addition, gene expression tends to change on the order of minutes to hours and thus NGS is ideal for capturing this level of response. Transcriptomic approaches can serve as exploratory studies but also as a technique to answer targeted hypothesis-driven questions. Specifically for *Mytilus spp*., the transcriptomic approaches have revealed how mussels are attuned to local conditions, such as tidal cycles, by the ability to capture a 'snapshot of [their] physiological state' (Lockwood et al. 2015).

For the purposes of this chapter, I explored oxygen consumption and gene expression among *M. californianus* individuals during their recovery in different water conditions (upwelling vs. relaxation) from heat stress experienced during aerial exposure during low tide. The experiment was conducted in the laboratory using a system that simulated aerial exposure during low tide and water conditions observed during natural upwelling and wind relaxation events. As gene expression can vary greatly across microhabitats in the field (Place et al. 2012), this investigation was conducted in a laboratory setting under tightly controlled pH and aerial temperature exposures. The focal physiological response that was investigated was the HSR, in order to test the hypothesis that low pH during upwelling, compared to periods of wind relaxation, alters the HSR initiated during emersion heat stress.

B. Materials and Methods

1. Field collections

This study was conducted on a mussel population at Fogarty Creek, Oregon (44°50.200 N, 124°03.517 W) that is known to experience hot emersion temperatures during low tides and strong summertime upwelling events. To best capture the first physiological response to summer conditions of emersion heat stress and upwelling, winter-acclimatized adult mussels were collected during a low tide on April 1, 2014 at Fogarty Creek, from a flat mussel bed in the mid to low intertidal zone. Approximately 300 mussels, 4 - 5 cm in length, were transported in a cooler to Hatfield Marine Science Center, Newport, Oregon. Mussels were cleaned of epibionts and placed in an outdoor flow-through seawater table overnight (~11 °C). The following morning, mussels were wrapped in seawater soaked paper towels, placed in open plastic bags and transported on newspaper and ice directly to the lab at University of California Santa Barbara.

In order to estimate the thermal history of experimental animals in the field, mussel mimics, made of real mussel shells (4 - 5 cm in length) filled with clear silicone and fitted with small temperature loggers (Maxim Integrated™ iButton®) (Jost and Helmuth 2007), were deployed in the mussel bed before mussel collections. Mussel mimics recorded temperature every 30 min for six weeks up until mussel collections. A second deployment of mussel mimics was conducted during the summer to document summer temperature exposures.

2. Experimental design

To investigate the impact of low tide heat stress on mussels during simulated upwelling (low pH, cold temperatures) and wind relaxation conditions (high pH, warm temperatures), the experimental design consisted of 4 treatments: two 'seawater treatments' x two 'low tide treatments' (Figure V-2). First, two seawater treatments were set up and represented summertime upwelling ('upwelling' from here onward) and wind relaxation ('relaxation' from here onward). The seawater treatments were based on pH and temperature time-series collected near Fogarty Creek, Oregon (Figure V-1) and were (1) pH 7.6 at 8 °C for upwelling and (2) pH 8.1 at 14 °C for relaxation. Second, following acclimation to seawater treatments and non-warming low tides in the lab (tidal simulator and experiment timeline are described below), two warm low tide treatments were simulated using a manual heat ramp in an incubator. Low tide treatments were (1) 20 °C maximum exposure temperature representing a non-HSR inducing temperature ('20 °C emersion stress' from here onward) and (2) 30 °C maximum exposure temperature representing a HSR inducing temperature

Figure V-2. Estimated mussel body temperature during the laboratory experiment, recorded by mimics. Mussels were held in simulated seawater conditions of wind relaxation (a, b) or upwelling events (c, d). Mussels were exposed to 2 or 3 non-warming low tides before exposure to one warm low tide of either 30 or 20 °C, respectively.

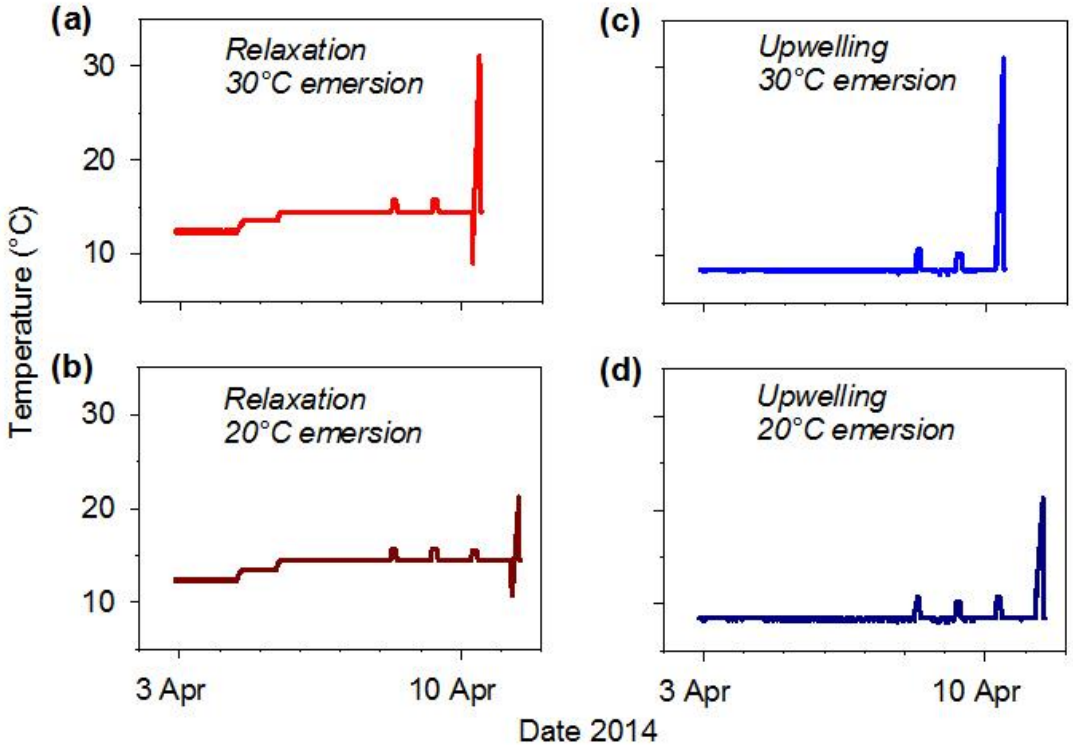

('30 °C emersion stress' from here onward). The response of mussels to warm low tides was measured by respiration rate and gene expression following a 1 h recovery in their respective seawater treatments (upwelling vs. relaxation).

Each seawater treatment consisted of two pseudo-replicate aquaria (receiving treatment water from the same header buckets). Low tide treatments were conducted in one incubator on separate days for the 20 and 30 °C emersion stress. Following the low tide treatment, mussels were allotted a 1 h recovery period in their respective seawater treatments before being sampled for respiration trials or gene expression. Respiration trials and dissections for gene expression were conducted at the time. For the respiration trials, either 2 or 3 mussels were sampled from each aquarium for a total of 5 mussels per treatment. For gene expression, gill tissue from 3 mussels per aquaria was collected (with the exception that for 30 °C emersion stress, 2 and 4 mussels were taken from each replicate upwelling treatment aquarium) for a total of 6 mussels per treatment.

3. Experimental system 1: seawater treatments and chemistry

Experimental aquaria with seawater treatments were set up in two separate and thermally controlled seawater tables (chillers, Aqua Logic, Inc. NEMA 4X). CO_2-acidification of 0.32 µm-filtered seawater generally followed Fangue et al. (2010) with a few modifications. A compressor, particle filters and CO_2-adsorber (Twin Engineering) were used to create dry-CO_2 free air. Pure CO_2 was mixed with CO_2-free air using mass flow control valves (Smart-Trak™ Sierra Instruments, Inc.) to create desired pH. Treatment air was bubbled into an 18 L header buckets via a venturi injector and a recirculating pump. Treatment water was then pumped into a second header bucket that received the same treatment air. This increased gas equilibration time of the treatment water was necessary to achieve target pH levels. From the

second header bucket, treatment water was delivered to two pseudo-replicate aquaria (72 L total volume) at a rate of 24 L per hour and to two smaller buckets at a rate of 2 L per hour, using irrigation drippers. The smaller buckets were used to isolate treatment water for respiration trials. All plumbing was flow-through.

Treatment water in aquaria was measured once a day for pH_T (spectrophotometric method, total hydrogen ion scale), temperature (OMEGA® HH81A wire probe), salinity (YSI 3100), and total alkalinity (A_T, Mettler-Toledo T50). Measurements of pH_T and A_T follow methods from Standard Operating Procedures 3b and 6b (Dickson et al. 2007). A_T measurements were calibrated by verifying Certified Reference Materials (CRMs) seawater standards, from Dr. Andrew M. Dickson at Scripps Institution of Oceanography, to within 10 µmol $kgSW^{-1}$ accuracy. *In situ* pH_{total} and other carbonate parameters were calculated in CO2calc (Robbins et al. 2010) using CO_2 constants from Mehrbach et al. (1973) refit by Dickson and Millero (1987).

4. Experimental system 2: tidal simulator

In an effort to synchronize tidal-driven gene expression across all individuals in the experiment (Gracey et al. 2008), mussels were simultaneously exposed to non-warming low tides using a custom tidal simulator, prior to warm low tide treatments (timeline described below, Figure V-3). The tidal simulator included a control panel, connecting each low tide simulator, which each used a timer-activated two-way pump with float valve control and timer-activated heat lamps with dimmers (not used in this experiment). Each aquarium (54 L seawater volume) was fitted with a PVC and Vexar® mesh frame at 10 cm depth to provide a platform for mussels above the low tide level. Briefly, timer-controlled pumps pumped water out of the aquaria during non-warming low tides. As incoming flow into the

Figure V-3. Schematic of fluid flow (a) and electrical set up (b) of the tidal simulator (a). The tidal system presented has more features than were used for the experiment (e.g. heat lamps, additional reservoir tank for fast refill of aquaria following a simulated low tide) and are presented here as a resource for the research community.

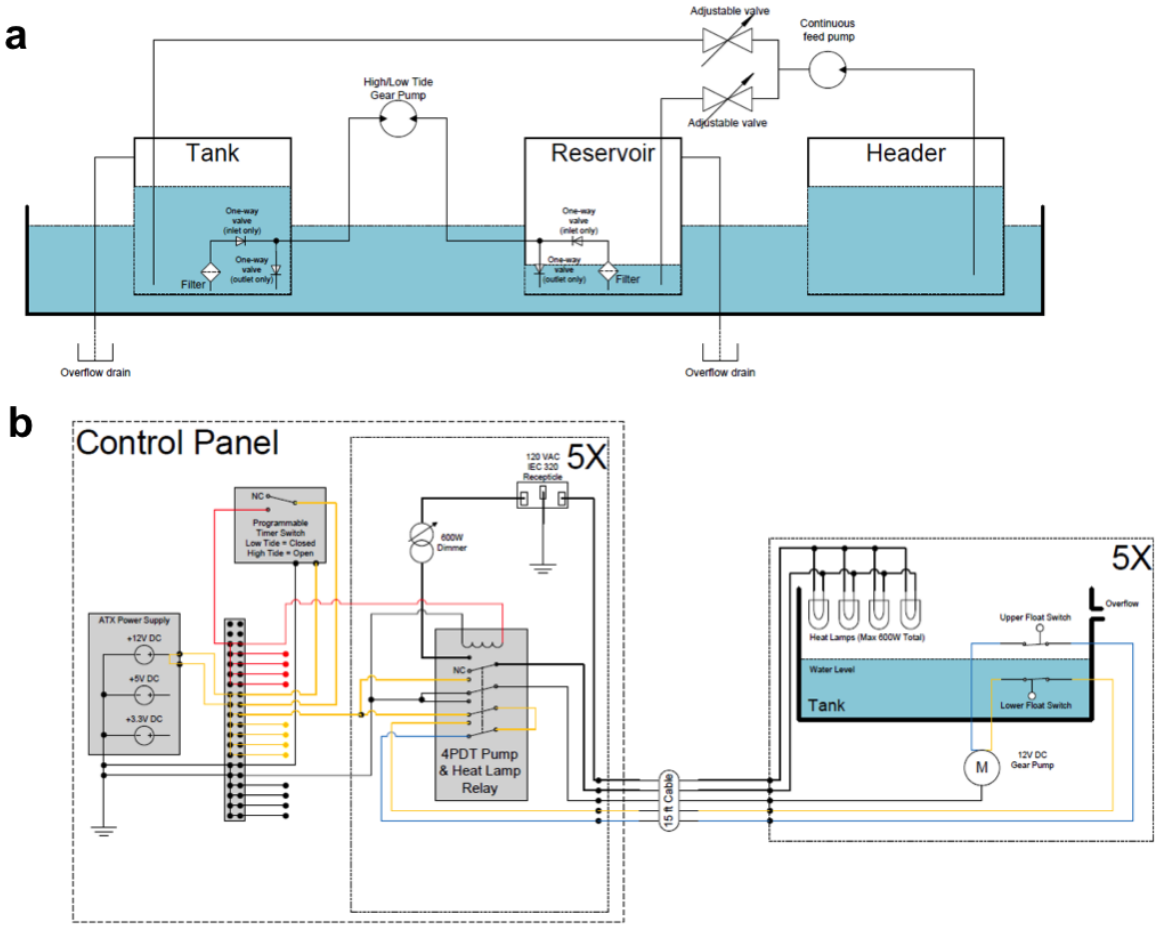

experiment aquaria was maintained by header buckets, a float valve was used to maintain pump activation and low water levels during the simulated low tide. The consistent incoming flow was necessary to ensure stable pH levels at high tide. While this simulator can have heat lamps and an additional reservoir for fast aquarium refill following the low tide, these features were not used in this experiment.

To provide a resource for the research community, the following section describes the full design of the tidal simulator (use for up to five aquaria with heat lamp warming, Figure V-3). *Fluid flow* (Figure V-3a): To start, flow-through aquaria receive incoming water flow from an upstream header tank. For each aquarium, a two-way pump (12V 3A DC Gear Pump, McMaster-Carr) serves to pump water between the experimental aquarium with animals and a reservoir tank. During low tide, the pump drains the primary aquarium to below the level of the animals and pumps the water into the reservoir tank. During high tide, the pump moves water from the reservoir tank back into the primary tank to submerge animals, if fast refill is necessary. The constant incoming flow of treatment water from the header tank can also refill the aquarium at high tide, after which high tide level is maintained by an overflow hole. The latter method was used for this experiment, as incoming water flow from header buckets was sufficient to refill the aquaria. *Electrical schematic* (Figure V-3b): The control panel for the tidal simulator was made from an existing desktop computer tower due to its ability to enclose the system safely, and the ease at which the sheet metal frame could be modified to mount all the required systems. All components were chosen to work on 12V, allowing the use of the computer's ATX power supply to power the system. The ATX power supply was mounted to the computer tower using the existing clips intended for this purpose. A screwed down terminal block served to distribute

the power and signals to each of the five subsystems. The timer relay and five 4PDT relays were mounted on a single DIN rail. The specific timer was chosen due to its ability to mount to a DIN rail, and the relays were inserted into DIN rail-mountable sockets. The dimmer switches for heat lamps and heat lamp power receptacles were mounted in custom cutouts to allow access from the outside of the computer tower.

Function: A 12V rail powers a timed relay that can be set by the user (THC15 12VDC Digital Programmable Switch, NITBUY). This relay switches a secondary 12V line (Figure V-3b, shown as red) to control a 4-pole-double-throw relay (4PDT Relay, McMaster-Carr). The four channels of the 4PDT relay have the following functions: (1) switch to turn on the heat lamps (one switch pole), drawing no more than 10A total, (2) pump H-bridge to control pumping direction (two switch poles), (3) switch to route the pump's power through snap-acting switches (Subminiature Snap-Acting Switch, McMaster-Carr, mounted above the water and attached to a float on an extended rod). Heat lamps can be mounted on a wooden frame suspended over open aquaria and were not used in this experiments as tight control of temperature was necessary for the gene expression experiment. When the timer relay is closed (e.g. low tide): (1) heat lamps are turned on, (2) snap-acting switch is set as the active switch (current runs through blue wire), (3) pump direction is set to pump water out of the aquarium until the water level drops below the float, and (4) steady inflow of fresh water from the header tank periodically pushes the float upward and trips the switch to allow the pump to move the excess water into the reservoir tank and maintain the desired low tide level.

When the timer relay is opened (e.g. high tide): (1) heat lamps turn off, (2) the other snap-acting switch is now active (current runs through yellow wire), and is closed. Because

the switch is closed, the pump begins pumping water from the reservoir tank into the primary aquarium thanks to the H-bridge having reversed the direction of current through the pump. Once the water level rises above the float, flipping the switch, the pump shuts off. Excess water introduced by the header tank is drained naturally via an overflow. All connections were made using either screwed down ring terminals, solder, or connectors.

5. Experiment timeline

To simulate the duration of an upwelling and wind relaxation event, the laboratory acclimation of mussels to seawater treatments (prior to low tide treatments) lasted 8 – 9 days and included 3 – 4 non-warming low tide exposures. Upon arrival in the lab, mussels were sorted for size (approximately 45 mm in length), and 54 mussels were immediately placed on the mesh frame in treatment aquaria (two seawater treatments each with two pseudo-replicate aquaria). One iButton® was placed among the mussels in each tank to track water and non-warming low tide temperatures throughout the experiment. Mussels were not fed during the experiment.

To acclimate mussels to a summertime temperature of 14 °C following wintertime field acclimatization, mussels in the relaxation treatment were exposed initially to 12 °C for one day. Seawater was warmed by 1 °C d^{-1} for two days while maintaining a pH of 8.1 until the desired relaxation treatment was reached (pH 8.1 at 14 °C). Mussels in the upwelling treatment did not undergo any thermal acclimation and were held at 8 °C for the duration of the experiment. On day 5, 10 mussels per tank were moved off the frame and placed below the low tide level as a non-tidal control treatment and were not used in this study.

Non-heated low tides were simulated starting on day 6 of the experiment to condition mussels to a simulated low tide series and increased in duration. The tidal cycle was based

on typical emersion time recorded by mussel mimics in the mussel bed at Fogarty Creek, Oregon during a low tide series. Laboratory emersion time started at 6 am and lasted for 3.5 h on day 6 and 4 h on day 7, 8, and 9 (20 °C emersion stress only). Warm low tide treatments were simulated using an incubator on day 9 (30 °C emersion stress) and 10 (20 °C emersion stress) and lasted for 4.5 h (Figure V-2). Due to labor and equipment restrictions, the 20 and 30 °C low tides could not be conducted on the same day. Thus, mussels exposed to a hot low tide of 20 °C experienced an additional day of seawater treatment acclimation and an additional non-warming low tide.

For the low tide treatments, immediately at the start of emersion at 6:00 am, 22 - 23 mussels per aquarium were moved to the incubator set at 10 °C. After 15 minutes, incubator temperature was incrementally increased every 10 min for a final temperature exposure of 20 °C or 30 °C that lasted 15 min, for a total emersion time of 4.5 h. Following the heat ramp, mussels were immediately returned to their respective aquarium and allowed a 1 h recovery period. Following the recovery, five mussels per treatment were prepped for respiration trials (described below). At the same time, gill tissue was dissected and preserved for gene expression analysis from the remaining mussels. Briefly, 80 mg of gill tissue was flash frozen in liquid nitrogen and promptly homogenized in 900 uL TRIzol®, re-frozen in liquid nitrogen, and stored at -80 °C, prior to analysis. A 1 h recovery was chosen as gene expression can first be detected 1 h following heat stress and provides the earliest snapshot of the HSR (Hofmann 2005).

6. Respiration trials

To connect cellular stress response (e.g. gene expression) to a physiological response, I measured mussel respiration rate as a proxy for metabolic rate. Mussel respiration was

measured in treatment seawater three times during the experiment: once one day before the first simulated non-warming low tide (control), and once following each low tide treatment.

Respiration was measured in custom respiration vials (screw top plexiglass vials, 300 mL) fitted with an oxygen sensing patch (RedEye® Ocean Optics), perforated second floor and a stir bar (~290 mL liquid volume with a live mussel). A NeoFox® LED optical sensor (Ocean Optics) was used to measure partial pressure of oxygen in the water via fluorescent excitation of ruthenium in the patch, every 12 min. Oxygen levels were calculated in associated software following manufacturer's calibration (Ocean Optics).

Immediately following the low tide treatment in the incubator, mussels were individually transferred to respiration vials situated in a bucket with their respective treatment water. The respiration vials were sealed underwater to avoid trapping air bubbles and placed in one of two large temperature controlled aluminum blocks. Aluminum blocks were maintained at seawater treatment temperatures (8 °C and 14°C). Oxygen measurements were taken over the course of 2.5 h, every 12 min, on mussel vials and two control vials filled with treatment seawater. After the 2.5 h, mussels were immediately dissected and all soft tissue was dried for 24 h at 65 °C and weighed. For each vials, the slope (μmol O_2 L^{-1} consumed per minute) was calculated and corrected for drift by subtracting the slope of a blank vial. Slope per g tissue was calculated for each individual mussel, respectively. Respiration rates are reported as oxygen consumption (μmol O_2 g^{-1} h^{-1}).

7. RNA extraction and sequencing

Total RNA was extracted using TRIzol®, following manufacture protocol. RNA was extracted from 3 mussels per pseudo-replicate aquarium (with the exception that for 30 °C emersion stress, 2 and 4 mussels were taken from each pseudo-replicate of the upwelling

treatment, respectively) for a total of 6 mussels per treatment (seawater x low tide, n = 24). Using NEBNext® Ultra™ Directional RNA Library Prep Kit for Illumina®, cDNA libraries (n = 24) were prepared from 1 μg total RNA. The libraries were sequenced in two lanes (n = 12 per lane) for 100 bp paired-end reads, at the University of California Berkeley on a HighSeq2000. Sequence data were trimmed using Trim Galore! (v0.4.0) with a Phred quality score threshold of 20 and for NEBNext® index adapters. FastQC (v0.11.3) was used to verify read quality and identify overrepresented sequences using Standard Nucleotide BLAST (http://www.ncbi.nlm.nih.gov/). Overrepresented sequences in all samples aligned to mitochondrial rRNA and were not removed prior to transcriptome assembly.

For the purposes of this dissertation chapter, only the most extreme treatments were analyzed for gene expression. Two libraries from mussels exposed to 30 °C emersion stress for both relaxation and upwelling seawater treatments were used for *de novo* assembly of the transcriptome, using Trinity (v2.0.6, Haas et al. 2013). Gene expression was analyzed using libraries from all 6 replicate mussels sampled from the two seawater treatments following the 30 °C emersion stress treatment. Read alignments to the *de novo* transcriptome assembly and abundance estimates for each sample was performed using Trinity and RSEM. Differential expression analysis of isoforms was conducted via Trinity using EdgeR. Differentially expressed isoforms were annotated using BLAST (National Center for Biotechnology Information) and gene ontologies were mapped to annotations using Blast2Go.

8. Emersion temperature stress in context

To put the low tide treatments used in this experiment in context with *M. californianus* thermal tolerance, respiration trials were also conducted on adult mussels in a second

experiment. The goal of this experiment was to generate a physiological response curve of oxygen consumption following a range of emersion stress temperatures using a larger sample size (N = 12 vs. 5). For this experiment, adult *M. californianus* were collected from Lompoc Landing, California (34°43'11.2" N, 120°36'31.8" W) in summer 2014. Mussels were held at 15 °C in the laboratory and exposed to 3 sequential low tides in the laboratory tidal simulator before being exposed to a manual warming or cooling ramp in an incubator, as described above. Seawater pH was not altered and all mussels were exposed to 14 - 15 °C seawater temperatures. Mussels were not fed during the experiment. Emersion temperatures in the incubator ranged from 3 – 43 °C following methods used above with a few changes described below.

Mussels were held in a seawater table. Batches of 12 mussels were placed in aquaria with a tidal simulator for 3 days before exposure to the low tide treatment in the incubator. On day 4, 12 mussels were moved to an incubator at control temperature (14.5 ± 0.2 °C). Mussels were held for 15 min at constant temperature after which the temperature was incrementally changed by 0.5 °C over the course of 3 h to achieve the final emersion temperature. Mussels were held at the endpoint temperature, ranging from 3 – 43 °C, for 15 minutes for a the total emersion time to 3.5 h. Immediately following the low tide in the incubator, respiration rate was measured at control temperature (14 - 15 °C) following methods described in *Respiration trials* above. Only one warming or cooling ramp was conducted per day and the order of end point temperatures was randomized by day. This experiment was conducted twice, once for low tide temperature exposures of 3 – 36 °C in increments of 3 °C using mussels collect from Lompoc Landing on 16 July 2014, and later on for mussels exposed to 10, 20, 30, 39, 41, and 43 °C collected in August 2014. Note that

low tide warming up to 45 °C led to 100 % mortality and was not included in the respiration trials. This experiment was part of a National Science Foundation Research Experience for Undergraduates and was conducted by University of California Santa Barbara undergraduate, Evan Barba.

C. Results and Discussion

1. Field and treatment conditions

Typical seawater pH and temperature exposures during the upwelling season at Fogarty Creek, Oregon, matched seawater treatments, with high agreement across aquarium replicates (Table V-1, Figure V-1). Mean (± SD) relaxation treatment conditions during the experiment were pH_T 8.09 ± 0.03 for both aquaria, at 13.4 ± 1.1 and 1.0 °C. The 1 °C SD was due to the acclimation warming from 12 to 14 °C at the start of the experiment. Mean upwelling treatment conditions were pH_T 7.58 and 7.59 ± 0.03 at 8.1 ± 0.1 °C, for both aquaria.

Mussel body temperatures in the field were estimated by 6 mussel mimics in winter (Figure V-4). From mid-February to the end of March during low tides, emersion temperatures generally deviated from seawater temperatures by 0.5 – 5 °C either positively or negatively. One mimic documented warmer emersion temperatures than the other mimics, with one maximum emersion temperature of 27.5 °C and second maxima of 20 °C two days later. This disparity across mussel mimics reflects the microscale variability in mussel body temperatures across mussel aggregates and patches within the mussel bed (Helmuth 1998). During transport from the field to the University of California Santa Barbara, temperature cooled from 11 °C to 7 °C over 8 hours and never reached temperatures above 12.5 °C. These results suggest that the mussels used in this experiment were generally cold

Table V-1. Treatment conditions of mussels held at upwelling or relaxation treatments over the course of the 10-day experiment.

Treatment	Tank	pH_T	pCO_2	Ω_{arag}	T (°C)	sal	A_T	*N*
Relaxation	1	8.09 ± 0.03	347 ± 27	2.36 ± 0.21	13.4 ± 1.1	33.1 ± 0.1	2228 ± 6	*12*
	2	8.09 ± 0.03	344 ± 28	2.38 ± 0.22	13.4 ± 1.0	33.1 ± 0.1	2227 ± 6	*12*
Upwelling	1	7.58 ± 0.03	1243 ± 85	0.67 ± 0.04	8.1 ± 0.1	33.1 ± 0.1	2227 ± 4	*13*
	2	7.59 ± 0.03	1227 ± 84	0.68 ± 0.04	8.1 ± 0.1	33.1 ± 0.1	2228 ± 5	*13*

Figure V-4. Estimated mussel body temperature in the field and during the laboratory experiment, recorded by mussel mimics. Field temperatures were recorded in the mussel bed at Fogarty Creek, Oregon in winter (a) and summer (b). Two of the four treatments are shown (a) for comparison of laboratory thermal exposure to field conditions.

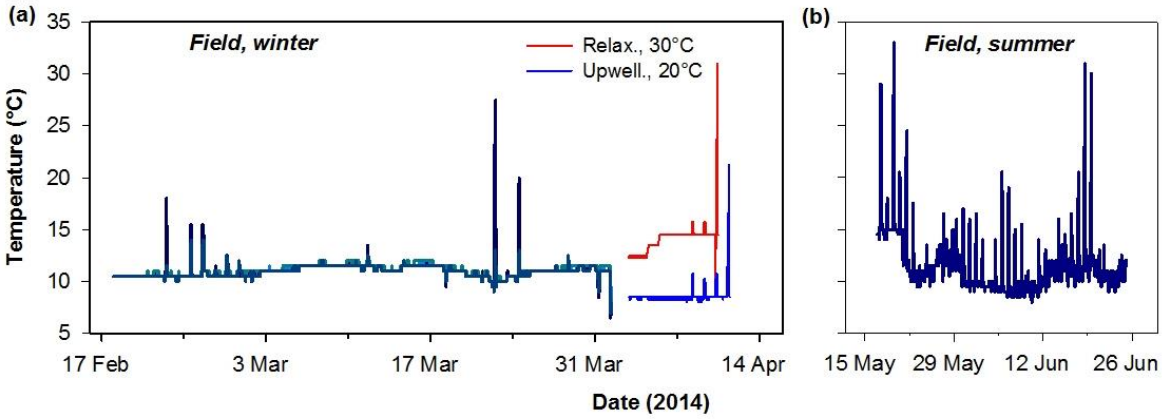

acclimatized, but some may have experienced one day of heat stress (> 20 °C) in the field depending on their exact exposure to solar radiation, wind, and ground and air temperatures (Helmuth 1998).

2. Respiration

Two respiration studies were conducted. To put the low tide treatments (20, 30 °C emersion stress) in context of *M. californianus* thermal tolerance, the second respiration experiment is reported first. Mussels collected from Lompoc Landing, California, exhibited highly variable oxygen consumption rates at different emersion temperatures (Figure V-5). Lowest mean respiration rates were detected at emersion temperatures above 36 °C. In other studies, this same temperature (36 °C) induced post-emersion stress mortality, as early as 1 day post-stress, in *M. californianus* individuals collected from populations along the CCS coastline (Logan et al. 2012). Interestingly, respiration rates first declined at 30 °C and increased twice at temperatures above 30 °C before consistently declining. This could reflect a response by mussels where metabolic depression is first induced, and then upregulated in response to increasing stress. Metabolic response to high temperatures decreased closer to the first immediate lethal temperature (45 °C) and delayed lethal temperature (36 °C, Logan et al. 2012). Heart rates of *M. californianus* have been shown to reach cardiac failure at maximum emersions temperatures of 34.7 ± 0.7 °C (mean ± SE) to 38.5 ± 0.6 °C during a heat ramp (Logan et al. 2012).

Respiration of mussels (5 individuals) was measured in treatment seawater simulating wind relaxation or upwelling, three times: no emersion, and following 20 and 30 °C emersion stress simulating hot low tides (Figure V-6, Table V-2). Lower respiration rates

Figure V-5. Mass-specific oxygen consumption rates of mussels following exposure to different emersion temperatures. Mussels were collected at Lompoc Landing, California, twice for two experiments. Mean ± SD, n = 12 per temperature.

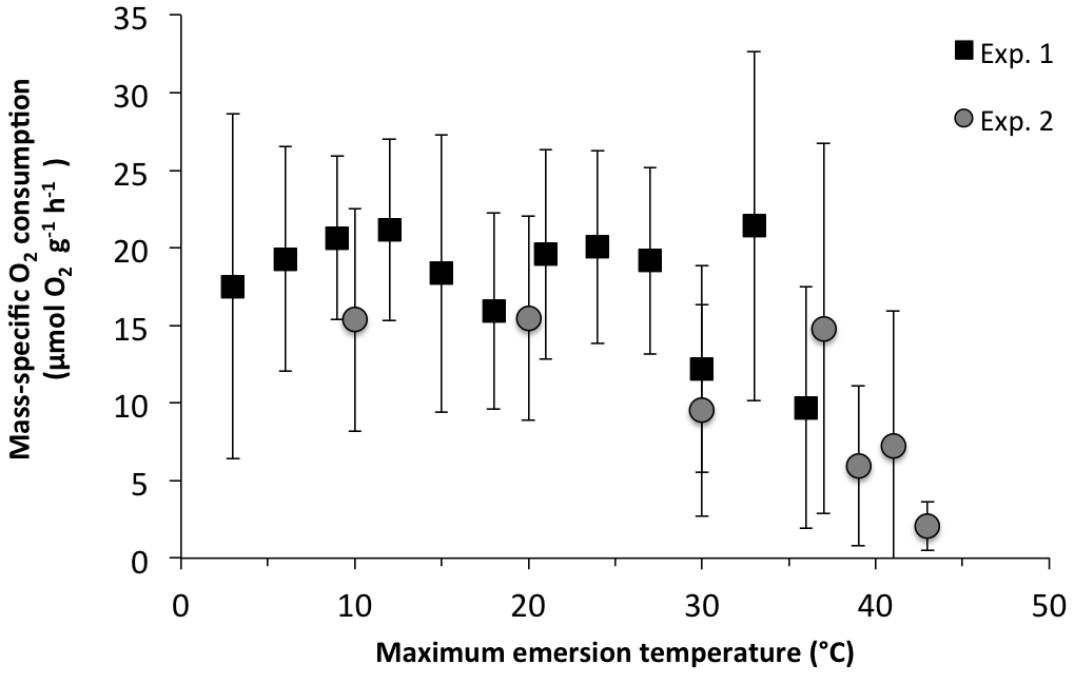

Figure V-6. Mass-specific oxygen consumption rates of mussels in seawater treatments simulating wind relaxation or upwelling events following either no emersion or maximum emersion heat stress of 20 or 30 °C. There were no significant differences in oxygen consumption across treatments (n = 5).

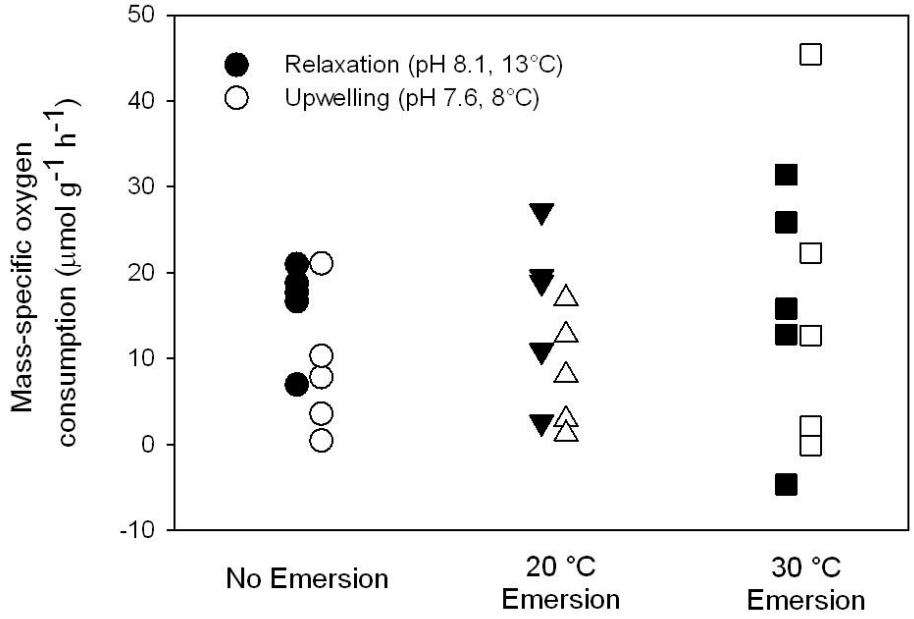

Table V-2. Starting conditions of seawater treatments used for respiration trials.

Salinity and total alkalinity represent samples taken from treatment tanks that day. pH was measured in triplicate.

Treatment	Tide	pH_T	pCO_2	Ω_{arag}	T (°C)	sal	A_T
Relaxation	none	8.07 ± 0.0	364 ± 4	2.33 ± 0.02	14	33	2232
	20°C	8.11 ± 0.0	329 ± 3	2.51 ± 0.02	14.1	33	2230
	30°C	8.10 ± 0.0	339 ± 4	2.46 ± 0.02	14.2	33	2230
Upwelling	none	7.62 ± 0.02	1141 ± 56	0.72 ± 0.03	8.1	33	2231
	20°C	7.60 ± 0.0	1212 ± 14	0.68 ± 0.01	8.2	33	2229
	30°C	7.61 ± 0.01	1150 ± 39	0.72 ± 0.02	8.2	33	2229

were expected in the upwelling treatment compared to the relaxation treatment due to cooler seawater temperatures (8 vs. 13 °C). However, no significant differences were detected based on seawater treatment and emersion heat stress (One-way ANOVA, *F-value* = 0.62, *p-value* = 0.683, *df* = 5, Anderson Darling test of normality passed, *p-value* = 0.522). Assuming that negative oxygen consumption means that the mussel did not respire, respiration rates ranged between 0 to > 40 µmol O_2 g^{-1} h^{-1} and fell within the observed range of *M. californianus* respiration rates from mussel collected at Lompoc Landing, California, following a range of emersion heat stress. These results show that mussel respiration is highly variable. It is possible that the high-plasticity and inter-individual variability of *M. californianus* metabolic response to environmental exposures facilitates its successful and extensive colonization across the intertidal.

Collectively, results from the respiration trials show that emersion temperatures can influence respiration rates during recovery from emersion heat stress (especially at temperatures nearing lethal exposures), suggesting a metabolic cost incurred by extreme emersion heat stress. This is reflected in gene expression research showing that mussels induce transcription of Hsps following low tide heat stress > 30 °C (Gracey et al. 2008). The results from the respiration trials suggest that the low tide treatments of 20 and 30 °C emersion stress fall within the physiological tolerance of *M. californianus*. In other words, exposure to 30 °C emersion stress does not compromise physiological processes beyond the ability of what *M. californianus* can tolerate. However, 30 °C emersion stress potentially nears levels of sub-lethal stress (e.g. temperatures that induce metabolic depression but do not result in mortality) and so may manifest in energy trade-offs that are detectable at the level of the transcriptome.

3. Gene expression

Although mussel gill tissue was collected from individuals exposed to all four treatments (seawater treatments simulating upwelling and wind relaxation, and two low tide treatments), this preliminary work investigates gene expression differences between individuals exposed to the two seawater treatments and only the 30 °C emersion stress. Following maximum emersion temperature of 30 °C during a simulated low tide, differential expression was found between 52 isoforms (FDR < 0.05) in mussels form the seawater treatment simulating wind relaxation as compared to that simulating upwelling (Figure V-7). Of these isoforms, 31 were up regulated and 30 were down regulated when mussels were exposed to the upwelling seawater treatment relative to simulated wind relaxation. Isoform sequences primarily mapped to the annotated transcriptome of *Crassostrea gigas* (Zhang et al. 2012) and second to *M. galloprovincialis*. Isoforms with sequence descriptions are described in Table V-3 and Table V-4. Overall, the presence of differential expression suggests that water mass qualities (e.g. temperature and pH combinations present in near-shore Oregon) influence cellular processes in *M. californianus* gill tissue following emersion heat stress. These preliminary results warrant future investigation of the effect of 20 vs. 30 °C emersion stress.

The primary goal of this experiment was to assess whether or not the HSR initiated during hot low tides differed between mussels under simulated wind relaxation or upwelling conditions. Changes in gene expression of Hsp70 were not detected in this analysis of comparing mussels exposed to simulated wind relaxation or upwelling seawater treatments following 30 °C emersion heat stress. In *M. californianus*, Hsp70 is inducible across a range of temperatures and initiation of expression changes with seasonal acclimatization to

Figure V-7. Volcano plot of log fold change in gene expression in mussel gill tissue of adult mussels exposed to 30 °C emersion stress under relaxed vs. upwelled treatment seawater. Red dots indicate genes with significant differential expression.

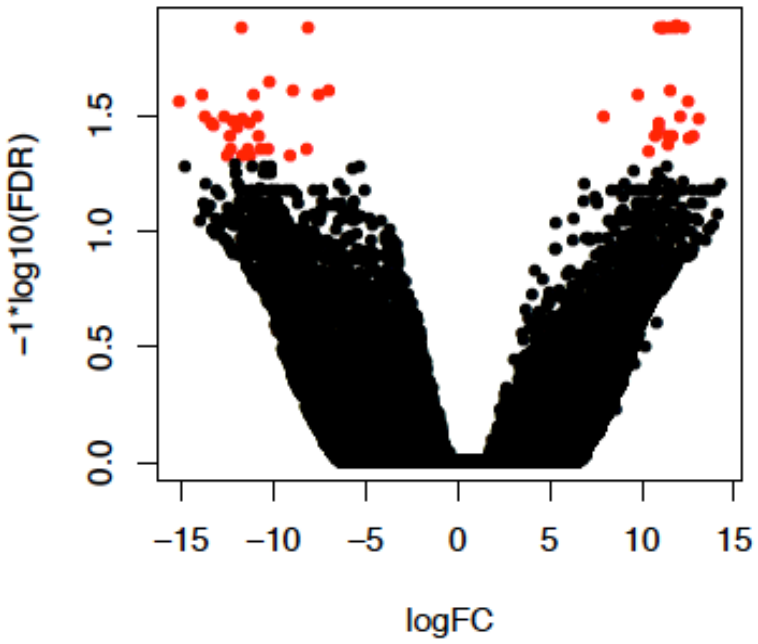

Table V-3. List of up regulated genes under simulated upwelling conditions relative to simulated wind relaxation for isoforms with sequence descriptions.

Sequence Name	Sequence Description	Gene Ontology
TR107520|c1_g1_i1	wsc domain-containing protein 2	
TR94779|c0_g1_i1	upf0764 protein c16orf89 homolog	
TR105881|c2_g1_i7	ubiquitin-conjugating enzyme e2 l3	ligase activity;metabolic process
TR124258|c0_g1_i2	stimulator of interferon genes partial	cytoplasmic part;binding;activation of innate immune response;positive regulation of type I interferon production
TR99463|c0_g1_i4	sal-like protein 1 isoform x2	intracellular organelle;nucleic acid binding;metal ion binding;kidney development;regulation of transcription, DNA-templated;nervous system development;anatomical structure morphogenesis;embryo development;tube development;positive regulation of cellular process;limb development;epithelium development
TR105212|c1_g2_i1	protein polybromo-1 isoform x1	chromatin binding;protein binding
TR105212|c1_g2_i4	protein polybromo-1 isoform x1	chromatin binding;protein binding
TR105212|c1_g2_i4|protein	protein polybromo-1 isoform x1	
TR138166|c1_g1_i2	protein mab-21-like 2	system development
TR98242|c0_g1_i1	perlucin-like protein	
TR144795|c5_g1_i1	mam and ldl-receptor class a domain-containing protein 1-like	membrane;scavenger receptor activity;protein binding
TR89398|c0_g1_i2	innexin unc-9-like isoform x1	plasma membrane;gap junction;integral component of membrane;ion transport
TR97740|c4_g3_i3	fibroblast growth factor receptor 2	protein binding
TR141391|c0_g1_i1	cell wall protein dan4-like isoform x2	extracellular region;protein binding;chitin binding;chitin metabolic process
TR96807|c2_g2_i1|---NA---	barrier-to-autointegration factor	
TR245|c0_g1_i1	astacin-like metalloendopeptidase	

Table V-4. List of down regulated genes under simulated upwelling conditions relative to simulated wind relaxation for isoforms with sequence descriptions.

Sequence Name	Sequence Description	Gene Ontology
TR101971|c0_g2_i2	vacuolar protein sorting-associated protein 13b isoform x1	
TR144820|c6_g1_i6	tubulin polyglutamylase ttll7-like isoform x1	cellular protein modification process
TR124864|c2_g1_i1	stress-induced protein 1	
TR124864|c3_g1_i1	small heat shock protein	
TR32157|c0_g1_i3	rna-binding protein musashi homolog rbp6 isoform x1	cytoplasm;polysome;nucleotide binding;mRNA binding;poly(U) RNA binding;stem cell development
TR6838|c0_g1_i1	reticulocyte-binding protein 2 homolog a-like isoform x1	cytoplasm;ubiquitin-protein transferase activity;ligase activity;protein ubiquitination involved in ubiquitin-dependent protein catabolic process
TR51609|c0_g1_i1	protein transport protein sec61 subunit alpha isoform 2	integral component of membrane;protein transport
TR134733|c0_g1_i13	protein fam46a-like	
TR82900|c3_g1_i1	protein deltex-3-like protein	metal ion binding
TR43825|c0_g1_i1	lysosomal-associated transmembrane protein 4a	integral component of membrane
TR136344|c1_g1_i3	hypothetical protein BRAFLDRAFT_76566	
TR16983|c0_g1_i1	elongation factor-1 gamma	translation elongation factor activity;protein binding;translational elongation
TR78156|c0_g2_i1	elongation factor 1 alpha	cytoplasm;translation elongation factor activity;GTPase activity;GTP binding;translational elongation
TR80768|c1_g1_i3	cytosolic carboxypeptidase 2	
TR138877|c3_g2_i2	cell wall protein dan4-like isoform x2	extracellular region;chitin binding;chitin metabolic process

changing temperatures (Roberts et al. 1997). *M. californianus* is known to reduce Hsp70 protein synthesis during the seasons with the highest temperature exposures (Roberts et al. 1997). As this experiment utilized winter-acclimatized individuals, the 30 °C emersion stress was potentially the first extreme heat exposure of the season. It is therefore possible that the influence of emersion heat stress was so great that it flooded any potential effect of the seawater treatments and induced high hsp70 expression in mussels equally regardless pH and temperature of the seawater. Future comparisons from this experiment using individuals exposed to 20 °C emersion stress will reveal the relative magnitude of heat stress induced in this experiment, as 20 °C is known to be one the warmest temperatures that does not induce a HSR in *M. californianus* (Roberts et al. 1997).

While differential expression was not detected for Hsp70, other Hsps did exhibit different patterns of expression. For example, small heat shock protein (hsp24.1) and stress-induced protein 1, also in the hsp20 family, were down regulated under upwelling conditions relative to simulated wind relaxation conditions. sHsps are molecular chaperones that bind proteins in non-native conformations, prevent protein aggregations, and are induced by increased temperature (Haslbeck et al. 2005). Mechanistically, sHsps bind to denatured proteins to build a reservoir of protected proteins that can be refolded with the assistance of ATP-dependent chaperones, such as Hsp70, and enhance the efficiency of such protein restoration (Haslbeck et al. 2005). The increased gene expression of sHsps under simulated wind relaxation suggests an increased need for protein repair processes, potentially due to the higher water temperatures compared to simulated upwelling conditions. As sHsps bind proteins that can later be refolded, sHsps may act as a first line of defense in extreme cellular stress. Potentially, cooler water temperatures following emersion heat stress may

reduce overall heat-induced protein damage. If so, upwelling of cold water may lessen the extent of cellular damage due emersion heat stress in *M. californianus*.

Another stress related gene that exhibited differential gene expression across simulated wind relaxation and upwelling was ubiquitin-conjugating enzyme e2 l3, a protein in the ubiquitin-proteasome cellular pathway. This E2 enzyme exhibited higher expression in mussels exposed to simulated upwelling compared to those held under simulated wind relaxation, following 30 °C emersion heat stress. E2 enzymes are involved in ubiquitin-tagging of damaged or short-lived proteins (Hershko and Ciechanover 1992). Ubiquitin tags signal proteins for cellular degradation by proteasomes. In contrast to the sHsp expression patterns, enhanced expression of E2 enzymes suggest that protein damage still occurred in mussels in the upwelling treatment. At the same time, down regulation of reticulocyte-binding protein 2 homolog a-like isoform x1 was detected under upwelling conditions. This reticulocyte-binding protein 2 homolog functions in ubiquitin-dependent protein catabolism. While down regulation might oppose the pattern observed for the E2 enzyme, it is challenging to interpret the meaning of, overall, few differentially expressed genes.

Future analyses using an annotated *de novo* transcriptome assembly using all samples sequenced in this study will allow for full pathway analyses and potentially provide a more complete picture of the changes in cellular processes induced by exposure to different water mass conditions and emersion heat stress. Such analyses may reveal how the other significantly differentially expressed genes contribute to the response of *M. californianus* to tidal emersion. The results presented here suggest that water mass conditions may change how *M. californianus* responds to emersion heat stress and deal with protein damage, and

this preliminary result warrants a more in-depth analysis using the full experimental design and dataset.

D. Acknowledgements

I thank Florian Kapsenberg for assistance with the design and construction of the tidal simulator and Angela Johnson and Roeland Kapsenberg for help with fieldwork. Mark Bitter, Alice Nguyen, Emily Rivest, Geoff Dilly, Kevin Johnson, Umi Hoshijima, Jay Lunden, Josh Hancock and Emily Ellis assisted with dissections and methods throughout the experiment. Kevin Johnson assisted with gene expression analyses.

E. References

Bakun, A. 1990. Global climate change and intensification of coastal ocean upwelling. Science **247:** 198-201.

Bograd, S. J., I. Schroeder, N. Sarkar, X. Qiu, W. J. Sydeman, and F. B. Schwing. 2009. Phenology of coastal upwelling in the California Current. Geophys. Res. Lett. **36**.

Breitburg, D. L. and others 2015. And on top of all that... coping with ocean acidification in the midst of many stressors. Oceanography **28:** 48-61.

Buckley, B. A., M.-E. Owen, and G. E. Hofmann. 2001. Adjusting the thermostat: the threshold induction temperature for the heat-shock response in intertidal mussels (genus *Mytilus*) changes as a function of thermal history. J. Exp. Biol. **204:** 3571-3579.

Dickson, A. G., and F. J. Millero. 1987. A comparison of the equilibrium constants for the dissociation of carbonic acid in seawater media. Deep-Sea Res. I **34:** 1733-1743.

Dickson, A. G., C. L. Sabine, and J. R. Christian. 2007. Guide to best practices for ocean CO_2 measurements. PICES Special Publication **3:** 191 pp.

Fangue, N. A., M. J. O'Donnell, M. A. Sewell, P. G. Matson, A. C. Macpherson, and G. E. Hofmann. 2010. A laboratory-based, experimental system for the study of ocean acidification effects on marine invertebrate larvae. Limnology and Oceanography-Methods **8:** 441-452.

Feder, M. E., and G. E. Hofmann. 1999. Heat-shock proteins, molecular chaperones, and the stress response: evolutionary and ecological physiology. Annu. Rev. Physiol. **61:** 243-282.

Feely, R. A., C. L. Sabine, J. M. Hernandez-Ayon, D. Ianson, and B. Hales. 2008. Evidence for upwelling of corrosive "acidified" water onto the continental shelf. Science **320:** 1490-1492.

Gaylord, B. and others 2011. Functional impacts of ocean acidification in an ecologically critical foundation species. J. Exp. Biol. **214:** 2586-2594.

Gracey, A. Y., M. L. Chaney, J. P. Boomhower, W. R. Tyburczy, K. Connor, and G. N. Somero. 2008. Rhythms of gene expression in a fluctuating intertidal environment. Curr. Biol. **18:** 1501-1507.

Gruber, N., C. Hauri, Z. Lachkar, D. Loher, T. L. Frölicher, and G.-K. Plattner. 2012. Rapid progression of ocean acidification in the California Current System. Science **337:** 220-223.

Haas, B. J. and others 2013. *De novo* transcript sequence reconstruction from RNA-seq using the Trinity platform for reference generation and analysis. Nature protocols **8:** 1494-1512.

Halpin, P. M., B. A. Menge, and G. E. Hofmann. 2004. Experimental demonstration of plasticity in the heat shock response of the intertidal mussel *Mytilus californianus*. Mar. Ecol. Prog. Ser. **276:** 137-145.

Harvey, B. P., D. Gwynn-Jones, and P. J. Moore. 2013. Meta-analysis reveals complex marine biological responses to the interactive effects of ocean acidification and warming. Ecology and Evolution **3:** 1016-1030.

Haslbeck, M., T. Franzmann, D. Weinfurtner, and J. Buchner. 2005. Some like it hot: the structure and function of small heat-shock proteins. Nat. Struct. Mol. Biol. **12:** 842-846.

Hauri, C. and others 2013. Spatiotemporal variability and long-term trends of ocean acidification in the California Current System. Biogeosciences **10:** 193–216.

Helmuth, B. and others 2006. Mosaic patterns of thermal stress in the rocky intertidal zone: implications for climate change. Ecol. Monogr. **76:** 461-479.

Helmuth, B., C. D. Harley, P. M. Halpin, M. O'Donnell, G. E. Hofmann, and C. A. Blanchette. 2002. Climate change and latitudinal patterns of intertidal thermal stress. Science **298:** 1015-1017.

Helmuth, B. S. 1998. Intertidal mussel microclimates: predicting the body temperature of a sessile invertebrate. Ecol. Monogr. **68:** 51-74.

Hershko, A., and A. Ciechanover. 1992. The ubiquitin system for protein degradation. Annu. Rev. Biochem. **61:** 761-807.

Hofmann, G. E. 2005. Patterns of Hsp gene expression in ectothermic marine organisms on small to large biogeographic scales. Integr. Comp. Biol. **45:** 247-255.

Hofmann, G. E. and others 2014. Exploring local adaptation and the ocean acidification seascape – studies in the California Current Large Marine Ecosystem. Biogeosciences **11:** 1053-1064.

Huyer, A. 1983. Coastal upwelling in the California Current system. Prog. Oceanogr. **12:** 259-284.

Iles, A. C., T. C. Gouhier, B. A. Menge, J. S. Stewart, A. J. Haupt, and M. C. Lynch. 2012. Climate-driven trends and ecological implications of event-scale upwelling in the California Current System. Global Change Biol. **18:** 783-796.

Jost, J., and B. Helmuth. 2007. Morphological and ecological determinants of body temperature of *Geukensia demissa*, the Atlantic ribbed mussel, and their effects on mussel mortality. The Biological Bulletin **213:** 141-151.

Kroeker, K. J. and others 2013. Impacts of ocean acidification on marine organisms: quantifying sensitivities and interaction with warming. Global Change Biol. **19:** 1884-1896.

Kültz, D. 2005. Molecular and evolutionary basis of the cellular stress response. Annu. Rev. Physiol. **67:** 225-257.

Kurihara, H. 2008. Effects of CO_2-driven ocean acidification on the early developmental stages of invertebrates. Mar. Ecol. Prog. Ser. **373:** 275-284.

Lindquist, S. 1986. The heat-shock response. Annu. Rev. Biochem. **55:** 1151-1191.

Lockwood, B. L., K. M. Connor, and A. Y. Gracey. 2015. The environmentally tuned transcriptomes of *Mytilus* mussels. J. Exp. Biol. **218:** 1822-1833.

Logan, C. A., L. E. Kost, and G. N. Somero. 2012. Latitudinal differences in *Mytilus californianus* thermal physiology. Mar. Ecol. Prog. Ser. **450:** 93-105.

Mehrbach, C., C. H. Culberso, J. E. Hawley, and R. M. Pytkowic. 1973. Measurement of apparent dissociation constants of carbonic acid in seawater at atmospheric pressure. Limnol. Oceanogr. **18:** 897-907.

Menge, B. A., and G. M. Branch. 2001. Rocky intertidal communities, p. 221-251. *In* M. D. Bertness, S. D. Gaines and M. E. Hay [eds.], Marine community ecology. Sinauer Associates Sunderland, Massachusetts, USA.

Menge, B. A., B. A. Daley, P. A. Wheeler, E. Dahlhoff, E. Sanford, and P. T. Strub. 1997. Benthic-pelagic links and rocky intertidal communities: bottom-up effects on top-down control? Proc. Natl. Acad. Sci. **94:** 14530-14535.

Michaelidis, B., C. Ouzounis, A. Paleras, and H. O. Pörtner. 2005. Effects of long-term moderate hypercapnia on acid-base balance and growth rate in marine mussels *Mytilus galloprovincialis*. Mar. Ecol. Prog. Ser. **293:** 109-118.

O'Donnell, M. J., M. N. George, and E. Carrington. 2013. Mussel byssus attachment weakened by ocean acidification. Nature Climate Change **3:** 587-590.

O'Donnell, M. J., L. M. Hammond, and G. E. Hofmann. 2008. Predicted impact of ocean acidification on a marine invertebrate: elevated CO_2 alters response to thermal stress in sea urchin larvae. Mar. Biol. **156:** 439-446.

Paganini, A. W., N. A. Miller, and J. H. Stillman. 2014. Temperature and acidification variability reduce physiological performance in the intertidal zone porcelain crab *Petrolisthes cinctipes*. The Journal of Experimental Biology **217:** 3974-3980.

Place, S. P., B. A. Menge, and G. E. Hofmann. 2012. Transcriptome profiles link environmental variation and physiological response of *Mytilus californianus* between Pacific tides. Funct. Ecol. **26:** 144-155.

Pörtner, H.-O. and others 2014. Ocean systems, p. 411-484. *In* C. B. Field et al. [eds.], Climate Change 2014: Impacts, Adaptation, and Vulnerability. Part A: Global and Sectoral Aspects. Contribution of Working Group II to the Fifth Assessment Report of the Intergovernmental Panel on Climate Change. Cambridge University Press.

Rastrick, S. P. and others 2014. Living in warmer, more acidic oceans retards physiological recovery from tidal emersion in the velvet swimming crab, *Necora puber*. The Journal of Experimental Biology **217:** 2499-2508.

Reum, J. C. and others 2015. Interpretation and design of ocean acidification experiments in upwelling systems in the context of carbonate chemistry co-variation with temperature and oxygen. ICES J. Mar. Sci.

Robbins, L. L., M. E. Hansen, J. A. Kleypas, and S. C. Meylan. 2010. CO2calc—A user-friendly seawater carbon calculator for Windows, Max OS X, and iOS (iPhone). U.S. Geological Survey Open-File Report 2010–1280.

Roberts, D. A., G. E. Hofmann, and G. N. Somero. 1997. Heat-shock protein expression in *Mytilus californianus*: acclimatization (seasonal and tidal-height comparisons) and acclimation effects. The Biological Bulletin **192:** 309-320.

Sanford, E. 1999. Regulation of keystone predation by small changes in ocean temperature. Science **283:** 2095-2097.

Somero, G. N. 1995. Proteins and temperature. Annu. Rev. Physiol. **57:** 43-68.

Stillman, J. H., and E. Armstrong. 2015. Genomics are transforming our understanding of responses to climate change. Bioscience**:** biu219.

Thomsen, J., and F. Melzner. 2010. Moderate seawater acidification does not elicit long-term metabolic depression in the blue mussel *Mytilus edulis*. Mar. Biol. **157:** 2667-2676.

Zhang, G. and others 2012. The oyster genome reveals stress adaptation and complexity of shell formation. Nature **490:** 49-54.